

ABSTRACT

Title of Document: ASSESSING THE UNCERTAINTY OF
EMERGY ANALYSES WITH MONTE
CARLO SIMULATIONS

Amy Hudson, Master of Science, 2012

Directed By: Associate Professor David R. Tilley,
Environmental Science and Technology

Crop production systems were used to show the presence and propagation of uncertainty in emergy analyses and the effect of source variance on the variance of the yield unit emergy value (UEV). Data on energy/masses and UEVs for each source and yield were collected from the emergy literature and considered as inputs for the Monte Carlo simulation. The inputs were assumed to follow normal, lognormal, or uniform probability distributions. Using these inputs and a tabular method, two models ran Monte Carlo simulations to generate yield UEVs. Supplemental excel files elucidate the Monte Carlo simulations' calculations. The nitrogen fertilizer UEV and net topsoil loss energy were the inputs with the largest impact on the variance of the yield's UEV. These two sources also make the largest emergy contributions to the yield and should be the focus of a manager intent on reducing total system uncertainty. The selection of a statistical distribution had an impact on the yield UEV and thus these analyses may need to remain system- or even source- specific.

ASSESSING THE UNCERTAINTY OF EMERGY ANALYSES WITH MONTE
CARLO SIMULATIONS

By

Amy Rebecca Hudson

Thesis submitted to the Faculty of the Graduate School of the
University of Maryland, College Park, in partial fulfillment
of the requirements for the degree of
Master of Science
2012

Advisory Committee:
Associate Professor David R. Tilley, Ph.D., Chair
Associate Professor Patrick C. Kangas, Ph.D.
Daniel E. Campbell, Ph.D.

© Copyright by
Amy Rebecca Hudson
2012

Table of Contents

Table of Contents	ii
List of Tables	iii
List of Figures	v
Chapter 1: Introduction	1
Emergy introduced.....	1
Emergy evaluation	3
Incorporating uncertainty into emergy.....	6
Monte Carlo simulation	9
Chapter 2: Objectives.....	15
Chapter 3: Plan of study.....	16
Chapter 4: Methodology	17
Systems descriptions.....	17
Original systems' descriptions.....	17
Monte Carlo simulations.....	22
Sensitivity analysis.....	45
Chapter 5: Results	48
Systems Descriptions	48
Original systems' descriptions.....	48
Monte Carlo simulations.....	53
Sensitivity analysis.....	99
Model 1: Energy/mass and UEV variance.....	100
Model 2: UEV variance	105
Model Comparison.....	110
Chapter 6: Discussion	113
Chapter 7: Summary	116
Appendices.....	120
Bibliography	128

List of Tables

Table 1:	Terms defined for use in this paper	2
Table 2:	Tabular method for emergy accounting	4
Table 3:	Selected Sources of Corn and Wheat Cropping Systems	19
Table 4a:	Energy/mass data collected from eight original systems for each source (1, 2, 3,...) and yield	19
Table 4b:	UEV data collected from eight original systems for each source (1, 2, 3,...) and yield	20
Table 4c:	Emergy found by multiplying corresponding cells in Table 4a and Table 4b	20
Table 5a:	Original eight cropping systems	49
Table 5b:	Emergy sum of squares partitioning for sources	50
Table 6a:	Monte Carlo output of Model 2 assuming normally distributed source UEVs	56
Table 6b:	Monte Carlo output of Model 2 assuming lognormally distributed source UEVs	58
Table 6c:	Monte Carlo output of Model 2 assuming uniformly distributed source UEVs	59
Table 7a:	Monte Carlo output of Model 2 assuming normally distributed source UEVs	63
Table 7b:	Monte Carlo output of Model 2 assuming lognormally distributed source UEVs	64
Table 7c:	Monte Carlo output of Model 2 assuming uniformly distributed	

	source UEVs	65
Table 8a:	The source partition of the energy yield uncertainty into the Energy/Mass Variance Model and the UEV Variance Model	69
Table 8b:	The 95% confidence interval of the yield UEV	70
Table 9a:	Model 1 sensitivity results	103
Table 9b:	Model 1 % difference of each output from the baseline	104
Table 10a:	Model 2 sensitivity results	107
Table 10b:	Model 2 % difference of each output from the baseline	108
Table 11:	A key of systems studied	120
Table 12a:	Energy/mass data of original eight systems studied	121
Table 12b:	UEV data of original eight systems studied	123
Table 13a:	Sensitivity analysis for Model 1: Exact data and p values	124
Table 13b:	Sensitivity analysis for Model 2: Exact data and p values	126

List of Figures

Figure 1:	Monte Carlo generation of weight	9
Figure 2:	Stochastic uncertainty propagation	10
Figure 3:	Simplified energy diagram showing driving forces of crop production	17
Figure 4:	Stochastic uncertainty propagation of corn and wheat production	23
Figure 5a:	Emergy signature of sources to the original crop systems without yield	52
Figure 5b:	Emergy signature of sources to the original crop systems with yield	53
Figure 6a:	Crop system emergy signature: Model 1	55
Figure 6b:	Crop system emergy signature: Model 2	61
Figure 7a:	Monte Carlo simulation graphs for sunlight source	74
Figure 7b:	Monte Carlo simulation graphs for evapotranspiration source	76
Figure 7c:	Monte Carlo simulation graphs for fuel source	78
Figure 7d:	Monte Carlo simulation graphs for net topsoil loss source	80
Figure 7e:	Monte Carlo simulation graphs for electricity source	82
Figure 7f:	Monte Carlo simulation graphs for labor source	84
Figure 7g:	Monte Carlo simulation graphs for seed source	86
Figure 7h:	Monte Carlo simulation graphs for steel machinery source	88
Figure 7i:	Monte Carlo simulation graphs for pesticides source	90
Figure 7j:	Monte Carlo simulation graphs for phosphate fertilizer source	92
Figure 7k:	Monte Carlo simulation graphs for nitrogen fertilizer source	95

Figure 71:	Monte Carlo simulation graphs for the output	98
Figure 8:	Relationships between uncertainty and emergy input for each of the 11 sources for crop production	117

Chapter 1: Introduction

Emergy introduced

There is a growing global effort to quantify the value of our surrounding natural systems. Embodied energy (emergy) analyses place value on systems using an energy-based process that measures and compares different quality levels and flows of energy in systems. The main principle of emergy is that every type of energy in a system can be transformed into a unit of energy of a single kind (solar emjoule) to document on a common basis the total energy that was required directly and indirectly to make another form of energy, a product, or provide a service (Odum 1996). A solar emjoule is equal to one joule of sunlight, and is the primary energy source that drives earth's planetary systems, including ecosystems.

Emergy is used in environmental accounting to specify performance indicators for systems. Table 1 defines popular indices such as EYR, ELR, percent renewability, and ESI, which respectively describe the yield, loading, reliance on renewable energy, and sustainability of a system. The appropriate index corresponds to the question of concern about the system.

Term:	Abbreviation:	Definition:
Solar Energy	Emergy	The amount of available energy of one type (usually solar) that is directly or indirectly required to generate a given output flow or storage of energy or matter.
Solar transformity	Transformity	Emergy investment required per unit process output of available energy
Specific emergy	Specific Emergy	Emergy investment required per unit process output of dry mass
Unit Emergy Value	UEV	Emergy investment required per unit of product or service
Emergy yield ratio	EYR	Emergy of the yield per unit of emergy invested or purchased from the economy
Environmental loading ratio	ELR	Total nonrenewable and imported emergy released per unit of local renewable resource
Emergy sustainability index	ESI	Emergy yield per unit of environmental loading
Emergy investment ratio	EIR	Emergy investment needed to use one unit of local (renewable and nonrenewable) resource.

(Odum 1996, Amponsah and Corre 2010, Ulgiati et al. 2010)

In accounting for all the types of energy that run the system, the three basic steps required to estimate the emergy of a type of energy, a product, or service are 1) decide on which sources are required for the system, 2) estimate the energy or mass required for each source, and 3) estimate the emergy content of a source's energy or mass (i.e. unit emergy value).

Not all energy is created equal: a joule of light from an electric bulb can serve a variety of purposes. To account for this inequality, each energy/mass unit is multiplied by a unit of emergy value (UEV), a way of describing an energy/mass unit in terms of efficiency, or the emergy source per unit of available yield (e.g. sej/J, sej/g). Depending on the energy/mass unit, the unit emergy values in this study can be

labeled as ‘transformity’ (sej/J), or ‘specific emergy’ (sej/g) (Ulgiati et al. 2010). For example, sunlight has a transformity of 1 sej/J of sunlight.

The emergy of a source is then the product of the energy/mass and its UEV. The emergy of the entire system is the sum of the emergy of the contributing sources. Therefore, there are three major pathways for uncertainty to enter the final estimate of how much emergy something required. First, the wrong model is used. For example, the list of sources required could exclude items that were actually required. Or rarely an item could be erroneously included. Second, the energy consumed by use of a source is often estimated using other models, but can be based on observed data. However, observed data will suffer from measurement error. Third, the UEV of the particular source may not be known so it is estimated using published UEVs for similar or identical items. This study aims to identify the significance of these three forms of uncertainty on the emergy estimate.

Emergy evaluation

Often, emergy analyses follow a tabular procedure where source flows of energy or mass are transformed to solar emergy and then summed to estimate the emergy of the yield (Table 2). In the example in Table 2 the source energy/mass for each item is multiplied by its corresponding solar transformity (sej/J) or specific solar emergy (sej/g) to estimate the solar emergy it contributes to the total solar emergy (sej) of the system. The emergy of the sources are summed to estimate the emergy of the yield. The solar transformity or specific solar emergy for the yield can then be estimated as the total solar emergy divided by the energy or mass of the yield.

Table 2: Tabular method for energy accounting.

Item	Energy/Mass	Units	UEV (sej/unit)	Energy flow (sej)
Source				
1	d_1	J	v_1	$m_1 = d_1 * v_1$
2	d_2	g	v_2	$m_2 = d_2 * v_2$
3	d_3	J	v_3	$m_3 = d_3 * v_3$
...
Yield	d_p	J	$v_p = m_p / d_p$	$m_p = m_1 + m_2 + m_3$

Estimates of the source energy/mass are supported with further information in footnotes or endnotes that include equations and data sources. Footnotes should clearly explain how the source energy/mass was generated and its intellectual basis.

For a given energy analysis, UEVs of the sources are not typically estimated from mathematical modeling. Rather, UEVs for the sources are selected from other studies or databases such as www.emergydatabase.org (Tilley et al. 2012) to best reflect the sources. For example, rather than estimate the UEV of freshwater for every study, a global mean UEV of rainfall is often used. Therefore, the source of all UEVs used in a study must be cited.

One of the main reasons for selecting UEVs, rather than estimating new ones for each study, is the limited amount of time an analyst has to conduct the study. The solar energy of any single source is the culmination of a complex web of energy transformations in its own right. Thus, the selection of UEVs is an accounting shortcut that saves the analyst vast amounts of computational time. Of course, one of the drawbacks is that the selected UEV is only the best guess of how much solar energy is actually embodied in the source. Another limitation is that only point estimates are typically available for the UEVs.

Emergy analysts recognize that point estimates are a limitation (Odum 1996, Campbell 2001, Cohen 2001, Ingwersen 2010a, Ingwersen 2010b, Brown et al.

2011). Multiple energy analyses of different systems that produce the same yield clearly show that multiple point estimates exist (Brandt-Williams 2002, Lefroy and Rydberg 2003, Rodrigues et al. 2003, Coppola et al. 2009, Franzese et al. 2009). Dynamic energy accounting has shown that the UEV of a particular product can vary over a range and may follow a probabilistic distribution (PDF) like the normal or lognormal (Tilley and Brown 2006). Thus, the point estimates are samples drawn from a population of UEVs that likely can be modeled with PDFs.

There is a growing demand by energy practitioners to model the uncertainty of unit energy values used or created (Hau and Bakshi 2004, Amponsah et al. 2010, Ulgiati et al. 2010). However, an important advantage of using point estimates for UEVs and specific energies is that it offers a simplified method for completing energy analyses quickly. Otherwise an energy analysis could involve making hundreds of calculations and estimations. Thus, there is a need to determine the most appropriate PDFs for modeling the uncertainty of UEVs. Once the nature of UEV uncertainty is better understood, future steps would be to adjust the methodology (e.g., tabular energy accounting in Table 2) to reduce overall levels of uncertainty and to provide the capability for estimating confidence intervals for key energy indices like the energy yield ratio.

In the related systems accounting field of life cycle assessment (LCA) uncertainty values are often required (Lloyd and Ries 2007, Ingwersen 2010a, Ingwersen 2010b). When LCA is used in a regulatory environment, the Federal Office of Management and Budget requires that LCAs include either a qualitative

discussion of the main uncertainties, a numerical sensitivity analysis, or a formal probabilistic analysis to communicate scientific uncertainty (Jaffe and Stavins 2007).

For energy analysis to be considered a formal policy analysis tool it too should include estimates of uncertainty and sensitivity. An energy database was created in part to assist in the *qualitative* and quantitative assessment of UEV uncertainty (Tilley et al. 2012). There have been a few recent energy publications that reported on UEV uncertainty (Campbell 2001, Cohen 2001, Tilley and Brown 2006, Ingwersen 2010a, Ingwersen 2010b, Brown et al. 2011). Ingwersen's (2010a) suggestion to standardize quantitative uncertainty propagation in energy analyses was in part the impetus for this study.

Incorporating uncertainty into energy

Before continuing on, it is important to clarify the terminology this study will use in discussing uncertainty in energy evaluations. In statistics, uncertainty is defined as having limited knowledge about the value of a parameter, while variability is the variation of the individuals in the population studied (Rai and Krewski 1998). Monte Carlo methods used in multiplicative models have been unable to separate total uncertainty *a)* due to uncertainty and *b)* due to variability in and between systems. Previous studies employing Monte Carlo methods have therefore lumped these uncertainty and variance terms together under the term uncertainty when discussing Monte Carlo method generated results (Llyod and Reis 2007, Ingwersen 2010a, Ingwersen 2010b). This study will be using both uncertainty and variance terms when they apply specifically, and uncertainty when addressing both cases.

LCA has many of the same data collection limitations as energy analysis. LCA relies on models to estimate inventory items and intensity factors similar to energy analysis. Therefore it could be useful to understand how the field of LCA has incorporated uncertainty characterization (Sonnemann et al. 2003). Ingwersen has taken LCA procedures on defining uncertainty and their conclusions on the effectiveness of uncertainty calculations, and applied them to energy calculation methods, introduced below.

The collection of data and modeling in energy analyses incorporates many sources of uncertainty, classified by the EPA as parameter, model, and scenario uncertainty (Lloyd and Ries 2007, Ingwersen 2010b). Parameter uncertainty is the uncertainty in observed or measured values used in a model, i.e. the source UEV in an energy analysis. Model uncertainty arises when there is more than one model available to use for appropriate estimations of UEV – differently representing the energy driving a system because of the structure and mathematical relationships of the models. Scenario uncertainty is the uncertainty of the fit of the model parameters to geographical, temporal, or technological contexts (Ingwersen 2010b). Scenario uncertainty is inherent in the types of systems selected for this study. Researchers will actively change levels of scenario uncertainty to examine how the output is affected. When scenario uncertainty is minimized, the interaction of parameter uncertainties and their effect on the yield will be emphasized. The original systems had slightly different sources that would change the interactions in their models. However, the manipulation of model uncertainty is outside the scope of this study. There is only

one type of model used- the traditional tabular-form energy analysis with specified sources.

To estimate UEV uncertainty, Ingwersen (2010a) presented an analytic model and a stochastic model. Analytic models are deterministic models used for formula-type UEVs (calculating UEV of raw materials) while stochastic models are used for table-form UEVs (calculating UEV of products concerning the ecosystem and human activities). The analytic model is better for simpler systems because it follows mathematical formulae and requires knowing the system output distribution as well as the system inputs' distributions. Stochastic models use random number generation to select input values from an assumed probability distribution function (PDF) that then interact with other randomly chosen input values to produce an output with its own PDF. In this study the stochastic modeling approach was used because the PDF of the output was not necessarily known, or even a defined distribution, but the PDFs of the inputs could be estimated from published studies.

It is necessary to differentiate between system sources and inputs, as well as yield and output. An item that enters the crop system to interact with other items in a process that 'yields' grain will be referred to as a system 'source'. This study has defined eleven sources for the crop production system. The values that are entered in to the Monte Carlo simulations will be referred to as 'inputs'. Each source has an energy/mass input and a UEV input that is dependent on the distribution chosen. When these parameters are entered in to the Monte Carlo simulations they generate 'outputs' such as the energy value for each source.

Monte Carlo simulation

The name Monte Carlo comes from the gambling scene at the Monte Carlo Casino, Monaco for the simulation's random number generation feature. Monte Carlo simulation is a stochastic sampling method, where parameter values (e.g. inputs) are randomly generated from PDFs for multiple iterations. PDFs are often modeled on observed data, but can be developed from expert opinion (Winston 1991, Ayyub and Klir 2006). The Monte Carlo simulation method was used in this study to examine uncertainty propagation in a modeled system.

An example of how the method can be employed is in determining the life expectancy of a population, where age, weight, eating habits, and exercising habits are important inputs into the system. These inputs all interact to form a life expectancy. These inputs all have assumed PDFs, for example, the 'weight of a person' input is assumed to follow a normal PDF (Figure 1). The points in green are the weights the researchers have measured on the study participants. Monte Carlo will follow this distribution characterized by the weight mean and standard deviation, and generate the points in red to obtain more sample weights for the study.

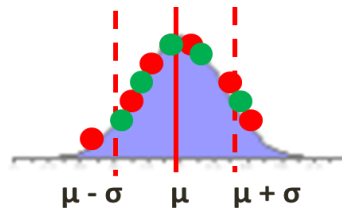


Figure 1: Monte Carlo generation of weight. A population's weight follows a normal distribution with a mean and standard deviation shown. The points in green

are the weights measured by researchers, while the red points are those generated by Monte Carlo to supplement the green.

This will be repeated for each input. The many options or values the Monte Carlo generates for each input can interact in a black box to create an output life expectancy (Figure 2). After running this model for a certain number of iterations, a PDF of the population's life expectancy can be determined. The generated data can be represented as probability distributions (or histograms) or converted to error bars, reliability predictions, tolerance zones, or confidence intervals.

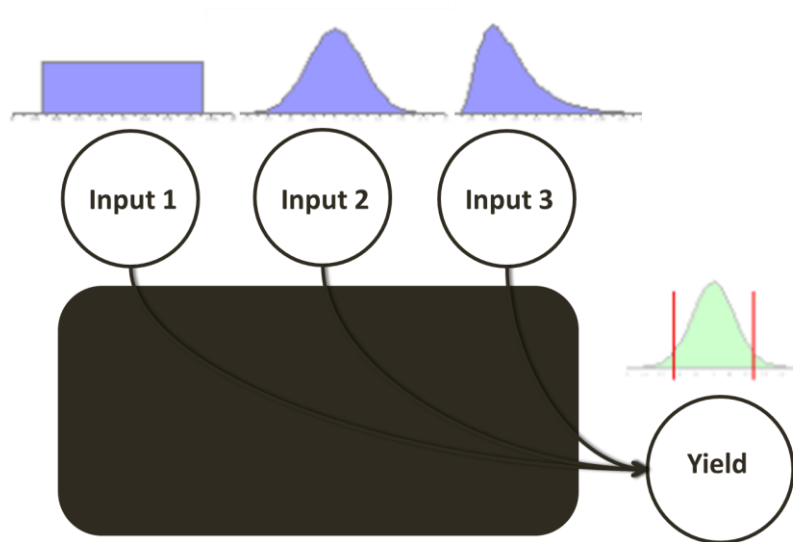


Figure 2: Stochastic uncertainty propagation. The input types are assumed to have a probability distribution (shown above the inputs in blue). The black box represents the interaction of the inputs to produce the outputs. The yields generated from the Monte Carlo simulation of the inputs are represented in a PDF and can be described using confidence intervals (i.e. the red lines intersecting the PDF).

Previous uses of Monte Carlo to simulate uncertainty in energy have employed various types of PDFs (e.g. normal, lognormal, and uniform distributions) (Campbell 2001, Cohen 2001, Limpert et al. 2001, Sonnemann et al. 2003, Brown et al. 2011). Normal distributions are used when the available input data represents the mean of data collection efforts (used in Campbell 2001, Cohen 2001, and Sonnemann et al. 2003). Uniform implies an insufficient collection of data for a more specific distribution (used in Brown et al. 2011). Lognormal PDFs (Sonnemann et al. 2003) produce all positive values and are skewed to the right. Ingwersen (2010a) cites Limpert et al. (2001) and other studies in LCA that use a lognormal PDF for all source inputs for environmental disciplines. With case studies for lead, petroleum and more UEV calculations, Ingwersen (2010a and 2010b) suggests that a lognormal CI of the original data set is the closest to the Monte Carlo generated CI when inputs are assumed to have a lognormal PDF. In this study we did not have enough systems to determine the PDFs of sources with confidence. Therefore, we ran separate Monte Carlo simulations that assumed normal, lognormal, or uniform PDFs.

Two types of models, each with a different type and amount of variation, were created for the Monte Carlo simulations. Model 1 (the energy/mass and UEV variance model) included the variance of the energy/mass input and the UEV input. Model 2 (the UEV only variance model) only included variance for the UEV input. Thus the models differed by the latter not including the variance of the energy/mass input. Simulations of the energy/mass and UEV variance model will reveal the total uncertainty due to uncertainty in both types of inputs, whereas the UEV only variance model will reveal uncertainty due to UEV inputs. Noting the differences in the output

means and variances generated by the two models will reveal the uncertainty due to energy/mass input estimates.

The Monte Carlo simulation models 1 and 2 were made to break down the uncertainty of energy analyses into energy/mass and UEV inputs. Ultimately, we will be able to say there is a 95% probability that a value within this range around the given yield UEV mean is returned. The uncertainty of the Energy/Mass and UEV inputs contributing to the total energy of a system can be broken down by the source. After removing the variance of a source from the system, the resulting confidence interval about the yield UEV mean can indicate the magnitude of the source's impact. This will aid in interpreting each source's Energy/Mass and UEV contribution to the confidence interval surrounding the mean of the yield UEV. The goal of the researcher in this study is to minimize the range of the confidence interval associated with the yield UEV.

Recent use of Monte Carlo simulation in energy analyses has highlighted the potential for incorporating uncertainties into the field. For example, many previous studies made for petroleum had one estimate for its UEV, even though analysts recognized there could be more due to several factors like plant source, geologic cycles, and geological age. Brown et al. (2011) used Monte Carlo simulation to show the uncertainty of using a singular petroleum UEV. They performed an energy analysis on the production of four types of fossil fuels: natural gas, crude oil, anthracite and bituminous coal, and sub-bituminous coal and lignite. The system sources were net primary productivity, preservation factors, and conversion efficiencies. The authors assumed a uniform distribution of the inputs based on the

minimum and maximums previously published for each input. A Monte Carlo simulation produced a mean and standard deviation for each type of fossil fuel UEV. The authors determined that the simulated UEVs were greater than fossil fuel UEVs provided in previous studies. The fossil fuel UEV increase from past calculations emphasized an increased importance of fossil fuels in human societies.

The energy community needs a transparent approach to document how uncertainty can be incorporated into an analysis to affect the estimate of a yield (specifically, the UEV of the yield). Many practitioners cite other studies in producing their own system's source UEVs, without regard to the range of values each UEV has. The tabular method's current practice is to provide singular values that actually represent a probability distribution around a mean value. The goals of this study are to present the benefits, opportunities, and necessity of incorporating uncertainty into an energy analysis, along with a framework for obtaining and presenting uncertainty results in evaluations. The framework is based on using Monte Carlo stochastic modeling with Excel and will be applied to crop production, with each step well documented. There is a need to produce uncertainties for at least a few key sources because of how much these UEVs can vary between systems and change the yield. Researchers can then calculate which sources most impact the yield UEV in terms of variance and mean value, and place more emphasis and resources on minimizing those source uncertainties. Since source uncertainties are dependent on choosing a distribution for the Monte Carlo methodology, this study attempted to outline the effect of distribution type on the output UEV. The effect of uncertainty levels included in the model was also examined. A quantitative assessment of the

variability in energy analyses of crop production systems was developed and discussed based on the model and distribution specific results.

Chapter 2: Objectives

The objective of this study was to show how to utilize random number generation effectively in table-form energy analyses of crop production systems to generate results for statistical review. This overarching objective was broken in to three questions addressed in this study.

1. Where does uncertainty originate in energy analyses, and how much uncertainty is propagated in a source's energy/mass and UEV components?
2. Which sources are more likely to influence the variance of the yield's UEV, and how much do energy/mass and UEV components of a source influence the yield UEV?
3. How does the distribution assigned to the Monte Carlo inputs impact the yield UEV variance?

Chapter 3: Plan of study

To achieve these objectives, this study investigated the energy literature on corn and wheat production systems to find systems with similar sources that have generated their own UEVs for crop production. Two models were created with different levels of variation incorporated. For each model, it was assumed that the source's energy/mass and UEV inputs follow one of the 3 distributions: normal, lognormal, or uniform. An additive system was created for each model and distribution that related the source energy values to the yield energy of crop systems. Energy output was generated with the Monte Carlo simulation for each distribution. The UEV of the output was determined by dividing the energy output by an energy constant, dependent on the distribution. Confidence intervals were constructed around the original systems' mean yield UEV for each model. Sensitivity analyses were run for each distribution on the effect of each source's variance level on the variance of the yield. Significant results were compared across the distributions and models. An increased knowledge of uncertainty propagation in crop production systems was created.

Chapter 4: Methodology

Systems descriptions

Original systems' descriptions

Crop systems (Figure 3) are useful for elucidating the source and propagation of uncertainty because of their multiple interacting sources and straight forward yield. Corn and wheat production in particular have been heavily analyzed by emergy scientists. They contain all of the common categories of sources analyzed in emergy evaluations, including renewable, locally non-renewable and purchased.

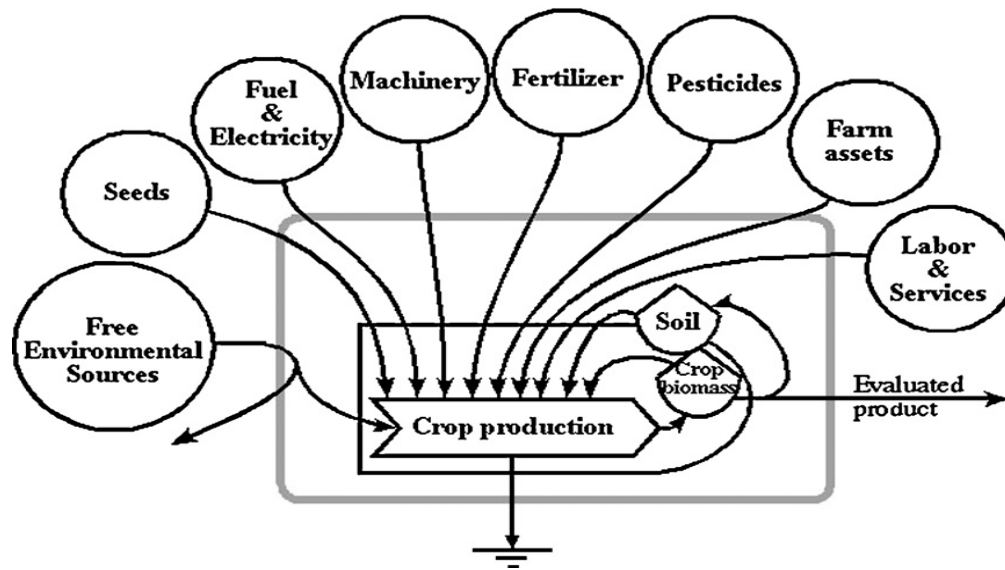


Figure 3: Simplified energy systems diagram showing the driving forces of crop production (Franzese et al. 2009) Renewable and non-renewable sources (seed, fuel and electricity, machinery, fertilizer, pesticides, farm assets, labor and services) all drive the crop production process. This production process creates a storage of crop biomass, part of which continues on to be an evaluated product. Another part of the biomass storage feeds into the soil and then into the crop production through a feedback loop.

Eight systems were identified in the emergy literature containing detailed analyses of wheat and corn crops that include calculations of their own output crop UEVs (Brandt-Williams 2002, Rodrigues et al. 2003, Lefroy and Rydberg 2003, Coppola et al. 2009, Franzese et al. 2009). Appendix i: Table 11 describes the specific systems chosen. Wheat and corn systems have similar types of sources that are used in comparable amounts. Analyzing both corn and wheat systems increased the sample size which improved the precision of probability distribution functions, while at the same time it increased the possible scenario uncertainty by adding to the locations and conditions of the harvested systems. Geographically, the systems span the globe to include the United States, Brazil, Italy, Australia, and Denmark. The temporal span covers only three years (2001 to 2004), which minimizes technological shifts in cropping practices. The studies included here as our original data set were studied to understand bioethanol production, agroforestry practices, harvesting techniques, or crop productivity in general. Three of the five papers compared two or more systems. Including more than one analysis from the same publication may have biased the Monte Carlo output obtained from those similar inputs.

Conventional and organic farming are two methods of farming that had been reported in the emergy literature. Conventional (or traditional) farming included fertilizer and/or pesticides as sources while organic systems excluded them as sources. Organic systems were removed from the list of systems studied because of the need to choose systems that had similar types of sources and relatively similar source values. In addition, the conventional farming technique was chosen for this study because it was the majority of farming systems reported in the emergy

literature. Systems with similar source types will eliminate some model uncertainty. Even limiting systems to conventional farming, the source types varied across systems. The eleven sources that were chosen for inclusion in the study were most representative of corn and wheat cropping systems (Table 3).

Table 3: Selected Sources of Corn and Wheat Cropping Systems
<i>Energy Sources:</i> Sunlight Evapotranspiration Fuel Net topsoil loss Electricity Labor
<i>Material Sources:</i> Seed Steel machinery Pesticides Phosphate (P) Fertilizer Nitrogen(N) Fertilizer

The eight observed systems were assembled to form a database. Tables were constructed for the energy/mass (Table 4a), UEV (Table 4b), and emergy (Table 4c) of each source and yield. The actual values, along with means and standard deviations summarizing the original dataset’s characteristics are shown in the Appendix ii.

Values are presented as hectare per year.

Table 4a: Energy/mass collected from eight original systems for each source (1, 2, 3,...) and yield.									
Item	Units	System							
		1	2	3	4	5	6	7	8
1	J	d ₁₁	d ₁₂	d ₁₃	d ₁₄	d ₁₅	d ₁₆	d ₁₇	d ₁₈
2	g	d ₂₁	d ₂₂	d ₂₃	d ₂₄	d ₂₅	d ₂₆	d ₂₇	d ₂₈
3	J	d ₃₁	d ₃₂	d ₃₃	d ₃₄	d ₃₅	d ₃₆	d ₃₇	d ₃₈
Yield (p)	J	d _{p1}	d _{p2}	d _{p3}	d _{p4}	d _{p5}	d _{p6}	d _{p7}	d _{p8}

Table 4b: UEV collected from eight original systems for each source (1, 2, 3,...) and yield.

Item	Units	System							
		1	2	3	4	5	6	7	8
1	sej/J	v ₁₁	v ₁₂	v ₁₃	v ₁₄	v ₁₅	v ₁₆	v ₁₇	v ₁₈
2	sej/g	v ₂₁	v ₂₂	v ₂₃	v ₂₄	v ₂₅	v ₂₆	v ₂₇	v ₂₈
3	sej/J	v ₃₁	v ₃₂	v ₃₃	v ₃₄	v ₃₅	v ₃₆	v ₃₇	v ₃₈
Yield (p)	sej/J	v _{p1}	v _{p2}	v _{p3}	v _{p4}	v _{p5}	v _{p6}	v _{p7}	v _{p8}

Table 4c: Emery found by multiplying corresponding cells in Table 4a and Table 4b.

Item	Units	System							
		1	2	3	4	5	6	7	8
1	sej	m ₁₁	m ₁₂	m ₁₃	m ₁₄	m ₁₅	m ₁₆	m ₁₇	m ₁₈
2	sej	m ₂₁	m ₂₂	m ₂₃	m ₂₄	m ₂₅	m ₂₆	m ₂₇	m ₂₈
3	sej	m ₃₁	m ₃₂	m ₃₃	m ₃₄	m ₃₅	m ₃₆	m ₃₇	m ₃₈
Yield (p)	sej	m _{p1}	m _{p2}	m _{p3}	m _{p4}	m _{p5}	m _{p6}	m _{p7}	m _{p8}

Partitioning of variance for the original systems

The sum of squared standard deviations was calculated to determine the relative contribution of each source’s variance (var_i) to both the system variance (var_{sys}) and the total source variance (var_{sum}).

The emery standard deviation for each source was squared, finding the emery variance for each source (var_i). These variances were summed to find the total variance of the sources (var_{sum}). The total system variance is the uncertainty present in the entire system and is the square of the yield emery standard deviation (var_{sys}). Total source variance (var_{sum}) is different from the system variance of the yield emery (var_{sys}) because of the added uncertainty in the yield energy and yield UEV that contribute to the system variance of the yield emery (var_{sys}). The percent difference between the total source variance and the total system variance ($[var_{sys} -$

$\text{var}_{\text{sum}}] / \text{var}_{\text{sys}}$) is the uncertainty that is unexplained by the sources, (scenario uncertainty). The uncertainty explained by the sources (parameter uncertainty) was found by dividing the total source variance by the total system variance ($\text{var}_{\text{sum}} / \text{var}_{\text{sys}}$).

The percentage that each source contributed to the total variance of the sources was recorded ($\text{var}_i / \text{var}_{\text{sum}}$). The percentage that each source contributed to the total system variance was also recorded ($\text{var}_i / \text{var}_{\text{sys}}$).

The uncertainty of the yield energy was not included in the Monte Carlo models. Therefore the total source variance (var_{sum}) was more representative of the uncertainty captured by the Monte Carlo models than the total system variance (var_{sys}). To further understand the original systems and their sources, an emergy signature was created based on the UEV and emergy tables shown above.

Emergy signature of original systems

Emergy signatures are traditionally created to visualize a system in terms of the nature of the sources driving the system. The sources are ordered along the x-axis in increasing emergy per unit, with the emergy values shown on the y-axis. If the graph is weighted towards the left, the system relies more on renewable sources, versus a system whose sources' emergy magnitudes are clustered to the right. Conventionally, emergy signature graphs are used to compare multiple systems and the nature of their sources.

The emergy signature method was used in this study to compare the sources within the average crop production system. The current study combined the eight original systems to produce average emergy values for each source, along with their

standard deviations. The sources were broken in to energy and material sources and ordered by increasing transformity and specific energy. For example, labor had the largest transformity and nitrogen fertilizer had the largest specific energy. The energy signature graph was analyzed based on the UEV, energy mean, and energy standard deviation of each source. These three features may influence the source's effect on the yield UEV. The source with the largest of each characteristic was hypothesized to have the largest impact on the output UEV. The sources with the largest impact would have the largest transformity or specific energy values, with the largest energy values on the y axis and the largest standard deviations.

Another energy signature graph was made that placed the sources' variances and energy values in context with the eight original systems' output. These graphs describing the original systems were later combined with the Monte Carlo generated systems for Model 1 and 2. Each distribution for the two models was compared to the original eight systems in an energy signature graph to identify prominent discrepancies or tendencies.

Monte Carlo simulations

The values of the sources were related to the yield of crop production systems using a table-form analysis. There were assumed to be no interactions between sources in the production process. The Monte Carlo simulation generated energy output values for multiple input values selected from a distribution (Figure 4).

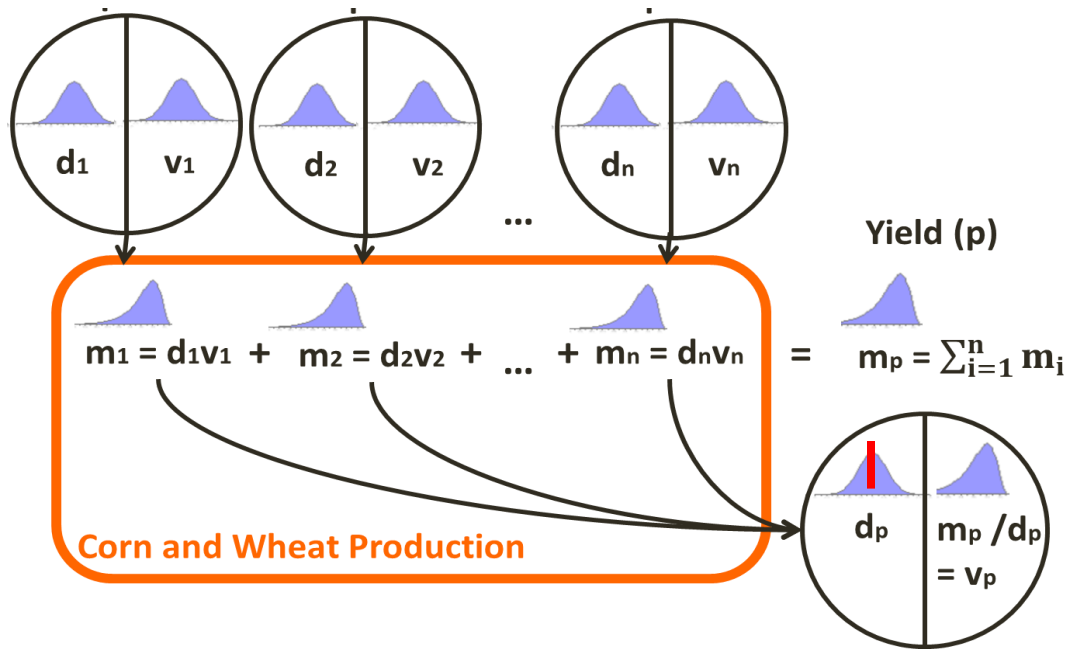


Figure 4: Stochastic uncertainty propagation in corn and wheat production.

Assuming Model 1. For each of the n sources, Monte Carlo simulation has generated energy/mass (d) and UEV (v) inputs. There is an assumption that the inputs follow a normal distribution (shown above the energy/mass and UEVs in blue). Energy is the product of the source's energy/mass and UEV. The energy values (m) are combined to produce the energy of the output, for which a PDF is developed. The energy values are then divided by an energy constant (in red) based on the normal distribution, to produce the PDF of the output UEV.

In order to generate input values, the Monte Carlo method required defining characteristics of an input's parent population. Two models were run in the Monte Carlo simulations for each input distribution. Model 1 included energy/mass variance (Figure 4), whereas Model 2 eliminated energy/mass variance. As such, there were different Monte Carlo inputs and generated outputs for each model and distribution.

Based on the type of distribution (normal, lognormal, or uniform) of the inputs' characteristics and a random number representing a probability distribution, the Model 1 Monte Carlo simulation generated energy/mass and UEV for inputs. The Model 2 Monte Carlo simulation generated only UEVs. The energy value for each source was found by multiplying together the source's energy/mass and UEV. The energy from each source was summed, giving the total energy. The UEV of the output was found by dividing the total energy by the energy yield, which was taken as a constant (i.e., non-random variable). By choosing a constant energy output instead of generating an estimate with Monte Carlo, the uncertainty of the model was isolated to the inputs. The energy output constant value was assumed to be a value that represented the majority of energy output studied in the original eight systems. Since each distribution shifts where the observations are clustered, the energy constant was determined to be dependent on the distribution type.

The methodology of the Monte Carlo simulations that varied for each model and distribution are described below in more detail. They are broken up by distribution into Monte Carlo Inputs and Monte Carlo Outputs.

Normal distribution

The normal distribution was used in determining crop production systems' uncertainty with the assumptions that there was a large enough sample size and the samples were distributed symmetrically about the mean of the samples.

Model 1: Energy/Mass and UEV Variance

- **Monte Carlo Inputs-**

There were 5 inputs that are fed in to the Monte Carlo simulation for the normal distribution. Equation 1.1 showed the arithmetic mean of the energy/mass input (d_{μ_i}) for the i^{th} source given the original eight systems.

$$1. \quad d_{\mu_i} = \frac{d_{i1} + d_{i2} + \dots + d_{iN}}{N} \quad 1.1$$

N was the total number of original systems with that source. Not every system studied had a value for each input, so N varied between sources. Equation 1.2 showed the sample standard deviation of the energy/mass input (d_{σ_i}) for the i^{th} source.

$$2. \quad d_{\sigma_i} = \sqrt{\frac{1}{N-1} * \sum_{k=1}^N (d_{ik} - d_{\mu_i})^2} \quad 1.2$$

k stood for the k^{th} original system with the value 1 to 8. Equation 1.3 showed the arithmetic mean of the UEV input (v_{μ_i}) for the i^{th} source given the original eight systems.

$$3. \quad v_{\mu_i} = \frac{v_{i1} + v_{i2} + \dots + v_{iN}}{N} \quad 1.3$$

N was the total number of original systems with that source. Not every system studied had a value for each input, so N varied between sources. Equation 1.4 showed the sample standard deviation of the UEV input (v_{σ_i}) for the i^{th} source.

$$4. \quad v_{\sigma_i} = \sqrt{\frac{1}{N-1} * \sum_{k=1}^N (v_{ik} - v_{\mu_i})^2} \quad 1.4$$

k stood for the k^{th} original system with the value 1 to 8.

5. j was a number from 0 to 1 that had been selected randomly, following a uniform distribution. The Excel code was

$$j = rand().$$

- **Monte Carlo Outputs-**

The Monte Carlo simulation produced 4 outputs for the normal distribution. Equation 2.1a returned the inverse of the normal cumulative distribution function of the energy/mass input for the i^{th} source.

$$1. \quad d_i = \text{norm.inv}(j, d_{\mu_i}, d_{\sigma_i}) \quad 2.1a$$

Equation 2.2 returned the inverse of the normal cumulative distribution function of the UEV for the i^{th} source given the three parameters described (a random number j , the arithmetic mean of the UEV input v_{μ_i} , and the sample standard deviation of the UEV input v_{σ_i}).

$$2. \quad v_i = \text{norm.inv}(j, v_{\mu_i}, v_{\sigma_i}) \quad 2.2$$

Equation 2.3 calculated the i^{th} source's emergy (m_i) and was found by multiplying the Monte Carlo generated energy/mass (d_i) by the Monte Carlo generated UEV (v_i) for that source.

$$3. \quad m_i = d_i * v_i \quad 2.3$$

This was repeated for each of the 11 sources. Equation 2.4 calculated the emergy of the output (m_p) and was the summation of the emergy of the 8 original systems for each source i .

$$4. \quad m_p = \sum_{k=1}^8 m_{ik} \quad 2.4$$

Equation 2.5 calculated the output UEV (v_p) and was found by dividing the output energy (m_p) by the output energy (d_p).

$$5. \quad v_p = \frac{m_p}{d_p} \quad 2.5$$

Equation 2.5 calculated the output energy (d_p) and was equal to the arithmetic mean of the energy of the original eight systems (d_{μ_p}).

$$\bullet \quad d_p = d_{\mu_p} \quad 2.6a$$

d_p was thus a constant rather than a random variable in the Monte Carlo simulations.

Model 2: Energy/Mass and UEV Variance

- **Monte Carlo Inputs-**

There were 4 inputs to the Monte Carlo simulation for Model 2 of the normal distribution. Model 1 included the variance of the energy/mass input ($d_{\sigma i}$) for each input, but Model 2 excluded this Monte Carlo simulation input. Equation 1.1 calculated the arithmetic mean of the energy/mass input ($d_{\mu i}$) for the i^{th} source given the original eight systems.

$$1. \quad d_{\mu i} = \frac{d_{i1} + d_{i2} + \dots + d_{iN}}{N} \quad 1.1$$

N was the total number of original systems with that source. Not every system studied had a value for each input, so N varied between sources. Equation 1.3

calculated the arithmetic mean of the input UEV ($v_{\mu i}$) for the i^{th} source given the original eight systems.

$$2. \quad v_{\mu i} = \frac{v_{i1} + v_{i2} + \dots + v_{iN}}{N} \quad 1.3$$

N was the total number of original systems with that input. Not every system studied had a value for each input, so N varied between inputs. Equation 1.4 calculated the sample standard deviation of the input UEV ($v_{\sigma i}$) for the i^{th} source.

$$3. \quad v_{\sigma i} = \sqrt{\frac{1}{N-1} * \sum_{k=1}^N (v_{ik} - v_{\mu i})^2} \quad 1.4$$

k stood for the k^{th} original system with the value 1 to 8.

4. j was a number from 0 to 1 that had been selected randomly, following a uniform distribution. The Excel code was

$$j = rand().$$

- **Monte Carlo Outputs-**

There were 5 outputs that were produced by the Monte Carlo simulation for Model 2 of the normal distribution. In Model 2 the energy/mass for each source (d_i) was the arithmetic average of the original systems for that source ($d_{\mu i}$) and thus was a constant rather than a random variable in the Monte Carlo simulations. This was shown in equation 2.1b.

$$1. \quad d_i = d_{\mu i} \quad 2.1b$$

Equation 2.2 returned the inverse of the normal cumulative distribution function of the UEV for the i^{th} source given the three parameters described (a random number j , the arithmetic mean of the UEV input v_{μ_i} , and the sample standard deviation of the UEV input v_{σ_i}).

$$2. \quad v_i = \text{norm.inv}(j, v_{\mu_i}, v_{\sigma_i}) \quad 2.2$$

Equation 2.3 calculated the i^{th} source's energy (m_i) found by multiplying the Monte Carlo generated energy/mass (d_{μ_i}) by the Monte Carlo generated UEV (v_i) for that source.

$$3. \quad m_i = d_{\mu_i} * v_i \quad 2.3$$

This was repeated for each of the 11 sources. Equation 2.4 calculated the energy of the output (m_p) as the summation of the energy of the 8 original systems for each source i .

$$4. \quad m_p = \sum_{k=1}^8 m_{ik} \quad 2.4$$

Equation 2.5 calculated the output UEV (v_p) by dividing the output energy (m_p) by the output energy (d_p).

$$5. \quad v_p = \frac{m_p}{d_p} \quad 2.5$$

$$\bullet \quad d_p = d_{\mu_p} \quad 2.6a$$

The output energy (d_p) was equal to the arithmetic mean of the energy of the original eight systems (d_{μ_p}) and thus was a constant rather than a random variable in the Monte Carlo simulations.

When the Monte Carlo simulation generated negative values, the negative values were taken out of the sample, lowering the sample sizes. The normal distribution's left tail extends to negative infinity, but it is impossible to have negative energy, mass, or unit energy value. The normally distributed inputs and outputs had different sample sizes.

Lognormal distribution

The lognormal distribution was used to generate crop production systems' uncertainty with the assumptions that there are only positive energy values for each input, and these values are large.

To run the Monte Carlo simulation for a lognormally distributed input, the inverse of the lognormal cumulative distribution function was needed. $\ln(B)$ was assumed to be normally distributed with parameters μ (the mean of $\ln(B)$) and σ (the standard deviation of $\ln(B)$). σ^2 was the variance of $\ln(B)$.

$$\ln(B) \sim N(\mu, \sigma) \quad 3.1$$

The mean (μ_B) and variance (σ_B^2) of B were then computed (Ayyub and Klir 2006)

$$\mu_B = e^{(\mu + \frac{1}{2}\sigma^2)} \quad 3.2$$

$$\sigma_B^2 = \mu_B^2 (e^{\sigma^2} - 1) \quad 3.3$$

These functions were then inverted, solving for μ and σ^2

$$\sigma^2 = \ln\left(1 + \left(\frac{\sigma_B}{\mu_B}\right)^2\right) \quad 3.4$$

$$\sigma = \sqrt{\ln\left(1 + \left(\frac{\sigma_B}{\mu_B}\right)^2\right)} \quad 3.5$$

$$\mu = \ln(\mu_B) - \frac{1}{2}\sigma^2 \quad 3.6$$

In applying these formulas to the distinct generation of energy/mass and UEVs, equations 3.1-3.6 were modified. d_B was used to symbolize energy/mass that was lognormally distributed, while v_B was used to symbolize UEVs that are lognormally distributed. They have been substituted for B seen in equation 3.1 in the following equations.

$$\ln(d_B) = N(d_\mu, d_\sigma) \text{ and } \ln(v_B) = N(v_\mu, v_\sigma) \quad 4.1$$

The symbols for the energy/mass mean d_μ and the energy/mass standard deviation d_σ signify the characteristics of a normal distribution. This was the same for the UEV symbols.

$$d_{\mu Bi} = e^{(d_{\mu i} + \frac{1}{2}d_{\sigma i}^2)} \quad 4.2$$

The normally distributed energy/mass mean $d_{\mu i}$ and normally distributed energy/mass standard deviation $d_{\sigma i}$ for each source i was distinguished from the lognormally distributed energy/mass mean $d_{\mu Bi}$ and lognormally distributed energy/mass standard deviation $d_{\sigma Bi}$ for each source i .

$$d_{\sigma^2 Bi} = (d_{\mu Bi})^2 (e^{d_{\sigma i}^2} - 1) \quad 4.3$$

In this set of simulations, the inputs were assumed to follow a lognormal distribution. The $d_{\mu Bi}$ and $d_{\sigma Bi}$ for each source were defined as the energy/mass mean and standard deviation for each source of the original eight systems. The inverses of $d_{\mu Bi}$ and $d_{\sigma Bi}$ ($d_{\mu i}$ and $d_{\sigma i}$) were then the actual inputs used in the Monte Carlo simulations.

$$v_{\mu Bi} = e^{(v_{\mu i} + \frac{1}{2}v_{\sigma i}^2)} \quad 4.4$$

The normally distributed UEV mean $v_{\mu i}$ and normally distributed UEV standard deviation $v_{\sigma i}$ for each source i was distinguished from the lognormally distributed UEV mean $v_{\mu Bi}$ and lognormally distributed UEV standard deviation $v_{\sigma Bi}$ for each source i .

$$v_{\sigma^2 Bi} = (v_{\mu Bi})^2 (e^{v_{\sigma^2 i}} - 1) \quad 4.5$$

The inputs were assumed to follow a lognormal distribution. The $v_{\mu Bi}$ and $v_{\sigma Bi}$ for each source were defined as the UEV mean and standard deviation for each source of the original eight systems. The inverses of $v_{\mu Bi}$ and $v_{\sigma Bi}$ ($v_{\mu i}$ and $v_{\sigma i}$) were then the actual inputs used in the Monte Carlo simulations.

Model 1: Energy/Mass and UEV Variance

- **Monte Carlo Inputs**

There were 5 inputs that were fed in to the Monte Carlo simulation for Model 1's lognormal distribution. Equation 5.1 calculated the energy/mass mean for each source i ($d_{\mu i}$).

$$1. \quad d_{\mu i} = \ln(d_{\mu Bi}) - \frac{1}{2} d_{\sigma^2 Bi} \quad 5.1$$

Equation 5.2 calculated the energy/mass standard deviation for each source i ($d_{\sigma i}$).

$$2. \quad d_{\sigma i} = \sqrt{\ln \left(1 + \left(\frac{d_{\sigma Bi}}{d_{\mu Bi}} \right)^2 \right)}$$

Equation 5.3 calculated the UEV mean for each source i ($v_{\mu i}$).

$$3. \quad v_{\mu i} = \ln(v_{\mu Bi}) - \frac{1}{2} v_{\sigma Bi}^2 \quad 5.3$$

Equation 5.4 calculated the UEV standard deviation for each source i ($v_{\sigma i}$).

$$4. \ v_{\sigma_i} = \sqrt[2]{\ln\left(1 + \left(\frac{v_{\sigma_{Bi}}}{v_{\mu_{Bi}}}\right)^2\right)} \quad 5.4$$

5. j was a number from 0 to 1 that had been selected randomly, following a uniform distribution. The Excel code was
- $$j = rand().$$

- **Monte Carlo Outputs**

There were 5 outputs that were produced by the Monte Carlo simulation for Model 2 of the normal distribution.

$$1. \ d_i = \text{lognorm.inv}(j, d_{\mu_i}, d_{\sigma_i}) \quad 6.1a$$

Equation 6.1a returned the inverse of the lognormal cumulative distribution function of the energy/mass input for the i^{th} source given the three parameters described above (a random number j , the arithmetic mean of the energy/mass input d_{μ_i} , and the sample standard deviation of the energy/mass input d_{σ_i}).

$$2. \ v_i = \text{lognorm.inv}(j, v_{\mu_i}, v_{\sigma_i}) \quad 6.2$$

Equation 6.2 returned the inverse of the lognormal cumulative distribution function of the UEV for the i^{th} source given the three parameters described above (a random number j , the arithmetic mean of the UEV v_{μ_i} , and the sample standard deviation of the UEV v_{σ_i}). In equation 2.3 the i^{th} source's energy (m_i) was found by multiplying the Monte Carlo generated energy/mass (d_{μ_i}) by the Monte Carlo generated UEV (v_i) for that source.

$$3. \quad m_i = d_{\mu_i} * v_i \quad 2.3$$

This was repeated for each of the 11 sources.

$$4. \quad m_p = \sum_{k=1}^8 m_{ik} \quad 2.4$$

Equation 2.4 calculated the energy of the output (m_p) is the summation of the energy of the 8 original systems for each source i .

$$5. \quad v_p = \frac{m_p}{d_p} \quad 2.5$$

Equation 2.5 calculated the output UEV (v_p) by dividing the output energy (m_p) by the output energy/mass (d_p).

- d_p = geometric mean of the eight original system yields

$$d_i = d_{\mu_{geoP}} = \sqrt[8]{\prod_{k=1}^8 d_{pk}} = \sqrt[8]{d_{p1} * d_{p2} * d_{p3} * d_{p4} * d_{p5} * d_{p6} * d_{p7} * d_{p8}} \quad 2.6b$$

The output energy/mass (dp) was equal to the geometric mean of the energy/mass of the original eight systems ($d_{\mu_{geoP}}$) and thus was a constant rather than a random variable in the Monte Carlo simulations.

Model 2: UEV Variance

- **Monte Carlo Inputs**

There were 5 inputs that were fed in to the Monte Carlo simulation for Model 2 of the lognormal distribution.

$$1. \quad d_{\mu_i} = \ln(d_{\mu_{Bi}}) - \frac{1}{2} d_{\sigma^2_{Bi}} \quad 5.1$$

Equation 5.1 calculated the energy/mass mean for each source i ($d_{\mu i}$).

$$2. \quad d_{\sigma_i} = \sqrt{\ln \left(1 + \left(\frac{d_{\sigma_{Bi}}}{d_{\mu_{Bi}}} \right)^2 \right)} \quad 5.2$$

Equation 5.2 calculated the energy/mass standard deviation for each source i (d_{σ_i}).

$$3. \quad v_{\mu_i} = \ln(v_{\mu_{Bi}}) - \frac{1}{2} v_{\sigma_{Bi}}^2 \quad 5.3$$

Equation 5.3 calculated the UEV mean for each source i ($v_{\mu i}$).

$$4. \quad v_{\sigma_i} = \sqrt{\ln \left(1 + \left(\frac{v_{\sigma_{Bi}}}{v_{\mu_{Bi}}} \right)^2 \right)} \quad 5.4$$

Equation 5.4 calculated the UEV standard deviation for each source i (v_{σ_i}).

5. j was a number from 0 to 1 that had been selected randomly, following a uniform distribution. The Excel code was $j = rand()$.

- **Monte Carlo Outputs**

1. d_i was defined in equation 6.1b as the geometric mean of the eight original systems for the i^{th} source. k represented one of the original eight systems.

$$d_i = d_{\mu_{gsoi}} = \sqrt[8]{\prod_{k=1}^8 d_{ik}} = \sqrt[8]{d_{i1} * d_{i2} * d_{i3} * d_{i4} * d_{i5} * d_{i6} * d_{i7} * d_{i8}}$$

6.1b

2. Equation 6.2 generated v_i for the i^{th} source

$$v_i = \text{lognorm.inv}(j, v_{\mu_i}, v_{\sigma_i}) \quad 6.2$$

Equation 6.2 returned the inverse of the lognormal cumulative distribution function of the UEV for the i^{th} source given the three parameters described above (a random number j , the arithmetic mean of the UEV v_{μ_i} , and the sample standard deviation of the UEV v_{σ_i}).

$$3. \quad m_i = d_{\mu_i} * v_i \quad 2.3$$

In equation 2.3 the i^{th} source's energy (m_i) was found by multiplying the Monte Carlo generated energy/mass (d_{μ_i}) by the Monte Carlo generated UEV (v_i) for that source. This was repeated for each of the 11 sources.

$$4. \quad m_p = \sum_{k=1}^8 m_{ik} \quad 2.4$$

Equation 2.4 calculated the energy of the output (m_p) to be the summation of the energy of the 8 original systems for each source i .

$$5. \quad v_p = \frac{m_p}{d_p} \quad 2.5$$

Equation 2.5 calculated the output UEV (v_p) by dividing the output energy (m_p) by the output energy/mass (d_p).

- $d_p =$
- **geometric mean of the eight original system outputs**

$$d_i = d_{\mu_{geoP}} = \sqrt[8]{\prod_{k=1}^8 d_{pk}} = \sqrt[8]{d_{p1} * d_{p2} * d_{p3} * d_{p4} * d_{p5} * d_{p6} * d_{p7} * d_{p8}}$$

2.6b

The output energy/mass (d_p) was equal to the geometric mean of the energy/mass of the original eight systems ($d_{\mu_{geoP}}$) and thus was a constant rather than a random variable in the Monte Carlo simulations. The geometric mean was used over the arithmetic mean because it is less influenced by the larger samples.

Uniform distribution

A uniform distribution was used to represent each input's probability distribution that then interact to produce output uncertainty for crop systems.

Model 1: Energy/Mass and UEV Variance

- **Monte Carlo Inputs**

There were 5 inputs that were fed in to the Monte Carlo simulation for Model 1 of the uniform distribution.

1. $d_{i_{min}}$ 7.1

Equation 7.1 calculated the minimum energy/mass value of the original eight systems for the i^{th} source.

2. $d_{i_{max}}$ 7.2

Equation 7.2 calculated the maximum energy/mass value of the original eight systems for the i^{th} source.

$$3. \ v_{i_{min}} \qquad 7.3$$

Equation 7.3 calculated the minimum UEV value of the original eight systems for the i^{th} source.

$$4. \ v_{i_{max}} \qquad 7.4$$

Equation 7.4 calculated the maximum energy/mass value of the original eight systems for the i^{th} source.

$$5. \ j$$

j was a number from 0 to 1 that had been selected randomly, following a uniform distribution. The Excel code was $j = rand()$

- **Monte Carlo Outputs**

This study used an equation where a probability returned a value from the specified the uniform distribution. The uniform distribution used the minimum (a) and maximum (b) values of the 8 systems studied in addition to the randomly generated probability mentioned in the normal and lognormal distributions. Every sample (x) from a uniformly distributed population had an equal probability of occurrence (P_x), which was equal to the difference between the sample and the minimum divided by the difference between the maximum and minimum.

$$P_x = \frac{(x - a)}{(b - a)} \qquad 8.1$$

To generate that sample's value, the equation was then solved for x :

$$x = P_x * (b - a) + a \qquad 8.2$$

These variables were then transformed into the energy/mass and UEV terms previously employed and placed as outputs of the Monte Carlo simulation. There were a total of 5 outputs for Model 1 of the uniform distribution.

$$1. \quad d_i = j * (d_{i_{max}} - d_{i_{min}}) + d_{i_{min}} \quad 8.3a$$

Equation 8.3a calculated the energy/mass value for the i^{th} source.

$$2. \quad v_i = j * (v_{i_{max}} - v_{i_{min}}) + v_{i_{min}} \quad 8.4$$

Equation 8.4 calculated the UEV value for the i^{th} source.

$$3. \quad m_i = d_{\mu_i} * v_i \quad 2.3$$

Equation 2.3 found the i^{th} source's energy (m_i) by multiplying the Monte Carlo generated energy/mass (d_{μ_i}) by the Monte Carlo generated UEV (v_i) for that source.

This was repeated for each of the 11 sources.

$$4. \quad m_p = \sum_{k=1}^8 m_{ik} \quad 2.4$$

Equation 2.4 calculated the energy of the output (m_p) as the summation of the energy of the 8 original systems for each source i .

$$5. \quad v_p = \frac{m_p}{d_p} \quad 2.5$$

Equation 2.5 found the output UEV (v_p) by dividing the output energy (m_p) by the output energy/mass (d_p).

$$\bullet \quad d_p = \frac{d_{p_{min}} + d_{p_{max}}}{2} \quad 2.6c$$

Equation 2.6c found the uniform distribution's energy output constant to be the arithmetic mean of the maximum and minimum of the eight original systems' output.

Model 2: UEV Variance

- **Monte Carlo Inputs**

There were 5 inputs that were fed in to the Monte Carlo simulation for Model 2 of the uniform distribution. These were the same inputs fed in to Model 1.

1. $d_{i_{min}}$ 7.1

Equation 7.1 calculated the minimum energy/mass value of the original eight systems for the i^{th} source.

2. $d_{i_{max}}$ 7.2

Equation 7.2 calculated the maximum energy/mass value of the original eight systems for the i^{th} source.

3. $v_{i_{min}}$ 7.3

Equation 7.3 calculated the minimum UEV value of the original eight systems for the i^{th} source.

4. $v_{i_{max}}$ 7.4

Equation 7.4 calculated the maximum energy/mass value of the original eight systems for the i^{th} source.

5. j

j was a number from 0 to 1 that has been selected randomly, following a uniform distribution. The Excel code was $j = rand()$.

- **Monte Carlo Outputs**

There were 4 outputs that were fed in to the Monte Carlo simulation for Model 2 of the uniform distribution. These varied from Model 1 in that the energy/mass variance has been removed from the simulation.

$$1. \quad d_i = \frac{d_{i_{min}} + d_{i_{max}}}{2} \quad 8.3b$$

Model 2 kept the energy/mass of the i^{th} source as the arithmetic mean of the maximum and minimum values for the original eight systems, shown in equation 8.3b.

$$2. \quad v_i = j * (v_{i_{max}} - v_{i_{min}}) + v_{i_{min}} \quad 8.4$$

Equation 8.4 calculated the UEV value for the i^{th} source.

$$3. \quad m_i = d_{\mu_i} * v_i \quad 2.3$$

Equation 2.3 calculated the i^{th} source's energy (m_i) by multiplying the Monte Carlo generated energy/mass (d_{μ_i}) by the Monte Carlo generated UEV (v_i) for that source.

This was repeated for each of the 11 sources.

$$4. \quad m_p = \sum_{k=1}^8 m_{ik} \quad 2.4$$

Equation 2.4 calculated the energy of the output (m_p) as the summation of the energy of the 8 original systems for each source i .

$$5. \quad v_p = \frac{m_p}{d_p} \quad 2.5$$

Equation 8.4 calculated the output UEV (v_p) by dividing the output energy (m_p) by the output energy/mass (d_p).

$$\bullet \quad d_p = \frac{d_{pmin} + d_{pmax}}{2} \quad 2.6c$$

Equation 2.6c calculated the uniform distribution's energy output constant as the arithmetic mean of the maximum and minimum of the eight original systems' output.

Model Comparison

Confidence intervals surrounding the yield UEV were constructed for different levels of uncertainty present in the models. These confidence intervals quantified how much removing different system sources of uncertainty could impact the yield UEV's variance. The process began with partitioning the energy variance using sums of squares for the normal PDF simulation as outlined in the previous methodology for the original systems. The coefficient of variation (COV) for the yield UEV was then calculated. By combining these methodologies, the sources of uncertainty were visible and were compared across the energy/mass + UEV variance, UEV only variance, and energy/mass only variance models.

The Monte Carlo simulation generated an energy and a UEV value for each crop system source which were multiplied together to obtain an energy value for each source. The standard deviations of the source energy values were squared to find the variance. The variance of each source was then divided by the sum of the variances for all the sources.

$$C_i = \frac{\sigma^2_i}{\sum_{k=1}^{11} \sigma^2_k} \quad 9.1$$

C_i in Equation 9.1 showed what percent each i^{th} source contributed to the combined source variance. This is written in the previous section as $\text{var}_i / \text{var}_{\text{sum}}$

The coefficient of variation (COV) of the emergy yield p was used to calculate the confidence interval. The COV was different dependent on the model. The coefficient of variation is a measure of dispersion of a normal probability distribution, equal to the standard deviation divided by the mean (Winston 1991).

$$COV_p = \frac{\sigma_p}{\mu_p} \quad 9.2$$

The emergy output COV was then multiplied by 2 because the mean plus and minus 2 standard deviations covers 95% of the area under the normal probability distribution curve (Winston 1991).

$$COV_{p95\%} = \frac{2 * \sigma_p}{\mu_p} \quad 9.3$$

Equation 9.3 was then multiplied by equation 9.1 to produce equation 9.4.

$$Y_i = \frac{2 * \sigma_p}{\mu_p} * \frac{\sigma^2_i}{\sum_{k=1}^{11} \sigma^2_k} \quad 9.4$$

The yield emergy mean and variance is the same as the yield UEV mean and variance multiplied by a constant. It was then possible to use the percentage Y_i from equation 9.4 to construct 95% confidence intervals around the mean yield UEV. This methodology was conducted on the normal distribution for both models. Then Model 2 was subtracted from Model 1 to obtain the energy/mass only variance model. The upper confidence interval was the mean output UEV plus Y_i times the mean output UEV. The lower confidence interval was the mean output UEV minus Y_i times the mean output UEV.

The effect the greatest sources of variance in the system had on the confidence interval was also visualized. The greatest sources of uncertainty were determined from the magnitude of their percent contribution to the total uncertainty. The new confidence intervals were formed after removing the greatest sources of uncertainty from Y_i .

Visual summary of Monte Carlo simulations

In determining where uncertainty originates in emergy analyses, frequency graphs were made using the Monte Carlo simulations to best visually show the resulting output distribution and each input's distribution. The curvature of each source's emergy PDF was dependent on the distribution of the input's energy/mass and UEVs. Each simulation generated 100 iterations, which were grouped into bins. Bin selection methodology suggests that there are at least 1 to 5 values in each bin (Winston, 1991). Splitting the 100 iterations into 5 bins allowed for at least 5 values in each bin for the output UEV. With the bin number 5, frequency distributions were created by grouping values into 5 bins using the minimum and maximum output values and size steps of 1/5 the range.

Once the bin number was selected and the methodology for splitting the iterations into bins conducted, a table for each source and yield was created, for a total of 12 tables. Each table showed graphs for models 1 and 2, the normal, lognormal, and uniform distributions, and the energy/mass, UEV and emergy, for a total of 18 graphs for each table. Placing the graphs in close proximity allowed for direct comparisons. The energy/mass differences were shown between models and

distributions. The UEV differences were shown between models and distributions. The energy differences were shown between models and distributions.

The methodology for graphically representing each Monte Carlo input and output's variance and curvature has been described. The generated graphs allowed for visual comparison between models and distributions. We will now focus on minimizing each source's variance and measuring the impact on the output in terms of variance and mean shift, for each model and distribution.

Sensitivity analysis

In energy analyses, emphasis should be placed on the collection of data for the sources that have the largest impact on the output UEV mean and variance. A sensitivity analysis was conducted for each model and distribution to determine which sources influenced the mean and the variance of the output UEV. For Model 1, the variance of the energy/mass and the UEV of 1 source were minimized, while the other sources energy/mass and UEVs were allowed to fluctuate for 100 iterations. Monte Carlo simulation generated output, which was titled under the name of the source whose energy/mass and UEV variance had been minimized. A baseline output was generated that allowed each source's energy/mass and UEV to fluctuate based on their variance. The baseline for Model 1 allowed every source's energy/mass and UEV to fluctuate and the resulting output UEV was recorded. The new Monte Carlo output was then compared to the Model 1 baseline to test whether that source had a significant impact on the mean or variation of the output UEV. This was repeated for each source. A table was created showing the percent difference of each generated output to the baseline.

% difference = $100 * (\text{the generated output value} - \text{the baseline value}) / \text{the baseline value}$

9.1

Since the percent difference was found (partly) by subtracting the baseline value from the generated output value, the sign of the resulting percent difference indicated whether the generated output value was larger (+) or smaller (-) than the baseline value. This was useful in a speedy analysis of which sources lowered the variance of the output UEV.

Another baseline was created for Model 2. The baseline for Model 2 kept the energy/mass values of each source constant while the UEV values were allowed to fluctuate and the resulting output UEV was recorded. Since the energy/mass was set constant for each source, only the UEV was minimized for one source at a time while the other source's UEVs were allowed to fluctuate.

The Student's t-test and the f-test were used to test for significant differences in mean and variation for each source's effect on the output for Models 1 and 2 and each distribution, respectively. The null hypothesis tested by the Student's t-Test was that the output produced by each source's variance being individually minimized was from the same underlying population, with the same mean, as the original Monte Carlo output. The test was set up as two samples with unequal variance (heteroscedastic) and a two-tailed distribution was used because if the source's variance is minimized, the mean could possibly shift to the left or right. When reviewing the results for significance, the alpha value of 0.05 was selected because of the convention of reporting a 95% confidence interval (Campbell 2001; Sonnemann

et al. 2003). A significant p -value ($\alpha \leq 0.05$) showed that when the variance of a source is minimized on an individual basis, the mean of the generated output differs significantly from the original output. The null hypothesis the f-Test tested was that the output produced by each source being minimized in their variance was from the same population, with the same variance, as the original output. A significant p -value ($\alpha \leq 0.05$) implied that the lowered source variance changes the output's variance.

The effect of the baseline source PDFs on the mean and variance of the yield UEV was also determined using these tests. The baselines for each PDF were compared to each other for each model and then between models and p values were recorded.

Chapter 5: Results

Systems Descriptions

The systems descriptions section of the results was split into the original systems' descriptions and the Monte Carlo simulation systems' descriptions. Both subsections were used to determine where uncertainty originates in emergy analyses, and how much uncertainty was propagated in a crop production source's energy/mass and UEV components. The Monte Carlo simulations were conducted dependent on the distribution of the inputs, and determined how the distribution assigned to the Monte Carlo inputs impacted the crop yield UEV variance.

Original systems' descriptions

The original systems energy/mass, UEV, and emergy values for each source and yield can be found in Appendix ii. The mean and standard deviations for the energy/mass, UEV, and emergy of the original systems were described in Table 5a. Table 5a is a reference to compare the Monte Carlo output simulations in later sections.

Table 5a: Original eight cropping systems. Energy/mass input, UEV input and emergy of sources given as arithmetic mean (mean) and standard deviation (stddev) for one hectare over a year.							
	Energy/Mass			UEV		Emergy	
	Unit	Mean	Stddev	(sej/unit)		(sej)	
		1E+06	1E+06	Mean	Stddev	Mean	Stddev
Energy Sources						1E+12	1E+12
Sunlight	J	53,800,000	12,200,000	1	0	53.8	12.2
Evapotranspiration	J	43,100	17,200	25,900	5.83	1,120	445
Fuel	J	4,290	4,500	107,000	7,610	474	501
Net topsoil loss	J	13,800	15,200	119,000	9,270	1,650	1,890
Electricity	J	785	758	251,000	42,100	183	186
Labor	J	37.9	87.4	12,700,000	5,120,000	314	660
Material Sources							
		1E+03	1E+03	1E+06	1E+06	1E+12	1E+12
Seed	g	84.2	78.6	666	595	84.8	109
Steel machinery	g	3.95	5.42	8,780	3,410	41.6	62.5
Pesticides	g	3.56	3.61	12,500	11,600	67.9	103
P Fertilizer	g	25.7	24.6	26,000	10,100	550	408
N Fertilizer	g	105	47.8	27,100	14,200	2,300	742
Yield							
		1E+06	1E+06	1E+03	1E+03	1E+12	1E+12
Grain	J	59,200	46,500	249	403	8,840	8,590

From Table 5a we see that nitrogen fertilizer (2.3E15 sej/ha/y) was the largest contributor to the yield emergy (i.e., 44% of the yield emergy) of the original systems, while net topsoil loss was the second largest contributor (1.65E15 sej/ha/y). These two major sources also had the first and second largest standard deviations (Table 5a).

Partitioning of variance in the original systems

Table 5b: Emergy sum of squares partitioning for sources. Source variance (var_i), total source variance (var_{sum}), total system variance* (var_{sys}) and percentages are shown.			
	var_i	$\text{var}_i/\text{var}_{\text{sum}}$	$\text{var}_i/\text{var}_{\text{sys}}$
Energy Sources	1.0E25 (sej^2)		
Sunlight	14.4	0.0%	0.0%
Evapotranspiration	19,800	3.8%	0.3%
Fuel	25,100	4.8%	0.3%
Net topsoil loss	357,000	68.2%	4.8%
Electricity	3,460	0.7%	0.0%
Labor	4,360	8.3%	0.6%
Material Sources			
Seed	1,190	0.2%	0.0%
Steel machinery	397	0.1%	0.0%
Pesticides	1,060	0.2%	0.0%
P Fertilizer	16,600	3.2%	0.2%
N Fertilizer	55,100	10.5%	0.7%
var_{sum}	523,000		
$\text{var}_{\text{sys}}^*$	7,380,000		
$\text{var}_{\text{sum}}/\text{var}_{\text{sys}}$	7.1%		

* System variance is the variance of the emergy yield of the original eight systems

Table 5b shows that only 7% of the variability in yield emergy, across the original eight systems, could be explained by the sum of variability in the emergy of individual sources ($\text{var}_{\text{sum}}/\text{var}_{\text{sys}}$). In other words, uncertainty in the energy/mass and UEV parameters contributed only 7% to total uncertainty of the yield. The vast majority (93%) of variability in the emergy value of the crop yield was due to scenario differences, indicating that the original eight systems varied greatly in the combinations of sources used to achieve different yields. The original systems were spread throughout the world in different climates on lands with different soils, suggesting that geographic location should be a major source of variability. The yield of corn is closely tied to nitrogen fertilization, and fertilization is closely linked with

water availability and soil properties. It is this situational or scenario difference that explained most of the variability in the UEV of corn produced around the world.

Of the 7% uncertainty contributed by the energy/mass and UEV parameters, by far the source that contributed the most variability (4.8%) was net topsoil loss, while no other source contributed more than 1% (Table 5b). Net topsoil loss rates varied greatly across the original eight systems with a standard deviation of $15.2E9$ J/ha/y that was greater than the mean of $13.8E9$ J/ha/y (Table 5a); a ratio of 1.1. In contrast the ratio of standard deviation to mean for net topsoil loss's UEV was only 0.08. Thus, most of the variability in energy of soil was due to uncertainty in net topsoil loss rates, not net topsoil loss UEV.

The uncertainty of the yield energy was not included in the Monte Carlo models. Therefore the total source variance (var_{sum}) was more representative of the uncertainty captured by the Monte Carlo models than the total system variance (var_{sys}).

Energy signature of the original systems

The energy signature graphs were used to visually compare the magnitude of the uncertainty associated with each source (Figure 5a). By convention the spectra arranged the sources according to their UEV in ascending order. However, note that arrangement for the first six sources on the left were in units of sej/J while the remaining five on the right were in sej/g (Figure 5a). The crop output was also shown on the energy signature to highlight the large amount of variance associated with the yield (Figure 5b).

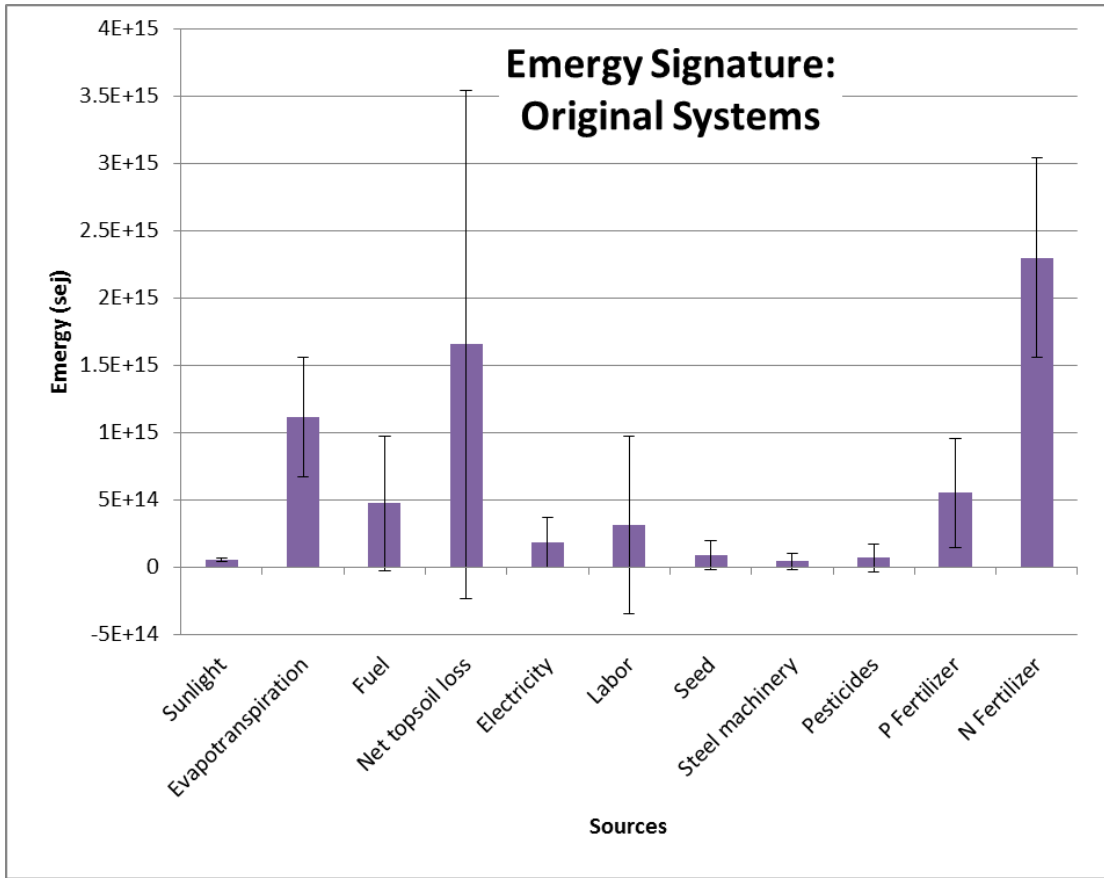


Figure 5a: Energy signature of the sources to the original crop systems without output. The original eight systems' mean energy values are shown for each source with the output to the right. The sources have been organized in order of increasing unit of energy value. One standard deviation is shown in both 5 and 5b. In the case of labor, steel machinery, and pesticides, the lower standard deviation extends below the x-axis. Nitrogen fertilizer and net topsoil loss are the sources with the highest energy means, and the largest variance.

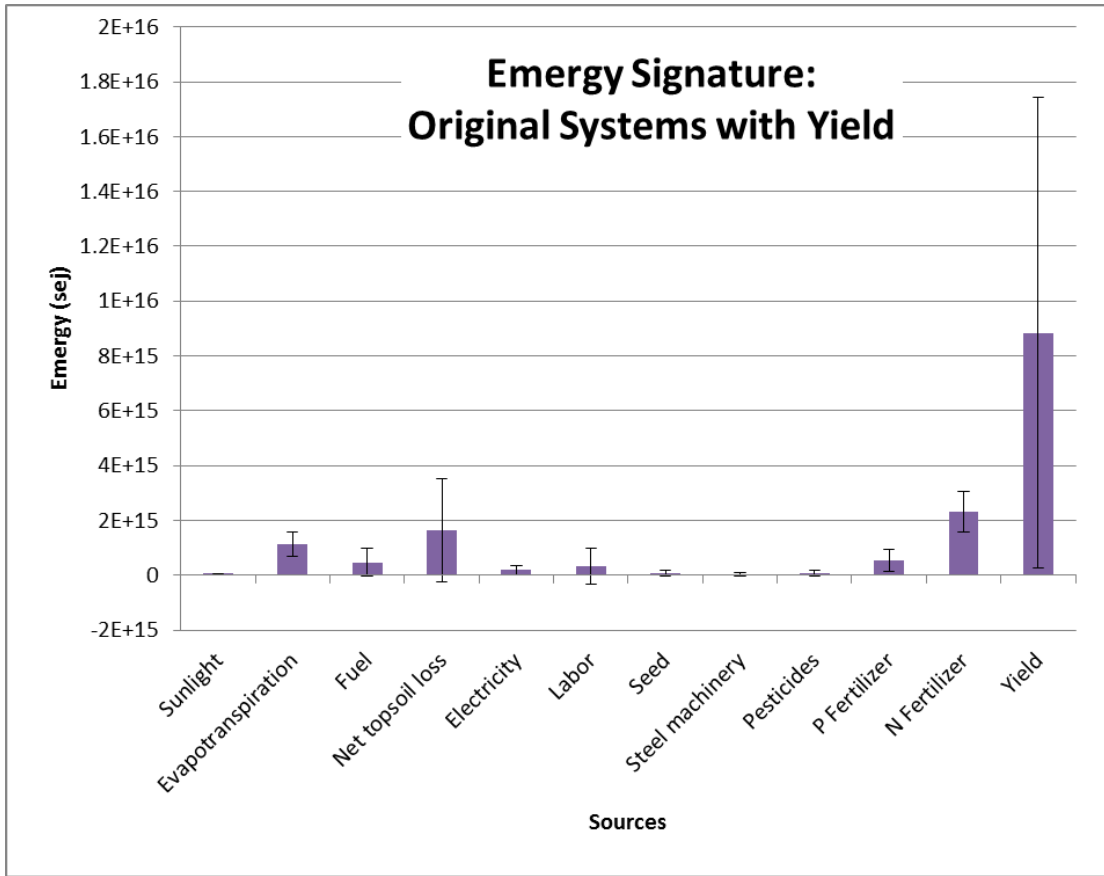


Figure 5b: Energy signature of the sources to the original crop systems with output. Showing the same information on energy sources as in Figure 5a but within the context of the output energy. The variance of the sources pales in comparison to the variance of the energy output.

Monte Carlo simulations

Model 1: Energy/mass + UEV variance

Comparison of energy signature of the original and three simulated systems from Model 1 showed, at first glance, that each PDF assumption gave values similar to the original energy/mass (Figure 6a). However, there were small differences among the PDFs for a few of the energy sources and the output (Figure 6a).

The variability predicted by each Monte Carlo simulation for the emergy output was much smaller than the original systems (Table 6a). Likely, this inability of the Monte Carlo simulations to replicate the total variability observed in the original eight systems is due to the lack of ability to model the scenario uncertainty. The Monte Carlo has no provisions for simulating the collinearity among the sources. That is, some sources will be highly correlated in real systems, like nitrogen fertilization rates and Evapotranspiration, but that correlation is ignored in the simulations. For example, nitrogen fertilization and Evapotranspiration rates are independently and randomly selected from their own PDFs. In the original systems, knowing the Evapotranspiration rate, and thus the approximate climatic conditions, would dictate how much nitrogen the farmer would add.

Thus, Model 1 is appropriate understanding parameter uncertainty, but can tell us little about scenario uncertainty. Only when the simulated results are compared to the original systems could we deduce something about scenario uncertainty.

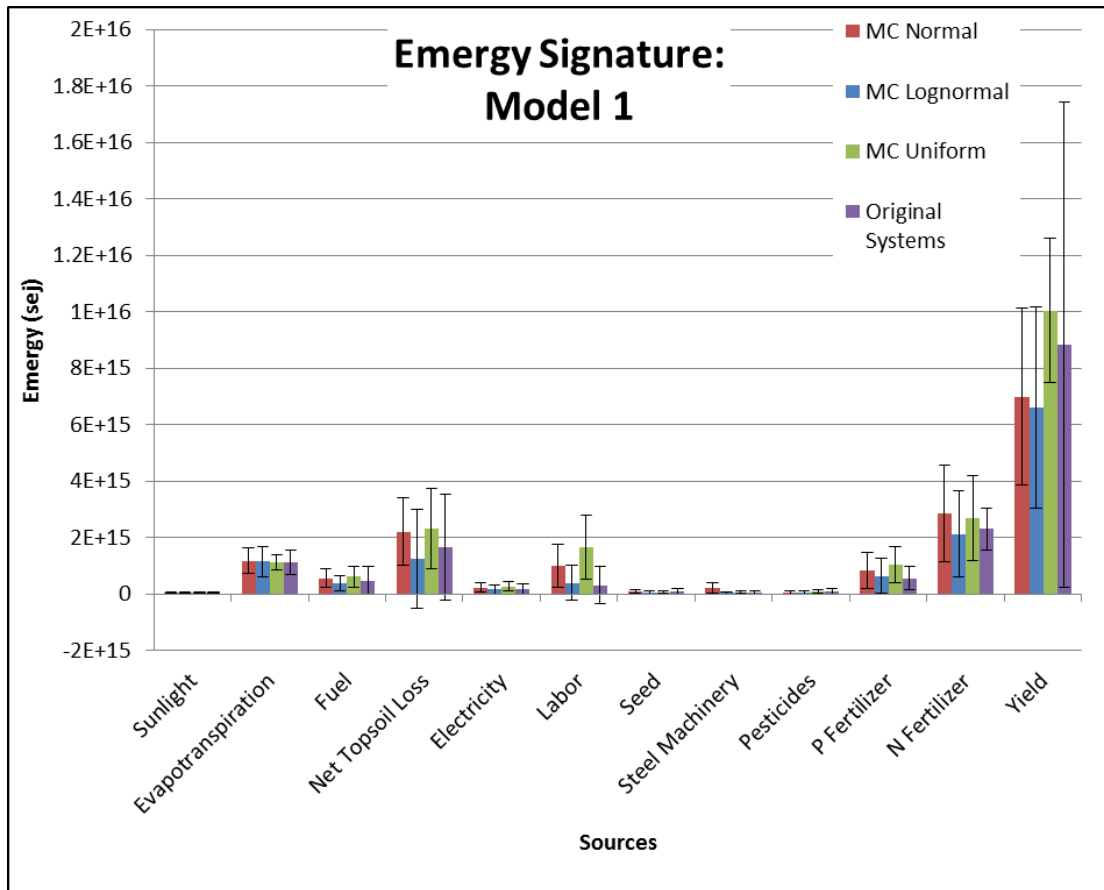


Figure 6a: Crop system emergy signatures: Model 1. The original eight systems' mean emergy values are shown and compared with Model 1 of the Monte Carlo simulations for each source and output. The Monte Carlo simulation results for Normal (MC Normal), Lognormal, and Uniform distributions are shown. The sources have been organized in order of increasing unit of emergy value. One standard deviation is shown.

In general, the simulations that assumed lognormal PDFs generated values most similar to the original systems for each source (Figure 6a). In addition, the lognormal PDF assumption was able to duplicate the negative value of the lower standard deviations observed for labor, steel machinery, and pesticides in the original systems, which no other PDF could do. However, since emergy values are positive,

the ability of the lognormal PDF to replicate a negative value may not be significant. Graphically, we see that the uniform PDF often overestimated the emergy of sources and the output when compared to the original systems (Figure 6a). Similarly, the normal PDF overestimated most of the largest emergy sources, but underestimated the output (Figure 6a).

The following tables showed the actual mean and standard deviation values for each source and output's energy/mass, UEV, and emergy generated in Monte Carlo using Model 1. Table 6a covered the normal distribution, Table 6b the lognormal distribution, and Table 6c the uniform distribution. These tables allowed for a quantitative assessment of the emergy signature graphs.

Table 6a: Monte Carlo output of Model 1 assuming normally distributed source energy/mass and UEVs							
	Energy/mass (unit/ha/year)			UEV (sej/unit/ha/year)		Emergy (sej/ha/year)	
	Unit	Mean	Stddev	Mean	Stddev	Mean	Stddev
Energy Sources		1E+06	1E+06			1E+12	1E+12
Sunlight	J	51,600,000	13,600,000	1	0	51.6	13.6
Evapotranspiration	J	45,300	18,000	25,900	6	1,170	466
Fuel	J	5,120	2,930	108,000	7,520	556	327
Net topsoil loss	J	18,800	10,300	118,000	9,370	2,200	1,200
Electricity	J	891	690	254,000	58,900	224	175
Labor	J	80	53	12,500,000	4,160,000	1,010	766
Material Sources		1E+03	1E+03	1E+06	1E+06	1E+12	1E+12
Seed	g	110	64.8	863	436	85.6	61.8
Steel machinery	g	21.3	18.4	30,900	24,700	206	181
Pesticides	g	4.46	2.81	14,900	9,870	62.4	59.1
P Fertilizer	g	30.7	19.5	26,500	10,300	823	637
N Fertilizer	g	99.9	44.3	29,600	14,300	2,850	1,720
Yield		1E+06	1E+06	1E+03	1E+03	1E+12	1E+12

Grain	J	59,200*	0	118	53.0	6,990	3,140
-------	---	---------	---	-----	------	-------	-------

*The energy arithmetic mean of the original eight systems' yield

The normally distributed Monte Carlo simulation of Model 1 showed that nitrogen fertilizer had the highest energy value (2.85E15 sej/ha/y) and standard deviation (1.72E15sej/ha/y), while net topsoil loss had the second largest energy value (2.20E15sej/ha/y) and standard deviation (1.20*10¹⁵sej/ha/y) (Table 6a). While this ranking of these top two sources was similar to the original systems, the ranking of their variability was flipped. While the ratio of net topsoil loss's standard deviation to its mean was 1.1 in the original systems (Table 5a), in Model 1 with the normal PDF assumption, the ratio was cut in half to 0.55 (Table 6a). In contrast the same ratio for the nitrogen fertilization source rose from 0.32 in the original system to 0.60 in the simulation. Thus, Model 1 altered the relative sources of variability from the original systems, but it is not clear how that happened.

Table 6b: Monte Carlo output of Model 1 assuming lognormally distributed source energy/mass and UEVs							
	Energy/mass (unit/ha/year)			UEV (sej/unit/ha/year)		Emergy (sej/ha/year)	
	Unit	Mean	Stddev	Mean	Stddev	Mean	Stddev
Energy Sources		1E+06	1E+06			1E+12	1E+12
Sunlight	J	46,800,000	12,100,000	1	0	46.8	12.1
Evapotranspiration	J	44,000	20,100	25,900	6	1,140	521
Fuel	J	3,400	2,460	107,000	8,090	368	275
Net topsoil loss	J	10,500	13,700	119,000	9,720	1,250	1,750
Electricity	J	631	624	256,000	45,100	161	157
Labor	J	33	61	12,400,000	4,600,000	394	620
Material Sources		1E+03	1E+03	1E+06	1E+06	1E+12	1E+12
Seed	g	63.7	67.4	608	526	36.7	56.8
Steel machinery	g	3.31	5.54	8,580	3,530	206	49.8
Pesticides	g	2.62	2.21	13,500	13,600	33.8	53.8
P Fertilizer	g	25.3	24.2	26,100	9,250	641	633
N Fertilizer	g	84.1	47.6	25,300	12,600	2,120	1,510
Yield		1E+06	1E+06	1E+03	1E+03	1E+12	1E+12
Grain	J	41,500*	0	159	86.0	6,620	3,570

*The energy geometric mean of the original eight systems' output

The lognormally distributed Monte Carlo generated systems showed that nitrogen fertilizer had the highest mean emergy value ($2.12E15$ sej/ha/y) and second largest standard deviation ($1.51E15$ sej/ha/y) while net topsoil loss had the second largest emergy value ($1.25E15$ sej/ha/y) and the largest standard deviation ($1.75E15$ sej/ha/y) (Table 6b). These rankings were identical to Model 1 above when normality was assumed.

Table 6c: Monte Carlo output of Model 1 assuming uniformly distributed source energy/mass and UEVs							
	Energy/mass (unit/ha/year)			UEV (sej/unit/ha/year)		Energy (sej/ha/year)	
	Unit	Mean	Stddev	Mean	Stddev	Mean	Stddev
Energy Sources		1E+06	1E+06			1E+12	1E+12
Sunlight	J	52,900,000	9,590,000	1	0	52.9	9.59
Evapotranspiration	J	43,400	10,900	25,900	3	1,120	282
Fuel	J	6,000	3,730	102,000	4,510	611	377
Net topsoil loss	J	20,300	12,200	114,000	5,270	2,320	1,420
Electricity	J	1,110	574	244,000	27,400	271	146
Labor	J	119	72	13,800,000	3,460,000	1,650	1,120
Material Sources							
		1E+03	1E+03	1E+06	1E+06	1E+12	1E+12
Seed	g	86.8	42.9	569	329	49.7	40.7
Steel machinery	g	7.12	3.73	8,260	1,840	206	34.6
Pesticides	g	7.08	2.67	14,500	7,060	98.9	62.4
P Fertilizer	g	45.8	21.8	22,500	8,460	1,030	652
N Fertilizer	g	113	34.1	23,700	10,900	2,680	1,510
Yield							
		1E+06	1E+06	1E+03	1E+03	1E+12	1E+12
Grain	J	65,200*	0	154	39.1	10,000	2,550

* The energy arithmetic mean found using the minimum and maximum of the original eight systems' output

The uniformly distributed Monte Carlo generated systems showed that nitrogen fertilizer had the highest energy value (2.68E15sej/ha/y) and standard deviation (1.51E15sej/ha/y), while net topsoil loss had the second largest energy value (2.32E15sej/ha/y) and std deviation (1.42E15sej/ha/y) (Table 6c). These rankings for the means were the same as the normal and lognormal assumptions for Model 1, but the standard deviation ranking was reversed. The mean energy of the

yield (10.0E15 sej/ha/y) for the uniform assumption was larger than for the normal and lognormal.

All three PDF assumptions for Model 1 and the original systems showed that nitrogen fertilizer and net topsoil loss were the sources that contributed the most energy to the yield and had the largest variances (Tables 5a, 6a, 6b, and 6c).

The normally and uniformly distributed Monte Carlo simulations of Model 1 both showed that nitrogen fertilizer and net topsoil loss as having comparable standard deviations (Tables 6a and 6c), while the original systems and the lognormally distributed Monte Carlo systems had net topsoil loss as having a larger standard deviation than nitrogen fertilizer (Tables 5a and 6b).

Model 2: UEV only variance

In Model 2 we assumed zero variance for all the energy sources in order to isolate parameter uncertainty to UEV variability solely. An energy signature was created to compare the three distributions used in the Model 2 Monte Carlo simulation to the original systems described earlier (Figure 5b). Like Model 1, in general, Model 2 often produced mean values similar to the original data (Figure 6b) with a few exceptions. Namely, the mean energy of top soil loss, labor, phosphorus and nitrogen often differed from the original data, upon visual inspection.

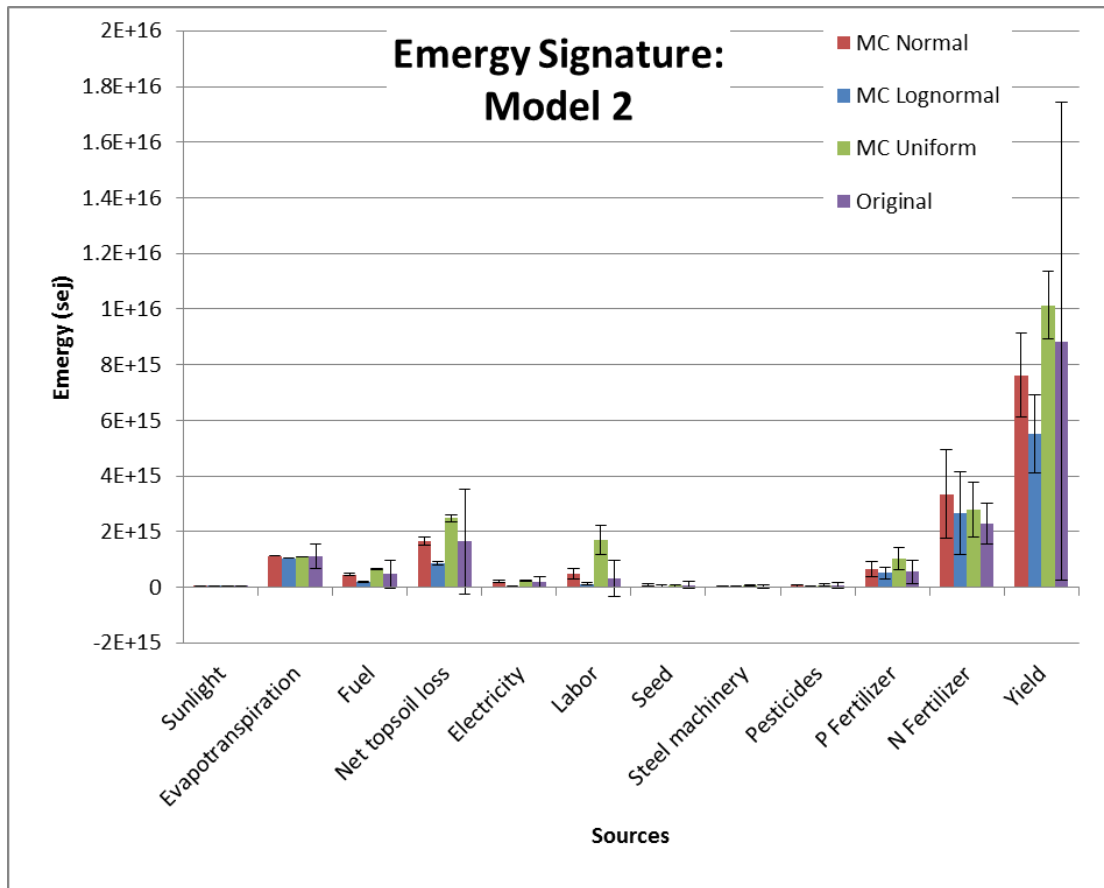


Figure 6b: Crop system energy signature: Model 2. The original eight systems' mean energy values are shown and compared with Model 2 of the Monte Carlo simulations for each source and output. The Monte Carlo simulation results for Normal (MC Normal), Lognormal, and Uniform distributions are shown. The variance of each source and output except for nitrogen fertilizer has obviously decreased from Model 1 in Figure 6a. This is somewhat expected since some uncertainty has been removed from the model.

Since the variance of the energy/mass input had been eliminated in Model 2, the standard deviations of each source's energy contributions were smaller than in Model 1 and due completely to variance in the UEV.

In general the normal and lognormal PDF assumptions for Model 2 generated mean energy values most similar to the original systems for each source (Figure 6b). The uniform distribution, on the other hand, often had larger values than the original systems (Figure 6b). Every distribution showed nitrogen fertilizer as the source with the highest mean energy input and the largest variance.

Similar to Model 1, the output for Model 2 had a much smaller standard deviation than the original systems. Also like Model 1, Model 2 did not represent any multicollinearity among the sources indicating that it could not represent scenario uncertainty. Nor did Model 2 have any uncertainty due to energy sources. Thus, Model 2 represented the fraction of uncertainty due solely to UEV uncertainty.

The following tables show the mean and standard deviation values simulated in Model 2 for each source UEV and energy. Table 7a covered the normal distribution, while Table 7b covered the lognormal distribution, and Table 7c covered the uniform distribution. These tables allowed for a quantitative assessment of the energy signature graphs.

	Energy/mass (unit/ha/year)			UEV (sej/unit/ha/year)		Emergy (sej/ha/year)	
	Unit	Mean	Stddev	Mean	Stddev	Mean	Stddev
Energy Sources		1E+06				1E+12	1E+09
Sunlight	J	53,800,000*	0	1	0	53.8	0
Evapotranspiration	J	43,100*	0	25,900	6	1,120	243
Fuel	J	4,290*	0	108,000	7,470	463	32,100
Net topsoil loss	J	13,800*	0	120,000	10,500	1,650	145,000
Electricity	J	785*	0	257,000	47,500	202	37,300
Labor	J	38*	0	12,900,000	5,260,000	488	199,000
Material Sources		1E+03		1E+06	1E+06	1E+12	1E+12
Seed	g	84.2*	0	841	456	70.8	38.4
Steel machinery	g	3.95*	0	8,320	3,330	206	13.2
Pesticides	g	3.56*	0	15,200	8,900	54.1	31.7
P Fertilizer	g	25.7*	0	26,000	10,600	669	273
N Fertilizer	g	105*	0	31,900	15,100	3,350	1,580
Yield		1E+06		1E+03	1E+03	1E+12	1E+12
Grain	J	59,200*	0	129	25.5	7,630	1,510

* The energy arithmetic mean of the respective source and yield of the original eight systems

The normally distributed Monte Carlo simulation of Model 2 showed that nitrogen fertilizer had the highest energy value (3.35E15 sej/ha/y) and standard deviation (1.58E15 sej/ha/y), while net topsoil loss had the second largest energy value (1.65E15 sej/ha/y) and the third largest standard deviation (1.45E14 sej/ha/y) (Table 7a).

	Energy/mass (unit/ha/year)			UEV (sej/unit/ha/year)		Emergy (sej/ha/year)	
	Unit	Mean	Stddev	Mean	Stddev	Mean	Stddev
Energy Sources		1E+06				1E+12	1E+09
Sunlight	J	52,500,000*	0	1	0	52.5	0
Evapotranspiration	J	40,200*	0	25,900	6	1,040	247
Fuel	J	1,700*	0	107,000	8,120	182	13,800
Net topsoil loss	J	7,160*	0	121,000	9,090	864	65,100
Electricity	J	157*	0	250,000	47,800	39.3	7,500
Labor	J	9*	0	13,600,000	5,700,000	118	49,700
Material Sources		1E+03		1E+06	1E+06	1E+12	1E+12
Seed	g	54.8*	0	782	611	42.8	33.5
Steel machinery	g	2.28*	0	8,940	3,430	206	7.82
Pesticides	g	2.58*	0	11,700	10,600	30.1	27.3
P Fertilizer	g	19.6*	0	25,900	10,500	508	205
N Fertilizer	g	95.5*	0	28,000	15,500	2,670	1,480
Yield		1E+06		1E+03	1E+03	1E+12	1E+12
Grain	J	41,500*	0	133	33.6	5,510	1,390

*The energy geometric mean of each respective source and yield for the original eight systems

The lognormally distributed Monte Carlo generated systems showed that nitrogen fertilizer had the highest mean emergy value ($2.67E15$ sej/ha/y) and the largest standard deviation ($1.48E15$ sej/ha/y) while net topsoil loss has the third largest emergy value ($8.64E14$ sej/ha/y) and the third largest standard deviation ($6.51E13$ sej/J) (Table 7b).

	Energy/mass (unit/ha/year)			UEV (sej/unit/ha/year)		Emergy (sej/ha/year)	
	Unit	Mean	Stddev	Mean	Stddev	Mean	Stddev
Energy Sources		1E+06				1E+12	1E+09
Sunlight	J	53,100,000*	0	1	0	53.1	0
Evapotranspiration	J	42,500*	0	25,900	2.84	1,100	121
Fuel	J	6,320*	0	102,000	4,850	644	30,700
Net topsoil loss	J	21,600*	0	115,000	5,600	2,480	121,000
Electricity	J	1,000*	0	244,000	27,400	245	27,500
Labor	J	128*	0	13,200,000	3,980,000	1,700	511,000
Material Sources		1E+03		1E+06	1E+06	1E+12	1E+12
Seed	g	93.1*	0	547	347	51.0	32.3
Steel machinery	g	7.30*	0	8,250	1,720	206	12.5
Pesticides	g	6.24*	0	13,100	6,480	81.6	40.5
P Fertilizer	g	46.5*	0	22,200	8,470	1,030	394
N Fertilizer	g	113*	0	24,600	8,680	2,780	981
Yield		1E+06		1E+03	1E+03	1E+12	1E+12
Grain	J	65,200*	0	156	18.8	10,100	1,230

* The energy arithmetic mean found using the minimum and maximum of the respective source and yield of the original eight systems

The uniformly distributed Monte Carlo generated systems showed that nitrogen fertilizer had the highest energy value (2.78E15 sej/ha/y) and standard deviation (9.81E14 sej/ha/y), while net topsoil loss had the second largest energy value (2.48E15 sej/ha/y) and the fourth largest standard deviation (1.21E14 sej/ha/y) (Table 7c).

All three PDFs and the original systems showed that nitrogen fertilizer was the source that contributed the most energy to the total energy and had the largest variability (Tables 5a, 7a, 7b, and 7c). Net topsoil loss was another source with large energy and variance contributions to the output. Model 2, without the variance

associated with energy and mass inputs, had sources that contributed more energy with larger variances than Model 1 (Tables 7a, 7b, and 7c)

The energy/mass values in normal PDF Model 2 were chosen to be the arithmetic mean of the original systems with no standard deviation. Judging by the large differences in energy/mass means between the Models (Tables 6a and 7a), this approach may not have been appropriate for a few sources. Steel machinery's and labor's mean values, in particular, shifted the most when the variance of the energy/mass inputs was removed from the model, and both were lower than the mean values of Model 1.

When variance of the energy/mass input was removed and only UEV uncertainty remained (Model 2), the energy variance was lowered in every source for the normal distribution (compare Tables 6a and 7a). Nitrogen fertilizer was interesting because its energy variance value was lowered the least (by ~8%) (Tables 6a and 7a), indicating that more of its uncertainty was generated from its UEV than its energy/mass input. Focusing on the yield UEV, the removal of energy/mass variance lowered the yield UEV variance by ~52% (Tables 6a and 7a), indicating that more than half of the uncertainty for crop production came from the sources' energy/mass inputs rather than the UEV inputs.

The energy/mass values were chosen in lognormal distribution Model 2 to be the geometric mean of the original systems (Tables 6b and 7b). There were larger differences in means of the inputs between Models 1 and 2 for the lognormal distribution than there were for the normal distribution. Electricity and labor's mean inputs in particular shifted the most, and both were lower in Model 2 than in Model 1.

Steel machinery had a much lower change in UEV variance between models in the lognormal distribution when compared to the normal distribution (comparing Tables 6a and 7a to 6b and 7b).

In removing energy/mass input variance, the variance of the energy output is lowered in every source in the lognormal distribution (Tables 6b and 7b) as was the case in the normal distribution. Nitrogen fertilizer is interesting in that its variance was lowered the least. The output UEV variance changed by ~61% between models, supporting the previous conclusion that more than half of the uncertainty for crop production comes from the energy/mass input rather than the UEV inputs.

The energy/mass values were chosen in uniform distribution Model 2 to be the arithmetic mean of the maximum and minimum of the original systems (Tables 6c and 7c). There were smaller differences in energy/mass, UEV, and energy means between the Models for the uniform distribution compared to the normal and lognormal distributions. This suggested that the uniform distribution's mean values were less dependent on the amount of uncertainty in the model when compared to the normal and lognormal distributions. While the normal and lognormal distributions had prominent shifts of the energy/mass means to the left on the number line, the uniform distribution shows energy/mass means scattered larger and smaller than their Model 1 counterparts.

In removing energy/mass variance, the energy variance was lowered in every source in the uniform distribution (Tables 6c and 7c) as in the normal and lognormal distributions, but much more evenly. Nitrogen fertilizer variance was the least lowered in both of the other distributions, but with a uniform distribution, seed's

energy variance was the least lowered and nitrogen fertilizer was the second least lowered. The yield UEV variance changed between models.

Model Comparison

The model comparisons made below were all based on the normal PDF assumption for the Monte Carlo inputs. This section outlines the percent contribution of each source's energy/mass and UEV component to the uncertainty of the energy yield when considering the normal distribution of inputs. The larger percentages of uncertainty are contributed by the sources that most likely influence yield UEV variance, shown in this section by the confidence intervals produced by removing specific uncertainties.

Energy/mass + UEV variance model results showed the crop yield UEV as having a coefficient of variance of 45%. This was found by dividing the yield UEV standard deviation by its mean. The COV was a measure of total system uncertainty relative to the mean yield UEV. The crop yield energy had the same COV of 45% because the yield UEV was a multiple of the yield energy. The yield UEV COV of 45% was partitioned among each source's energy/mass variance and UEV variance (Table 8a). Of the 45%, 25% was from energy/mass variance and 20% was from UEV variance.

Of all the sources of uncertainty, nitrogen fertilizer UEV variance was the largest (19%), followed by net topsoil loss energy (11%), nitrogen fertilizer mass (4%), and labor energy (5%). Out of 22 inputs (11 energy/mass inputs and 11 UEV inputs), 4 inputs contributed more than 86% of the uncertainty of the yield UEV. These 4 inputs were net topsoil loss energy, labor energy, nitrogen fertilizer UEV and

nitrogen fertilizer mass data. As for uncertainty due to UEV variance, only two sources (labor and phosphorus fertilizer) other than nitrogen fertilizer contributed more than 0.5% (Table 8a). More often, the uncertainty associated with how much energy or mass was used in the system added more uncertainty than the UEV.

Table 8a: The source partition of the energy yield uncertainty into the Energy/Mass Variance Model and the UEV Variance Model. Normal PDF was assumed.

	Energy/Mass and UEV Variance (Model 1)	UEV Variance (Model 2)	Energy/Mass Variance (Model 1 minus Model 2)
Energy Sources			
Sunlight	0%	0%	0%
Evapotranspiration	1.69%	0%	1.69%
Fuel	0.83%	0.01%	0.82%
Net topsoil loss	11.18%	0.16%	11.02%
Electricity	0.24%	0.01%	0.23%
Labor	4.56%	0.30%	4.26%
Mass Sources			
Seed	0.03%	0.01%	0.02%
Steel machinery	0.25%	0%	0.25%
Pesticides	0.03%	0.01%	0.02%
P Fertilizer	3.15%	0.56%	2.59%
N Fertilizer	22.97%	18.74%	4.23%
Coefficient of Variance of yield UEV			
	44.92%	19.79%	25.13%

Confidence intervals (95%) around the original systems' mean crop yield UEV were estimated to demonstrate the effect of removing some of the sources of uncertainty (Table 8b). The total parameter coefficient of variance of 45% was multiplied by 2 to obtain 90%. The partitioned variances ($\text{var}_i / \text{var}_{\text{sum}}$) for the i^{th} source were then multiplied by 90% to obtain for each source the percentage of the

mean that when added to and subtracted from the mean, resulted in the 95% confidence interval.

When the nitrogen UEV variance was removed from the model, the 95% confidence interval was reduced dramatically to 4% of the mean (Table 8b). This was much smaller than energy/mass + UEV only variance model, the energy/mass variance only model, and the UEV variance only model with the nitrogen variance included.

Table 8b: The 95% confidence interval of the yield UEV. The confidence intervals (+/- 2σ) are surrounding the yield UEV mean of the original systems. The original systems' yield UEV variance represents the scenario and parameter uncertainty in crop production. This is compared to the Monte Carlo models where only parameter uncertainty is present. The Monte Carlo models are shown below: energy/mass + UEV variance, UEV only variance, UEV only variance minus the variance of the nitrogen fertilizer source, and energy/mass only variance.

	Lower 95% Confidence Interval	Mean	Upper 95% Confidence Interval	Range of CI	Range/mean
Original Systems' yield UEV	-557,000	249,000	1,060,000	1,610,000	647%
Energy/Mass and UEV only variance (M1)	25,300	249,000	473,000	447,000	180%
UEV only variance (M2)	150,000	249,000	348,000	197,000	79%
UEV only variance minus nitrogen fertilizer	244,000	249,000	254,000	10,500	4%
Energy/mass only variance (M1-M2)	124,000	249,000	374,000	250,000	101%

The visual summary section below focused on comparing the models qualitatively by source.

Visual summary of Monte Carlo simulations

The following figures were created to visualize where uncertainty originates in energy analyses and applied in the current case of crop production systems. These figures focused on uncertainty originating at a specific point in the tabular procedure-

when the source's energy/mass and UEV inputs were multiplied together to form the source's energy. The Monte Carlo simulation results for each source ($n = 11$) and yield were graphed below (Figure 7a-7l) using 5 bins. One standard deviation was shown about the mean providing context between the graphs. Model 2 was shown below Model 1 for each distribution for direct comparison vertically, with the x-axis showing the same scale. The axes were different between the energy/mass, UEV, and energy values, so a visual comparison between them was not directly applicable. However, since the axes were still present, it was possible to make comparisons taking the axes of energy/mass, UEV, and energy into consideration.

The objective of determining where uncertainty originates in energy analyses was broken down into 2 parts for the analysis of this section:

- 1) visualize the shift in the energy column from Model 1 to Model 2 rows, and
- 2) visualize the effect of the energy/mass PDF and the UEV PDF (columns 1 and 2) on the energy PDF (column 3). This part also partially addressed the objective of determining the impact of the PDF on the yield UEV.

The shift between Model 1 and Model 2 showed the impact of the energy/mass input on the source's energy variance. If there was a large shift, there was a large amount of energy/mass input variance. If there was a smaller shift, there was a smaller amount of energy/mass input variance, meaning the UEV input variance contributed significantly to the source's energy variance. The sensitivity analysis will quantitate this shift between models. For now, the distance between the dashed red lines qualitatively showed the shift between models.

To visualize the effects of the multiplied PDF types on the energy PDF, only the Model 1 rows were examined. The Model 2 rows multiplied the UEV PDF by a constant, so that the resulting energy PDF was the same UEV PDF.

Normal M1	<p style="text-align: center;">Sunlight</p>	<p style="text-align: center;">Sunlight</p>	<p style="text-align: center;">Sunlight</p>
Normal M2	<p style="text-align: center;">Sunlight</p>	<p style="text-align: center;">Sunlight</p>	<p style="text-align: center;">Sunlight</p>
Lognormal M1	<p style="text-align: center;">Sunlight</p>	<p style="text-align: center;">Sunlight</p>	<p style="text-align: center;">Sunlight</p>
Lognormal M2	<p style="text-align: center;">Sunlight</p>	<p style="text-align: center;">Sunlight</p>	<p style="text-align: center;">Sunlight</p>
Uniform M1	<p style="text-align: center;">Sunlight</p>	<p style="text-align: center;">Sunlight</p>	<p style="text-align: center;">Sunlight</p>
Uniform M2	<p style="text-align: center;">Sunlight</p>	<p style="text-align: center;">Sunlight</p>	<p style="text-align: center;">Sunlight</p>

Figure 7a: Monte Carlo simulation graphs for sunlight source. The rows show the graphs specific for each distribution (Normal, Lognormal, and Uniform) and model (M1 and M2). The columns show on the x-axis the energy/mass, UEV, and energy for each graph, while the y-axis is the frequency of occurrence. The arithmetic mean is shown in a solid red line with one standard deviation shown as dashed red lines.

All of the variance in the sunlight solar energy source was from the energy/mass estimate (Figure 7a). Assumption of the PDF for sunlight affected the PDF of the solar energy contributed by sunlight directly, since the UEV of sunlight is 1 (Figure 7a). Assuming a normal PDF for the sunlight energy produced a bell-shaped PDF for the sunlight solar energy. Assuming a lognormal PDF for the sunlight energy produced a lognormal PDF with a right-skewed tail (Figure 7a). Assuming a uniform PDF for the sunlight source's energy/mass produced a uniform PDF with a similar probability for each value (Figure 7a). Regardless of which type of PDF was assumed, all of the variance originated from the estimate of the sunlight energy rather than its UEV (Figure 7a).

Normal M1	<p style="text-align: center;">Evapotranspiration</p>	<p style="text-align: center;">Evapotranspiration</p>	<p style="text-align: center;">Evapotranspiration</p>
Normal M2	<p style="text-align: center;">Evapotranspiration</p>	<p style="text-align: center;">Evapotranspiration</p>	<p style="text-align: center;">Evapotranspiration</p>
Lognormal M1	<p style="text-align: center;">Evapotranspiration</p>	<p style="text-align: center;">Evapotranspiration</p>	<p style="text-align: center;">Evapotranspiration</p>
Lognormal M2	<p style="text-align: center;">Evapotranspiration</p>	<p style="text-align: center;">Evapotranspiration</p>	<p style="text-align: center;">Evapotranspiration</p>
Uniform M1	<p style="text-align: center;">Evapotranspiration</p>	<p style="text-align: center;">Evapotranspiration</p>	<p style="text-align: center;">Evapotranspiration</p>
Uniform M2	<p style="text-align: center;">Evapotranspiration</p>	<p style="text-align: center;">Evapotranspiration</p>	<p style="text-align: center;">Evapotranspiration</p>

Figure 7b: Monte Carlo simulation graphs for evapotranspiration source. The rows show the graphs specific for each distribution (Normal, Lognormal, and Uniform) and model (M1 and M2). The columns show on the x-axis the energy/mass, UEV, and energy for each graph, while the y-axis is the frequency of occurrence. The arithmetic mean is shown in a solid red line with one standard deviation shown as dashed red lines.

The majority of the variance in the evapotranspiration solar energy source was from the energy/mass estimate, while only a small amount was from the UEV of evapotranspiration (Figure 7b). Assumption of the PDFs for evapotranspiration energy and UEV affected the PDF of the solar energy contributed by evapotranspiration (Figure 7b). Assuming normal PDFs for both the evapotranspiration energy and UEV produced a bell-shaped PDF for the evapotranspiration solar energy. Assuming a log-normal for both the evapotranspiration energy and UEV produced a PDF that more closely resembled a log-normal distribution with its right-skewed tail (Figure 7b). Assuming uniform PDFs for both evapotranspiration energy and UEV produced a PDF resembling a uniform distribution (Figure 7b). Regardless of which type of PDF was assumed, most of the variance originated from the estimate of the evapotranspiration energy rather than its UEV (Figure 7b).

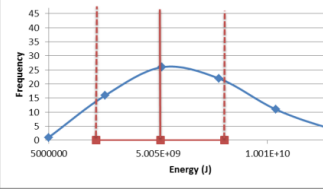
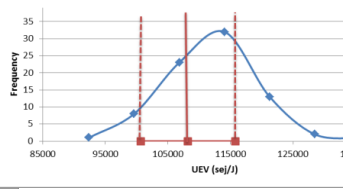
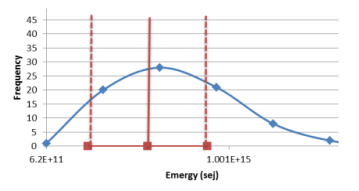
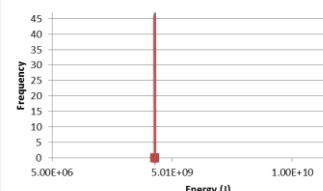
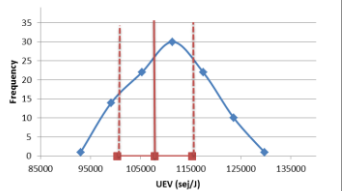
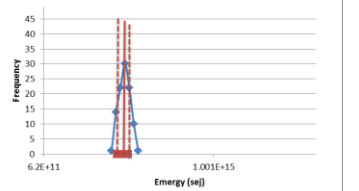
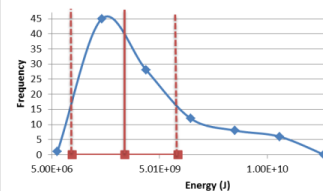
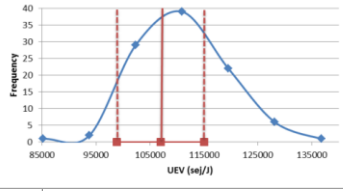
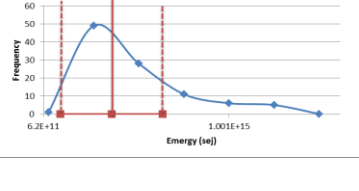
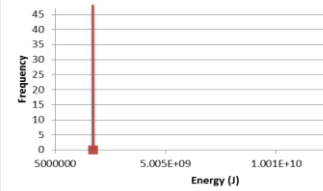
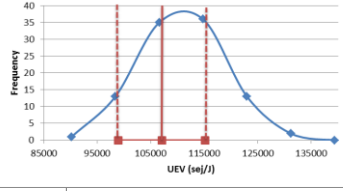
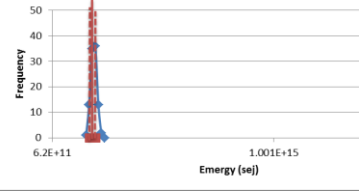
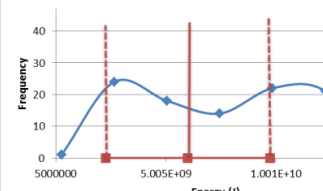
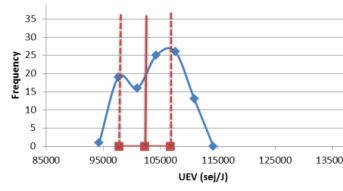
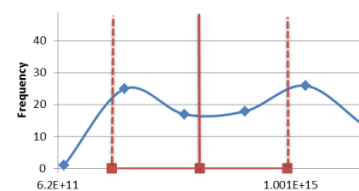
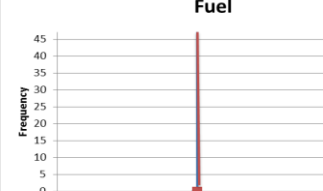
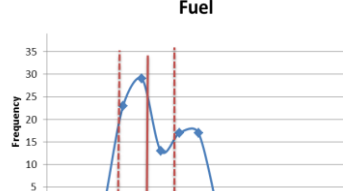
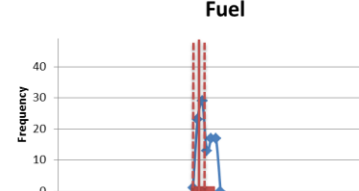
Normal M1	<p style="text-align: center;">Fuel</p> 	<p style="text-align: center;">Fuel</p> 	<p style="text-align: center;">Fuel</p> 
Normal M2	<p style="text-align: center;">Fuel</p> 	<p style="text-align: center;">Fuel</p> 	<p style="text-align: center;">Fuel</p> 
Lognormal M1	<p style="text-align: center;">Fuel</p> 	<p style="text-align: center;">Fuel</p> 	<p style="text-align: center;">Fuel</p> 
Lognormal M2	<p style="text-align: center;">Fuel</p> 	<p style="text-align: center;">Fuel</p> 	<p style="text-align: center;">Fuel</p> 
Uniform M1	<p style="text-align: center;">Fuel</p> 	<p style="text-align: center;">Fuel</p> 	<p style="text-align: center;">Fuel</p> 
Uniform M2	<p style="text-align: center;">Fuel</p> 	<p style="text-align: center;">Fuel</p> 	<p style="text-align: center;">Fuel</p> 

Figure 7c: Monte Carlo simulation graphs for fuel source. The rows show the graphs specific for each distribution (Normal, Lognormal, and Uniform) and model (M1 and M2). The columns show on the x-axis the energy/mass, UEV, and energy for each graph, while the y-axis is the frequency of occurrence. The arithmetic mean is shown in a solid red line with one standard deviation shown as dashed red lines.

The majority of the variance in the fuel solar energy source was from the energy/mass estimate, while only a small amount was from the UEV of fuel. This is seen by the similarities between the energy and energy graphs (Figure 7c).

Assumption of the PDFs for fuel energy and UEV affected the PDF of the solar energy contributed by fuel (Figure 7c). Assuming normal PDFs for both the fuel energy and UEV produced a bell-shaped PDF for the fuel solar energy. Assuming a log-normal for both the fuel energy and UEV produced a PDF that more closely resembled a log-normal distribution with its right-skewed tail (Figure 7c). Assuming uniform PDFs for both fuel energy and UEV produced a PDF resembling a uniform distribution (Figure 7c). Regardless of which type of PDF was assumed, most of the variance originated from the estimate of the fuel energy rather than its UEV (Figure 7c).

Normal M1	<p style="text-align: center;">Net Topsoil Loss</p>	<p style="text-align: center;">Net Topsoil Loss</p>	<p style="text-align: center;">Net Topsoil Loss</p>
Normal M2	<p style="text-align: center;">Net Topsoil Loss</p>	<p style="text-align: center;">Net Topsoil Loss</p>	<p style="text-align: center;">Net Topsoil Loss</p>
Lognormal M1	<p style="text-align: center;">Net Topsoil Loss</p>	<p style="text-align: center;">Net Topsoil Loss</p>	<p style="text-align: center;">Net Topsoil Loss</p>
Lognormal M2	<p style="text-align: center;">Net Topsoil Loss</p>	<p style="text-align: center;">Net Topsoil Loss</p>	<p style="text-align: center;">Net Topsoil Loss</p>
Uniform M1	<p style="text-align: center;">Net Topsoil Loss</p>	<p style="text-align: center;">Net Topsoil Loss</p>	<p style="text-align: center;">Net Topsoil Loss</p>

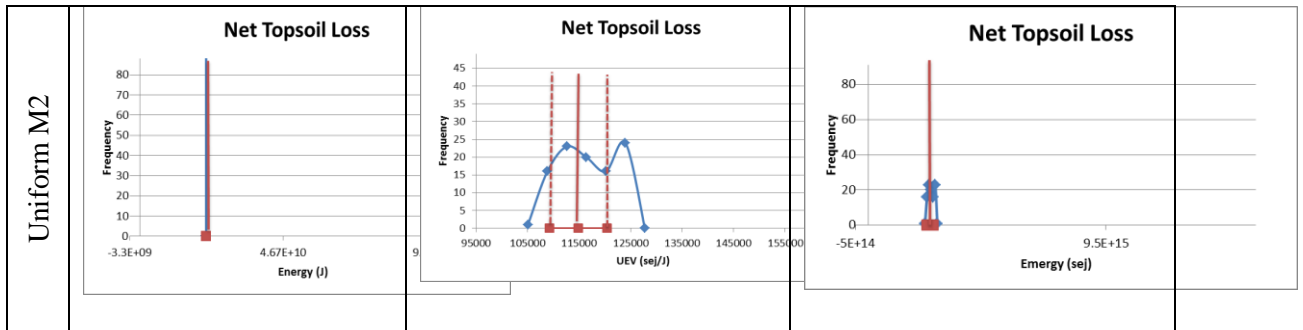


Figure 7d: Monte Carlo simulation graphs for net topsoil loss source. The rows show the graphs specific for each distribution (Normal, Lognormal, and Uniform) and model (M1 and M2). The columns show on the x-axis the energy/mass, UEV, and energy for each graph, while the y-axis is the frequency of occurrence. The arithmetic mean is shown in a solid red line with one standard deviation shown as dashed red lines.

The majority of the variance in the net topsoil loss solar energy source was from the energy/mass estimate, while only a small amount was from the UEV of net topsoil loss. This is seen by the similarities between the energy and energy graphs (Figure 7d), as well as the much lower variance of the energy graphs in the Model 2 rows compared to the Model 1 rows. Assumption of the PDFs for net topsoil loss energy and UEV affected the PDF of the solar energy contributed by net topsoil loss (Figure 7d). Assuming normal PDFs for both the net topsoil loss energy and UEV produced a bell-shaped PDF for the net topsoil loss solar energy. Assuming a log-normal for both the net topsoil loss energy and UEV produced a PDF that more closely resembled a log-normal distribution with its right-skewed tail (Figure 7d). Assuming uniform PDFs for both net topsoil loss energy and UEV produced a PDF resembling a uniform distribution (Figure 7d). Regardless of which type of PDF was assumed, most of the variance originated from the estimate of the net topsoil loss energy rather than its UEV (Figure 7d).

Normal M1	<p style="text-align: center;">Electricity</p>	<p style="text-align: center;">Electricity</p>	<p style="text-align: center;">Electricity</p>
Normal M2	<p style="text-align: center;">Electricity</p>	<p style="text-align: center;">Electricity</p>	<p style="text-align: center;">Electricity</p>
Lognormal M1	<p style="text-align: center;">Electricity</p>	<p style="text-align: center;">Electricity</p>	<p style="text-align: center;">Electricity</p>
Lognormal M2	<p style="text-align: center;">Electricity</p>	<p style="text-align: center;">Electricity</p>	<p style="text-align: center;">Electricity</p>
Uniform M1	<p style="text-align: center;">Electricity</p>	<p style="text-align: center;">Electricity</p>	<p style="text-align: center;">Electricity</p>

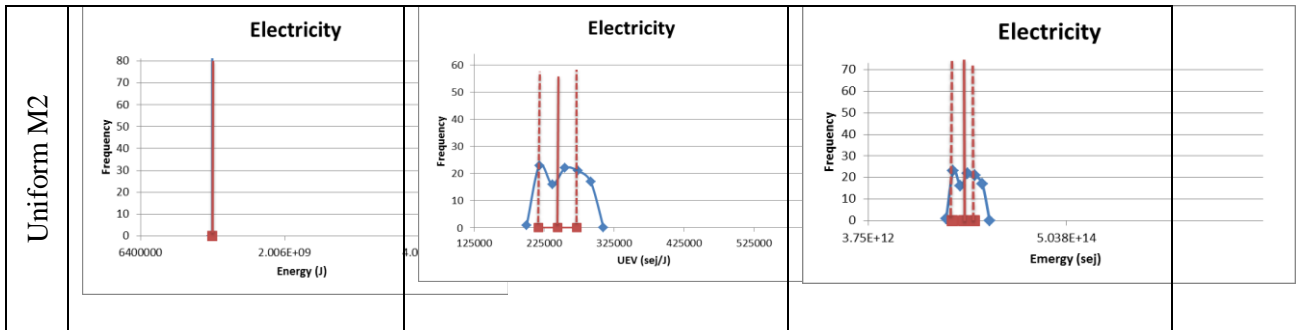


Figure 7e: Monte Carlo simulation graphs for electricity source. The rows show the graphs specific for each distribution (Normal, Lognormal, and Uniform) and model (M1 and M2). The columns show on the x-axis the energy/mass, UEV, and energy for each graph, while the y-axis is the frequency of occurrence. The arithmetic mean is shown in a solid red line with one standard deviation shown as dashed red lines.

The majority of the variance in the electricity solar energy source was from the energy/mass estimate, while a smaller amount was from the UEV of electricity.

The variance of the electricity is larger than the other sources studied so far, and seems to affect the shape of the energy curve (Figure 7e). Assumption of the PDFs for electricity energy and UEV affected the PDF of the solar energy contributed by electricity (Figure 7e).

Assuming normal PDFs for both the electricity energy and UEV produced a bell-shaped PDF for the electricity solar energy. Assuming a log-normal for both the electricity energy and UEV produced a PDF that more closely resembled a log-normal distribution with its right-skewed tail (Figure 7e).

Assuming uniform PDFs for both electricity energy and UEV produced a PDF resembling a uniform distribution (Figure 7e).

Normal M1	<p style="text-align: center;">Labor</p>	<p style="text-align: center;">Labor</p>	<p style="text-align: center;">Labor</p>
Normal M2	<p style="text-align: center;">Labor</p>	<p style="text-align: center;">Labor</p>	<p style="text-align: center;">Labor</p>
Lognormal M1	<p style="text-align: center;">Labor</p>	<p style="text-align: center;">Labor</p>	<p style="text-align: center;">Labor</p>
Lognormal M2	<p style="text-align: center;">Labor</p>	<p style="text-align: center;">Labor</p>	<p style="text-align: center;">Labor</p>
Uniform M1	<p style="text-align: center;">Labor</p>	<p style="text-align: center;">Labor</p>	<p style="text-align: center;">Labor</p>

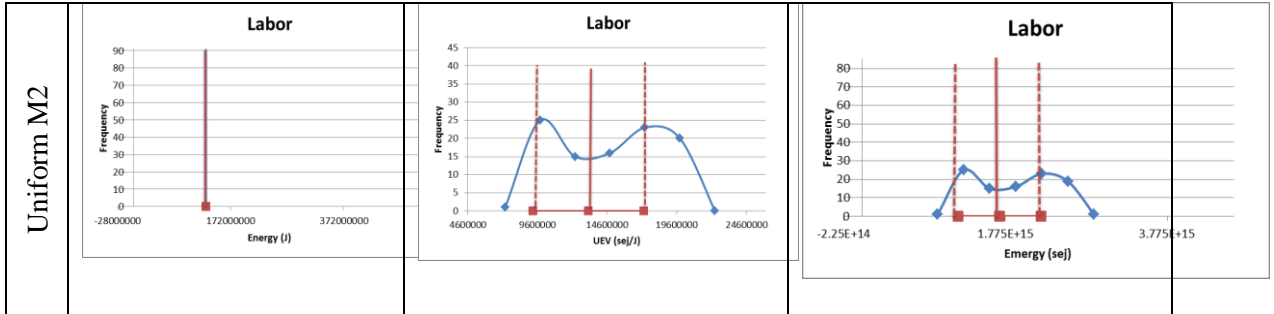
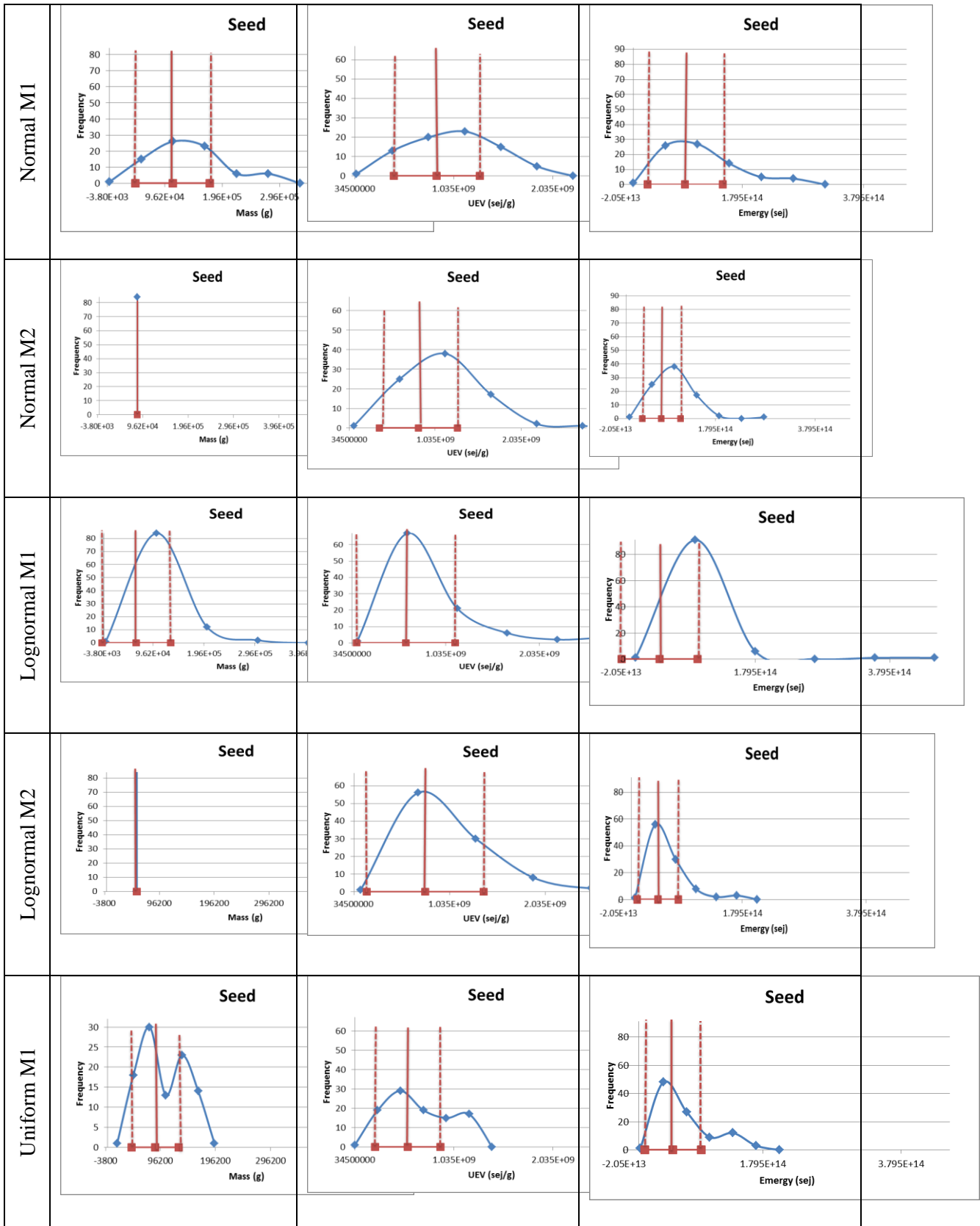


Figure 7f: Monte Carlo simulation graphs for labor source. The rows show the graphs specific for each distribution (Normal, Lognormal, and Uniform) and model (M1 and M2). The columns show on the x-axis the energy/mass, UEV, and energy for each graph, while the y-axis is the frequency of occurrence. The arithmetic mean is shown in a solid red line with one standard deviation shown as dashed red lines.

The majority of the variance in the labor solar energy source was from the energy/mass estimate, while a smaller amount was from the UEV of labor (Figure 7f). Assumption of the PDFs for labor energy and UEV affected the PDF of the solar energy contributed by labor (Figure 7f). Assuming normal PDFs for both the labor energy and UEV produced a skewed bell-shaped PDF for the labor solar energy. The standard deviation of the original systems for labor was large, meaning that some values produced by the model were negative. These values were discarded, making a smaller left tail and skewed curve shape for the normal PDF. Assuming a log-normal for both the labor energy and UEV produced a PDF that more closely resembled a log-normal distribution with its right-skewed tail (Figure 7f). Assuming uniform PDFs for both labor energy and UEV produced a PDF resembling a uniform distribution (Figure 7f). The uniform PDF shows less of energy/mass parameter variance than the other two distributions (Figure 7f).



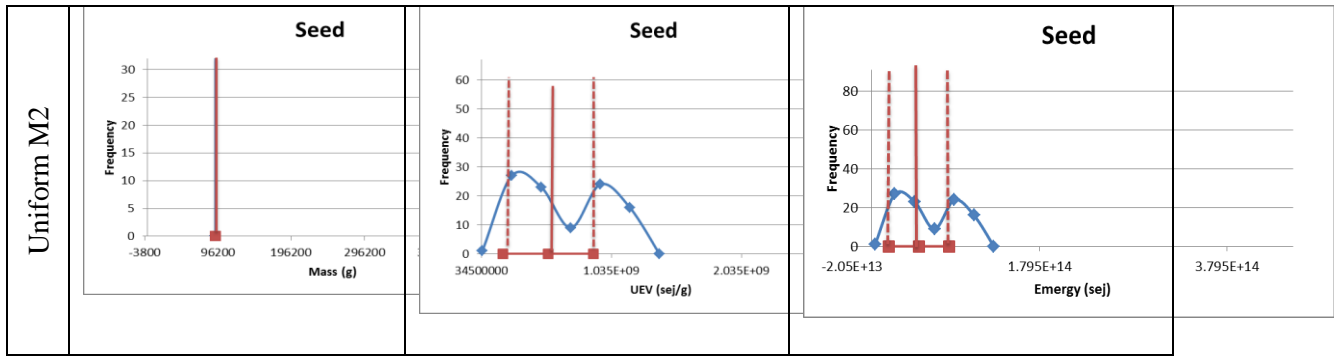
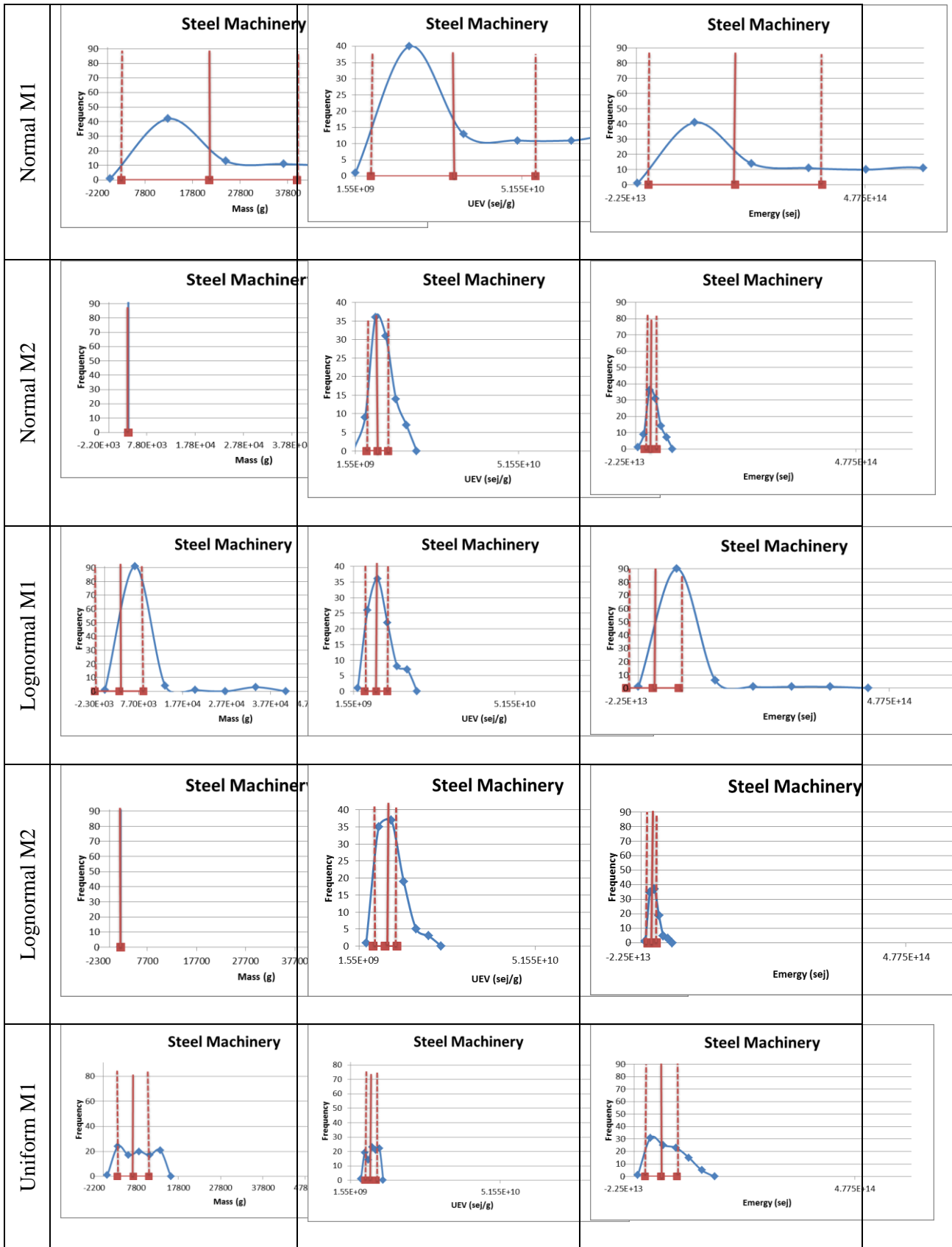


Figure 7g: Monte Carlo simulation graphs for seed source. The rows show the graphs specific for each distribution (Normal, Lognormal, and Uniform) and model (M1 and M2). The columns show on the x-axis the mass, UEV, and energy for each graph, while the y-axis is the frequency of occurrence. The arithmetic mean is shown in a solid red line with one standard deviation shown as dashed red lines.

The variance in the seed solar energy source was split somewhat evenly between the mass estimate and the UEV of seed (Figure 7g). When energy/mass variance is removed from the system (moving from Model 1 to Model 2), the distance of the red lines in the energy graphs shorten slightly (Figure 7g). For sources such as evapotranspiration, the change from Model 1 to Model 2 in the energy column has greatly decreased the distance of the red lines (Figure 7b). This implies that the energy variance is much more significant for evapotranspiration than seed. Assumption of the PDFs for seed mass and UEV affected the PDF of the solar energy contributed by seed (Figure 7g). Assuming normal PDFs for both the seed mass and UEV produced a bell-shaped PDF for the seed solar energy. Assuming a log-normal for both the seed mass and UEV produced a PDF that more closely resembled a log-normal distribution with its right-skewed tail (Figure 7g). Assuming uniform PDFs for both seed mass and UEV produced a PDF resembling a uniform distribution (Figure 7g).



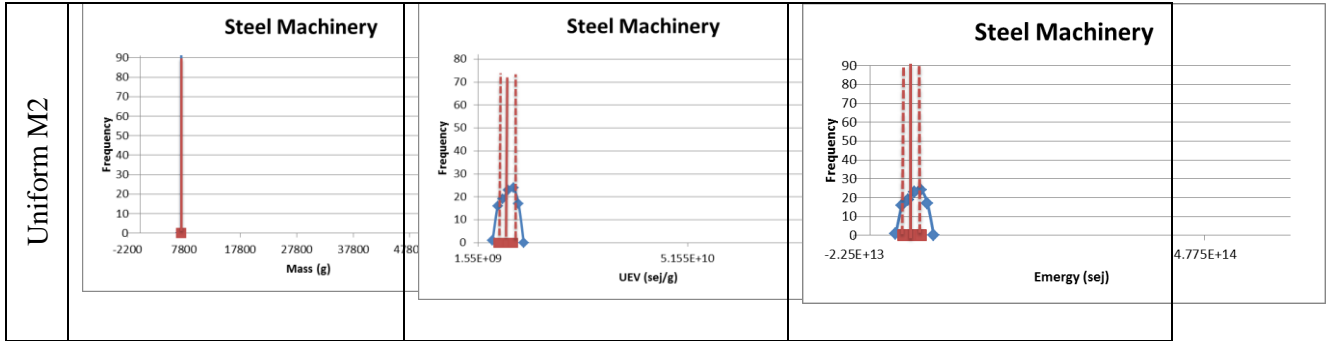
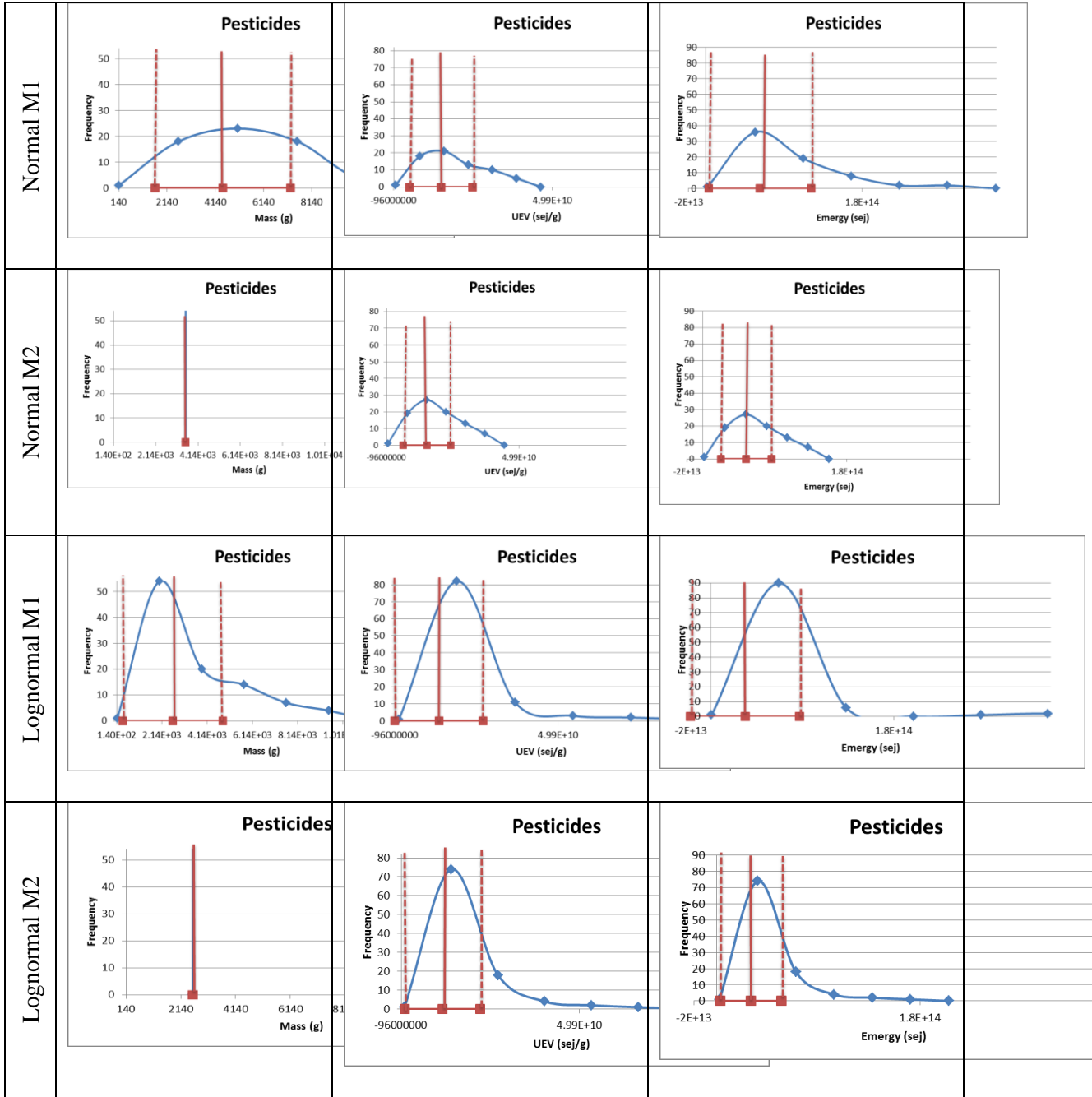


Figure 7h: Monte Carlo simulation graphs for steel machinery source. The rows show the graphs specific for each distribution (Normal, Lognormal, and Uniform) and model (M1 and M2). The columns show on the x-axis the mass, UEV, and energy for each graph, while the y-axis is the frequency of occurrence. The arithmetic mean is shown in a solid red line with one standard deviation shown as dashed red lines.

The majority of the variance in the steel machinery solar energy source was from the mass estimate, while a smaller amount was from the UEV of steel machinery (Figure 7h). Assumption of the PDFs for steel machinery energy and UEV affected the PDF of the solar energy contributed by steel machinery (Figure 7h). Assuming normal PDFs for both the steel machinery mass and UEV produced a PDF for the steel machinery solar energy that was not quite bell shaped due to the need to take out negative values from the model. Assuming a log-normal for both the steel machinery mass and UEV produced a PDF that more closely resembled a log-normal distribution with its right-skewed tail (Figure 7h). Assuming uniform PDFs for both steel machinery mass and UEV produced a PDF resembling a uniform distribution (Figure 7h). The normal PDF shows most of the variance originating from the estimate of the steel machinery mass rather than its UEV (Figure 7h). The lognormal

and uniform PDFs were also affected by the removal of the energy/mass variance, but to a lesser extent.



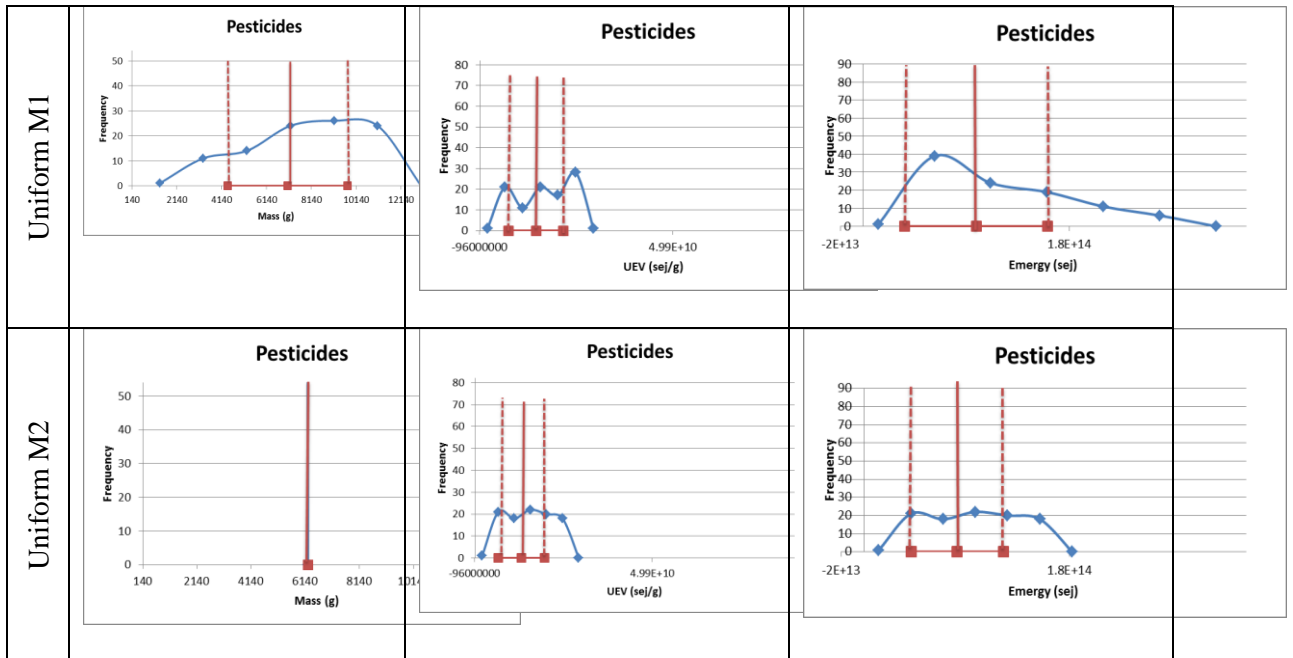
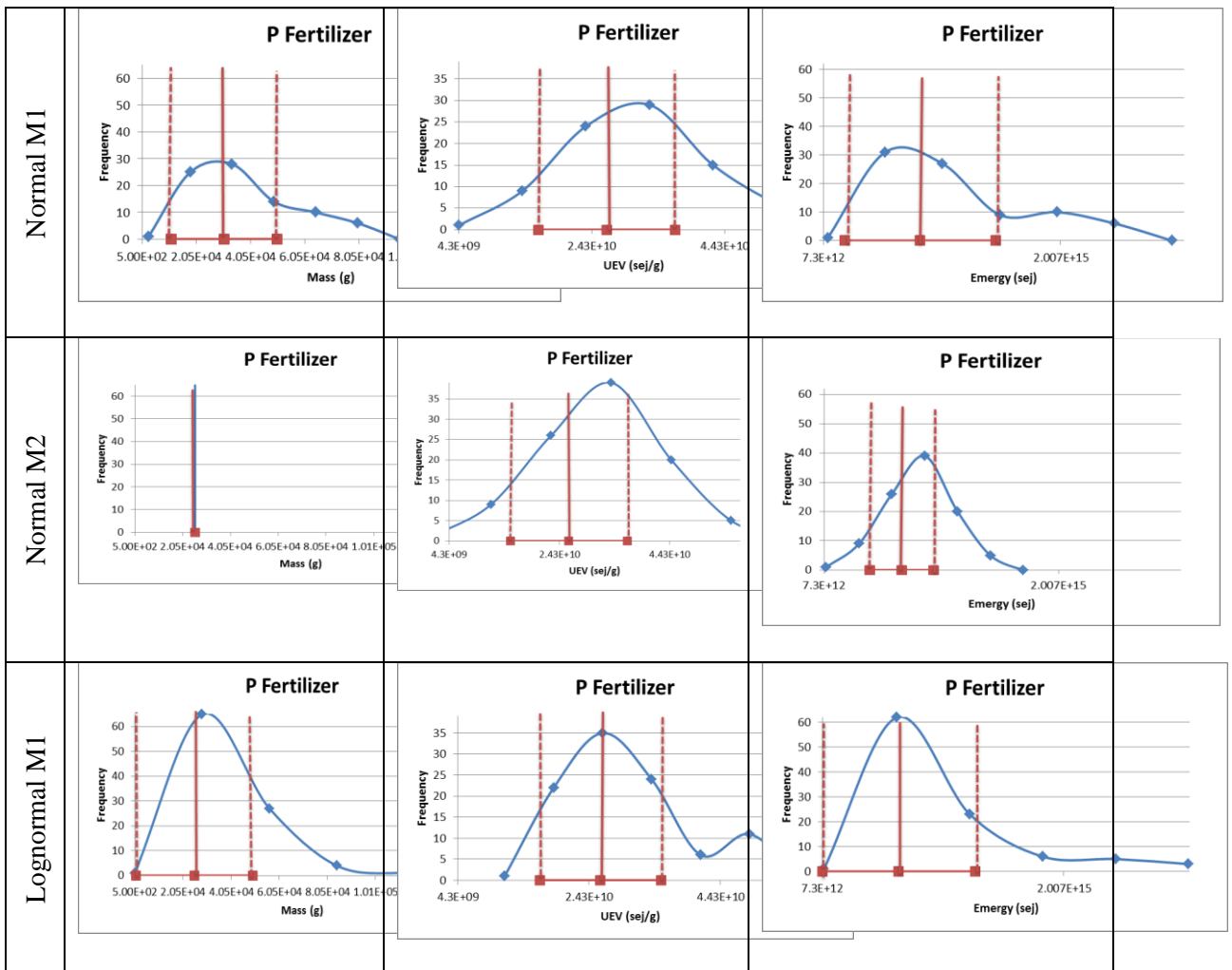


Figure 7i: Monte Carlo simulation graphs for pesticides source. The rows show the graphs specific for each distribution (Normal, Lognormal, and Uniform) and model (M1 and M2). The columns show on the x-axis the mass, UEV, and energy for each graph, while the y-axis is the frequency of occurrence. The arithmetic mean is shown in a solid red line with one standard deviation shown as dashed red lines.

The variance in the pesticides solar energy source was split somewhat evenly between the mass estimate and the UEV of pesticides (Figure 7i). When energy variance is removed from the system (moving from Model 1 to Model 2), the distance of the red lines in the energy graphs shorten slightly (Figure 7i). For sources such as evapotranspiration, the change from Model 1 to Model 2 in the energy column has greatly decreased the distance of the red lines (Figure 7b). This implies that the energy/mass variance is much more significant for evapotranspiration than pesticides. Assumption of the PDFs for pesticides mass and UEV affected the PDF of the solar energy contributed by pesticides (Figure 7i). Assuming normal PDFs for both the pesticides mass and UEV produced a skewed bell-shaped PDF for the pesticides solar

energy. The standard deviation of the original systems for pesticides was large, meaning that some values produced by the model were negative. These values were discarded, making a skewed curve shape for the normal PDF. Assuming a log-normal for both the pesticides mass and UEV produced a PDF that more closely resembled a log-normal distribution with its right-skewed tail (Figure 7i). Assuming uniform PDFs for both pesticides mass and UEV produced a PDF resembling a uniform distribution (Figure 7i).



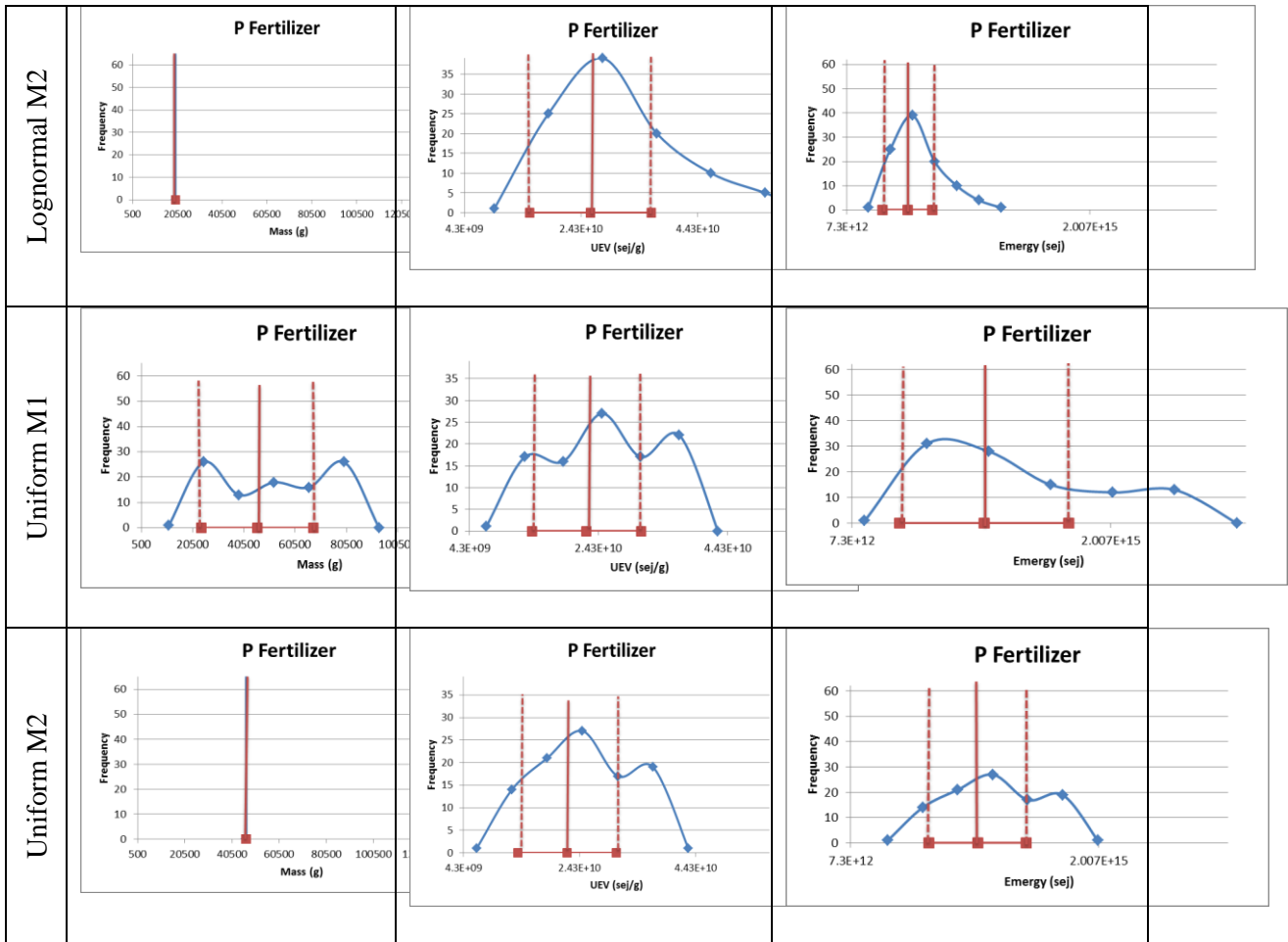
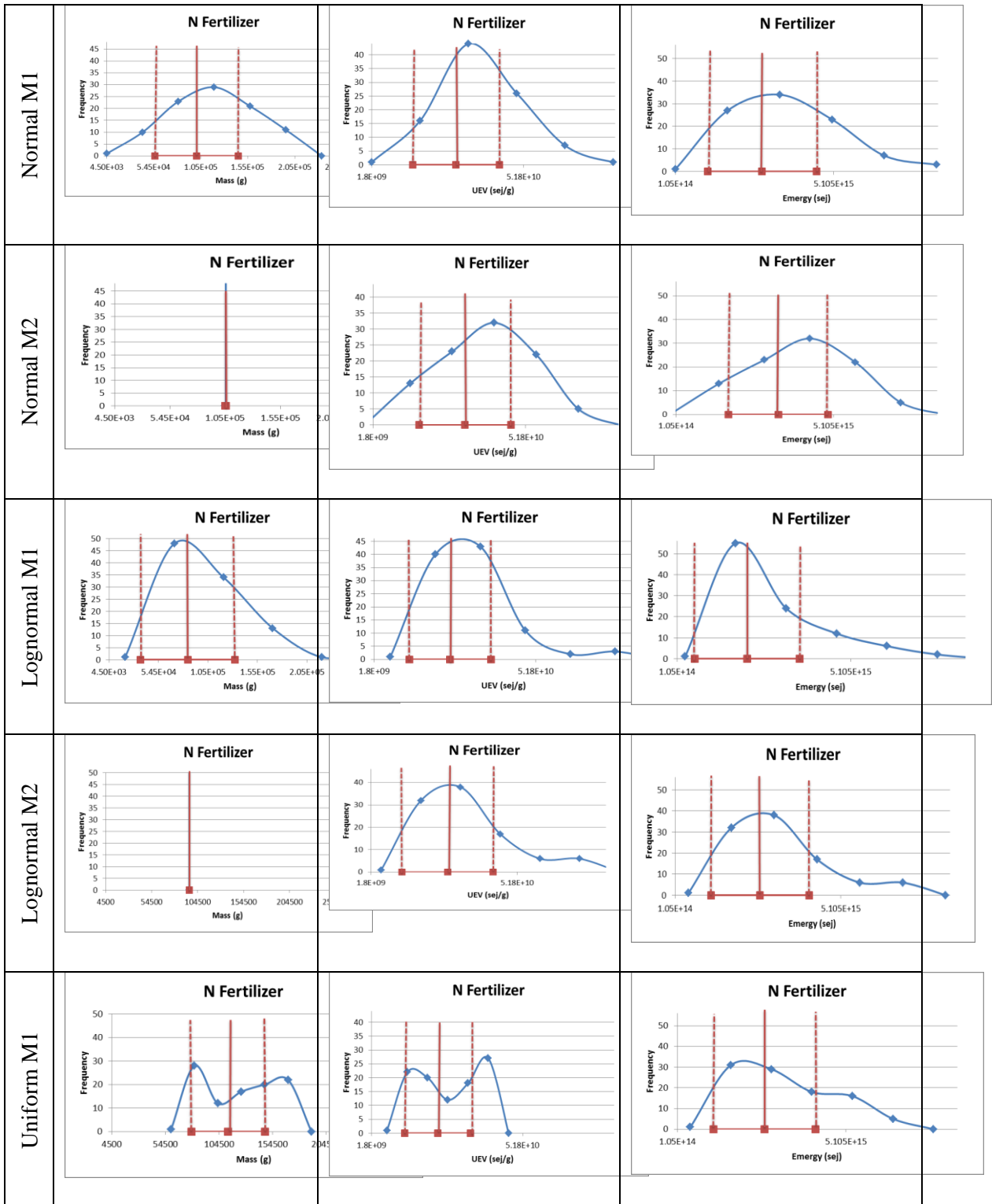


Figure 7j: Monte Carlo simulation graphs for phosphate fertilizer source. The

rows show the graphs specific for each distribution (Normal, Lognormal, and Uniform) and model (M1 and M2). The columns show on the x-axis the mass, UEV, and energy for each graph, while the y-axis is the frequency of occurrence. The arithmetic mean is shown in a solid red line with one standard deviation shown as dashed red lines.

A smaller amount of the variance in the phosphate fertilizer solar energy source was from the mass estimate. The UEV variance of phosphate fertilizer was a major component of uncertainty in solar energy of the phosphate fertilizer source (Figure 7j). Assumption of the PDFs for phosphate fertilizer mass and UEV affected the PDF of the solar energy contributed by phosphate fertilizer (Figure 7j). Assuming

normal PDFs for both the phosphate fertilizer mass and UEV produced a bell-shaped PDF for the phosphate fertilizer solar energy. Assuming a log-normal for both the phosphate fertilizer mass and UEV produced a PDF that more closely resembled a log-normal distribution with its right-skewed tail (Figure 7j). Assuming uniform PDFs for both the phosphate fertilizer mass and UEV produced a PDF resembling a uniform distribution (Figure 7j).



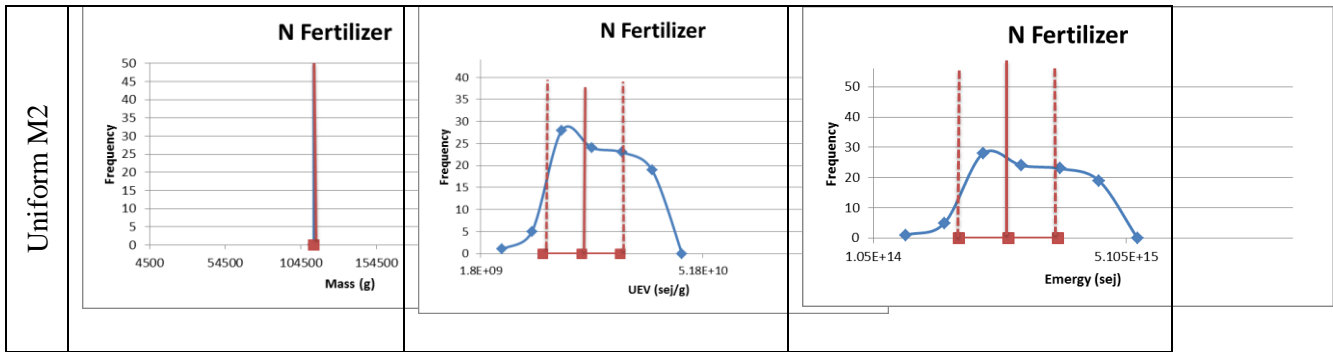


Figure 7k: Monte Carlo simulation graphs for nitrogen fertilizer source. The

rows show the graphs specific for each distribution (Normal, Lognormal, and Uniform) and model (M1 and M2). The columns show on the x-axis the mass, UEV, and energy for each graph, while the y-axis is the frequency of occurrence. The arithmetic mean is shown in a solid red line with one standard deviation shown as dashed red lines.

The majority of the variance in the nitrogen fertilizer solar energy source was from the UEV input (Figure 7k). There was barely any change in the distance between the red lines in the energy graphs when energy/mass variance was removed from the system (moving from Model 1 to Model 2) (Figure 7k). For sources such as evapotranspiration, the change from Model 1 to Model 2 in the energy column had greatly decreased the distance of the red lines (Figure 7b). This implies that the energy variance is much more significant for evapotranspiration than nitrogen fertilizer. Assumption of the PDFs for nitrogen fertilizer mass and UEV affected the PDF of the solar energy contributed by nitrogen fertilizer (Figure 7k). Assuming normal PDFs for both the nitrogen fertilizer mass and its UEV produced a bell-shaped PDF for the nitrogen fertilizer solar energy. Assuming a log-normal for both the nitrogen fertilizer mass and UEV produced a PDF that more closely resembled a log-normal distribution with a right-skewed tail (Figure 7k). Assuming uniform PDFs for

both nitrogen fertilizer mass and UEV produced a PDF that ended up resembling a lognormal PDF (Figure 7k). The Model 1 graphs of both the normal and uniform PDFs showed a slight lognormal tendency.

Normal M1			
Normal M2			
Lognormal M1			
Lognormal M2			
Uniform M1			

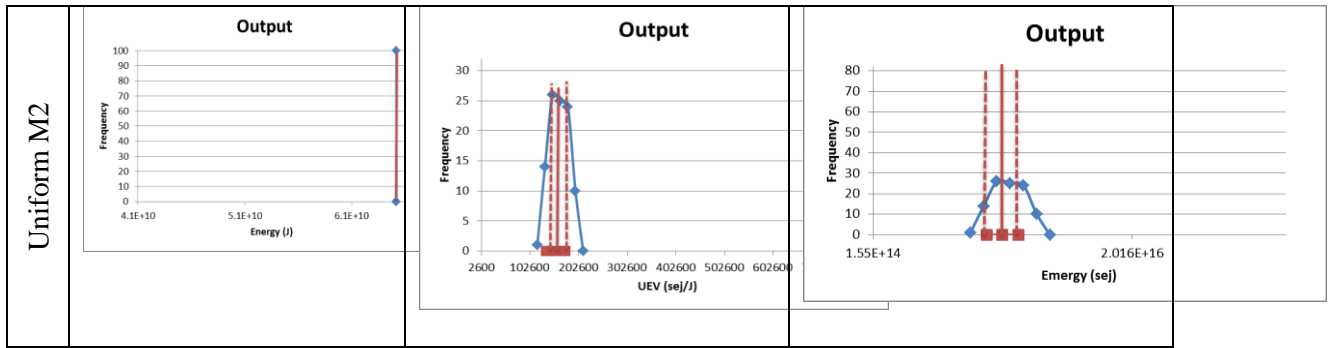


Figure 71: Monte Carlo simulation graphs for the output. The rows show the graphs specific for each distribution (Normal, Lognormal, and Uniform) and model (M1 and M2). The columns show on the x-axis the energy, UEV, and energy for each graph, while the y-axis is the frequency of occurrence. The arithmetic mean is shown in a solid red line with one standard deviation shown as dashed red lines.

The variance in the output energy was split somewhat evenly between the energy input energy estimate and the UEV of Seed (Figure 71). There was some change in the distance between the red lines in the energy graphs when energy/mass variance was removed from the system (moving from Model 1 to Model 2) (Figure 71). The shift was not as extreme as in the cases of sunlight and evapotranspiration, implying that the energy variance is much more significant for sunlight and evapotranspiration than the output. Assumption of the PDFs for the energy and UEV affected the PDF of the solar energy of the output (Figure 71). Assuming normal PDFs for both the energy and UEV produced a bell-shaped PDF. Assuming a log-normal PDF for both the energy and UEV produced a PDF that resembled a log-normal distribution with a right-skewed tail (Figure 71). Assuming a uniform PDF for the input energy and UEV produced a PDF resembling a uniform distribution (Figure 71).

In summary, there were seven sources with a large energy/mass variance. These sources were sunlight, evapotranspiration, fuel, net topsoil loss, electricity, labor, and steel machinery. Energy/mass variance for the seeds, pesticides, phosphate and nitrogen fertilizer sources and the output seem to be less of a major influence on their energy variance than the afore-mentioned sources. The energy variance for nitrogen fertilizer in particular barely changed as energy/mass variance was removed from the model. This implies that nitrogen fertilizer had a UEV variance that contributed the majority of the variance to the energy variance.

For the most part, the PDFs assigned to the inputs matched the PDF of the resulting energy output. However, some inputs with a normal or uniform PDF produced a lognormal PDF for the energy output.

Objectives 1 and 3 have been qualified in this section visually. In the previous Monte Carlo simulations' model comparison section, the normal distribution was used to quantify the effect of specific sources on output UEV variance. Now we move on to quantify by each PDF for each source the energy/mass and UEV inputs' impact on the variance of the output UEV.

Sensitivity analysis

Sensitivity analyses were conducted to determine which energy/mass and UEVs influenced the mean value of the yield UEV and its variance and by how much. Each probability distribution was tested in the sensitivity analysis to also determine the impact of the source's PDF on the yield UEV variance.

The first sensitivity analysis involved sequentially removing the variance of each source's energy/mass and UEV inputs in the energy/mass and UEV variance

model, while the second analysis removed the UEV variance of each source sequentially. The sensitivity of yield UEV to the variance of each source was determined by comparing to baseline conditions.

The yield UEV's and their standard deviations for the baseline and each run of the sensitivity analysis are given in Table 8a for the Energy/Mass and UEV Model, while the same type of energy/mass for the UEV Only Model is given in Table 9a. Tables 8b and 9b show the percent difference between the baseline and the Monte Carlo generated output for each system input.

Model 1: Energy/mass and UEV variance

The mean UEV for crop yield was 120,000 sej/J with a standard deviation of 53,000 sej/J when all the variance of all energy/mass and UEV inputs were included in the simulations and the normal PDF was assumed (Table 9a). When the variance of each input was removed, only three energy/mass inputs were found to affect the mean UEV of crops (ET, machinery and phosphorus), but two different energy/mass inputs (soil loss and nitrogen fertilizer) affected the uncertainty in the UEV (Table 9a).

Removing the variance due to ET, machinery and phosphorus increased the yield UEV by about 15% to 140,000 sej/J (Table 9a and 9b). Removing the variance due to net topsoil loss and nitrogen fertilizer reduced the standard deviation of the corn by about 23% to 41,000 sej/J. The mean shifts for the normal distribution hint that variance was lowered by eliminating values from a specific tail, which may be an interesting path to pursue. It is assumed that the variance would be removed from the left tail as it extends to negative infinity, since energy can't be expressed negatively. This is confirmed by seeing a shift in the means to the right, as all new means have

larger values than the original output with generally smaller standard deviations.

While the natural variance of five of the eleven sources was large enough to affect the uncertainty of the output UEV, the simulation also indicated that six of eleven had no affect because their natural variance was too small.

The mean UEV for crop yield was 160,000 sej/J with a standard deviation of 86,000 sej/J when all the variance of all energy/mass and UEV inputs were included in the simulations and the lognormal PDF was assumed (Table 9a). When the variance of each input was removed, only two energy/mass inputs were found to affect the mean UEV of corn (ET, and nitrogen fertilizer), but seven different energy/mass inputs (sunlight, et, fuel, soil loss, steel machinery, pesticides, and nitrogen fertilizer) affected the uncertainty in the UEV (Table 9a). Removing the variance due to ET, and nitrogen fertilizer decreased the mean yield UEV by about 18% to 130,000 sej/J and 41% to 94,000 respectively (Table 9a and 9b). As variance is lowered, the lognormal distribution would have fewer values come from the right tail as it extends to positive infinity, explaining the shift of the mean to the left on the x-axis. Removing the variance due to sunlight, Evapotranspiration, fuel, net topsoil loss, steel machinery, and pesticides reduced the standard deviation of the corn by about 30% to 60,000 sej/J. When the variance due to nitrogen fertilizer is removed, the standard deviation was reduced by 57% to 37,000. While the natural variance of seven of the eleven sources was large enough to affect the uncertainty of the output UEV, the simulation also indicated that 4 of 11 had no affect because their natural variance was too small.

The mean UEV for crop yield was 170,000 sej/J with a standard deviation of 43,000 sej/J when all the variance of all energy/mass and UEV inputs were included in the simulations and the uniform PDF was assumed (Table 9a). When the variance of each input was removed, three energy inputs were found to affect the mean UEV of corn (fuel, net topsoil loss, and labor), and four different energy inputs (soil loss, labor, pesticides, and nitrogen fertilizer) affected the uncertainty in the UEV (Table 9a). Removing the variance due to fuel and labor decreased the mean output UEV by about 10% to 150,000 sej/J. When the variance due to net topsoil loss was removed, the mean output UEV was reduced by 21% to 130,000 (Table 9a and 9b). Removing the variance due to soil loss, labor, pesticides, and nitrogen fertilizer reduced the standard deviation of the corn by about 23% to 60,000 sej/J. While the natural variance of seven of the eleven sources was large enough to affect the uncertainty of the output UEV, the simulation also indicated that four of eleven had no affect because their natural variance was too small.

Table 9a: Model 1 sensitivity results. The mean and standard deviation for the generated output UEV when minimizing the variance of a source, and its significance in comparison to the baseline. † (Values are shown below multiplied by 1E3)						
	Normal		Lognormal		Uniform	
	Mean	Stddev	Mean	Stddev	Mean	Stddev
Baseline output	118	53.0	159	85.9	170	43
Sunlight	118	53.0	127	55.1**	174	39.7
Evapo-transpiration	135*	57.9	131**	64.4**	170	42.9
Fuel	127	48.9	147	61**	154**	41.4
Net topsoil loss	125	41.2**	139	63.8**	134**	33.4**
Electricity	126	47.6	164	78.9	170	42.3
Labor	122	46.2	148	73.9	146**	34.1*
Seed	127	47.9	159	75.2	166	42.5
Steel machinery	137*	51.7	158	63.8**	182	43.3
Pesticides	132	50.4	159	63.1**	167	34.3**
P Fertilizer	135*	46.5	153	74.0	166	40.1
N Fertilizer	125	40.9**	93.3**	37.3**	161	32.3**

† Specific *p* values are provided in Appendix iii

*Significance of $p < 0.05$

**Significance of $p < 0.01$

We can see from Table 9a that nitrogen fertilizer and net topsoil loss were the only sources that had a significant impact on the output UEV variance across the distributions ($p < 0.01$). Table 9b was created to quantify the mean and variance shift from the baseline when a source's energy and UEV variances were removed from Model 1.

Table 9b: Model 1 % difference of each output from the baseline. †						
	Normal		Lognormal		Uniform	
	Mean	Stddev	Mean	Stddev	Mean	Stddev
Baseline output	0	0	0	0	0	0
Sunlight	0	0	-20.1	-35.9**	2.35	-7.67
Evapo-transpiration	14.4*	9.25	-17.6**	-25.0**	0	-0.233
Fuel	7.63	-7.74	-7.55	-29.0**	-9.41**	-3.72
Net topsoil loss	5.93	-22.3**	-12.6	-25.7**	-21.2**	-22.3**
Electricity	6.78	-10.2	3.14	-8.15	0	-1.63
Labor	3.39	-12.8	-6.92	-14.1	-14.1**	-20.7*
Seed	7.63	-9.62	0	-12.5	-2.35	-1.16
Steel machinery	16.1*	-2.45	-0.629	-25.7**	7.06	0.698
Pesticides	11.9	-4.91	0	-26.5**	-1.76	-20.2*
P Fertilizer	14.4*	-12.3	-3.77	-13.9	-2.35	-6.74
N Fertilizer	5.93	-22.8**	-41.3**	-56.6**	-5.29	-24.9**

† Specific *p* values are provided in Appendix iii

*Significance of $p < 0.05$

**Significance of $p < 0.01$

The nitrogen fertilizer and net topsoil loss sources had the most consistent impact on the output UEV across the distributions. Minimizing the variance of the nitrogen fertilizer source lowered the variance of the output UEV by ~23% for the normal distribution, ~57% for the lognormal distribution, and ~25% for the uniform distribution (Table 9b). Minimizing the variance of the net topsoil loss source lowered the variance of the output UEV by ~22% for the normal distribution, ~26% for the lognormal distribution, and ~22% for the uniform distribution (Table 9b).

Seed and electricity were the only sources that did not have a significant effect on the mean or variance of the output UEV, for any distribution according to the sensitivity analysis. Phosphate fertilizer had the next weakest showing, only

significantly changing the mean of the output UEV in the normal distribution (~14%, $p < 0.05$).

Sunlight and evapotranspiration were expected to have no real impact on the output UEV. The original eight systems had minimal variance in the UEV of evapotranspiration, and no variance for the UEV of sunlight (by definition). However, minimizing these source's variances produced a significant difference in the output UEV's variance and means for certain distributions. The evapotranspiration source showed a significant mean shift in the output for the normal (~14%, $p < 0.03$) and lognormal (~18%, $p < 0.01$) distributions. The lognormal distribution also produced a significant change in the variance of the output UEV when the Evapotranspiration source was minimized in variance (~25%, $p < 0.01$). There are large amounts of uncertainty in Model 1 for sunlight and Evapotranspiration with the energy values being able to fluctuate. These unexpected results for the sunlight and evapotranspiration sources are indicators that Model 1 may include too much uncertainty to allow for an accurate depiction of an source's effect on the output.

Model 2: UEV variance

The mean UEV for crop yield was 124,000 sej/J with a standard deviation of 26,400 sej/J when all the variance from UEVs were included in the simulations and the normal PDF was assumed (Table 10a). When the variance of each UEV was removed, three sources were found to affect the mean UEV of crops (fuel, labor and machinery), while only machinery and nitrogen fertilizer affected the variance (Table 10a). Removing the variance due to fuel, labor, and machinery increased the UEV by 5 to 10% to 131,000-137,000 sej/J (Table 10a and 10b). Removing the variance due

to machinery and nitrogen fertilizer reduced the standard deviation of the crops by 19% to 21,400 sej/J and 76% to 6,300 sej/J respectively.

The mean UEV for crop yield was 136,000 sej/J with a standard deviation of 33,800 sej/J when all the variance from UEVs were included in the simulations and the lognormal PDF was assumed (Table 10a). When the variance of each UEV was removed, only the nitrogen fertilizer source was found to affect the mean UEV of crops and the variance (Table 10a). Removing the variance due to nitrogen fertilizer lowered the mean UEV by 11% to 115,000 sej/J (Table 10a and 10b) and lowered the standard deviation of the crops by 85% to 5,070 sej/J.

The mean UEV for crop yield was 154,000 sej/J with a standard deviation of 20,300 sej/J when all the variance from UEVs were included in the simulations and the uniform PDF was assumed (Table 10a). When the variance of each UEV was removed, no sources were found to affect the mean UEV of crops, while nitrogen fertilizer effected the variance (Table 10a). Removing the variance due to nitrogen fertilizer lowered the standard deviation of the crops by 55% to 9,140 sej/J.

When non-normal PDFs were assumed, the UEV of nitrogen fertilizer was the only system source that affected the UEV of the output (Table 10a). Thus, the effect of UEV uncertainty depends on which PDF is assumed. It is also worth noting that the non-normal PDFs produced larger UEVs for the output (136,000 and 154,000 sej/J) than the normal PDF (124,000 sej/J) (Table 10a).

Table 10a: Model 2 sensitivity results. The mean and standard deviation for the generated output UEV when minimizing the variance of a source, and its significance in comparison to the baseline. † (Values are shown below multiplied by 1E3)

	Normal		Lognormal		Uniform	
	Mean	Stddev	Mean	Stddev	Mean	Stddev
Baseline output	124	26.4	136	33.8	154	20.3
Sunlight	128	26.9	130	27.6	155	19.4
Evapo-transpiration	128	27.1	132	29.5	157	20.7
Fuel	137**	28	132	38.5	155	19.7
Net topsoil loss	127	24.7	128	28.4	159	20.5
Electricity	127	28.1	133	38	157	20.1
Labor	132*	24.4	131	31.5	155	16.9
Seed	125	25.7	131	35.6	154	20.7
Steel machinery	131*	21.4*	130	29.4	156	21.2
Pesticides	129	25.8	132	35.8	158	18.5
P Fertilizer	129	25	132	34.8	151	19.9
N Fertilizer	128	6.3**	120**	5.1**	155	9.1**

† Specific p values are provided in Appendix iii

*Significance of $p < 0.05$

**Significance of $p < 0.01$

We can see from Table 10a that nitrogen fertilizer was the only source that significantly lowers the output UEV variance across the distributions ($p < 0.01$). Table 10b was created to quantify the mean and variance shift from the baseline when a source's energy/mass and UEV variances were removed from Model 1.

Table 10b: Model 2 % difference of each output from the baseline. †						
	Normal		Lognormal		Uniform	
	Mean	Stddev	Mean	Stddev	Mean	Stddev
Baseline output	0	0	0	0	0	0
Sunlight	3.23	1.89	-4.41	-18.3	0.649	-4.43
Evapo-transpiration	3.23	2.65	-2.94	-12.7	1.95	1.97
Fuel	10.5*	6.06	-2.94	13.9	0.649	-2.96
Net topsoil loss	2.42	-6.44	-5.88	-16.0	3.25	0.990
Electricity	2.42	6.44	-2.21	12.4	1.95	-0.990
Labor	6.45*	-7.58	-3.68	-6.80	0.650	-16.8
Seed	0.810	-2.65	-3.68	5.33	0	1.97
Steel machinery	5.65*	-18.9*	-4.41	-13.0	1.30	4.43
Pesticides	4.03	-2.27	-2.94	5.92	2.60	-8.87
P Fertilizer	4.03	-5.30	-2.94	2.96	-1.95	-1.97
N Fertilizer	3.23	-76.1**	-11.0**	-84.9**	0.650	-55.0**

† Specific *p* values are provided in Appendix iii

*Significance of *p* <0.05

**Significance of *p* <0.01

Machinery and nitrogen fertilizer were the only two system sources whose UEV uncertainty had a significant effect on the uncertainty of the output UEV (Table 10a). This was true for nitrogen fertilizer regardless of the PDF assumed. Examining Table 10b shows that minimizing the variance of the nitrogen fertilizer source has lowered the variance of the output UEV by ~76% for the normal distribution, ~85% for the lognormal distribution, and ~55% for the uniform distribution. Thus, the uncertainty in the UEV of nitrogen has a large impact on the uncertainty of crop production. In contrast, removing the uncertainty of each of the other system sources, with the exception of machinery, did not change the uncertainty in corn (output) UEV (Table 10a). When energy input data is known with high certainty, the uncertainty of input UEVs can affect the uncertainty of a crop's UEV. During the practice of

conducting an emergy evaluation of a modern cropping system that employs sources similar to the crop system studied here, this indicates that care should be given to selecting the most appropriate UEV for nitrogen, but that using a point estimate for the UEV of the other system sources is sufficient. From a general perspective, the observation that the uncertainty of the UEV of only 2 of 11 system sources affected the output UEV indicates that uncertainty in emergy evaluations is likely concentrated in a few system sources rather than broadly based.

Nitrogen fertilizer UEV was the only UEV input to have a significant effect on crop production output UEV across three input distributions. Crop system output has been known to correlate positively with nitrogen fertilizer use (Blumenthal et al. 2008). The large emergy value of nitrogen fertilizer source is supported by the literature that suggests that nitrogen is usually the most limiting factor on crop (corn and wheat) output. An increase in nitrogen fertilizer source generally results in increased protein concentration in grain crops (Blumenthal et al. 2008). Concerning Florida corn for grain production, nitrogen is the largest primary energy source (43.5%) (Fluck 1992). An emergy analyst can use the information in the current literature that nitrogen fertilizer is important to crop production combined with the fact that it contributes a large portion of emergy to the total emergy. Add a large variance, and the nitrogen fertilizer source stood out in importance. Doing a preliminary analysis should further specify whether more energy/mass data was needed or whether a source UEV needed to be calculated to best lower output UEV.

Model Comparison

The only two inputs that lowered the variance of the yield for all distributions were nitrogen fertilizer UEV and net topsoil loss energy/mass.

Removing the sources that impacted the standard deviation of the output UEV according to both models 1 and 2 left the sources whose energy/mass impacted the standard deviation of the output UEV. These sources were sunlight, Evapotranspiration, fuel, net topsoil loss, labor, steel machinery, and pesticides. This is seven out of twenty two parameters in the Monte Carlo simulation that significantly impacted the output UEV variance. Combined with the two UEV parameters of nitrogen fertilizer and steel machinery, there were nine out of twenty two parameters in a Monte Carlo simulated energy analysis that significantly impacted the output UEV for one of the three described distributions. Use of a specific distribution further narrowed down the list of inputs. Energy analysts of crop production should focus lowering the uncertainty of these specified inputs, thereby saving resources.

A trend was shown in comparing the two models conducted with different amounts of variance of energy/mass and the way distribution results differ between them. When more uncertainty was present in the system, the uniform distribution and the lognormal distribution had larger numbers of sources with significant differences in variance (uniform-4, lognormal-7) than the normal distribution (2 sources). There was a similar number of significantly different means between the distributions. When uncertainty was removed from the model (2), the lognormal and uniform distributions became much more conservative, with only one source having a significant variance shift. The normal distribution was much more consistent between

models in number of sources with significant differences in output. While the lognormal and uniform distributions converged to the case of the nitrogen fertilizer source providing the most significant effect on crop output, the normal distribution was only consistent with nitrogen fertilizer variance and steel machinery mean shift and changes the other 3 sources that significantly impacted the output.

To test the impacts of the PDF on the yield UEV variance quantitatively, the sensitivity analysis baselines for each distribution and model were compared for statistical significance. The distribution assigned to the Monte Carlo inputs was determined to affect the mean and the variance of the yield UEV. For Model 1, differences between the yield UEV means and standard deviations of the uniform PDF and the normal PDF were significant ($p < 0.001$). This was also the case for the lognormal and the normal PDFs ($p < 0.001$). The uniform and the lognormal PDF had a similar mean ($p = 0.734$) but the uniform PDF standard deviation was smaller ($p < 0.001$). Even when the mean yield UEV is similar between PDFs, the standard deviation was still dependent on the PDF selected. For Model 2, differences between the means and standard deviations for each PDF were significant ($p < 0.001$).

The models were then compared to each other for each PDF. The variance of the output UEV was smaller in Model 2 for each PDF ($p < 0.001$). The normal PDF and uniform PDF yield UEV means did not change significantly between models ($p < 0.362$ and $p < 0.579$). The lognormal PDF yield UEV mean was lowered when going from Model 1 to Model 2 ($p < 0.012$). This was explained by the right tail holding most of the variance so that the removal of variance for the lognormal PDF would shift the mean to the right.

This study concluded that the crop production system did not promote one distribution over the other. While this study did not promote one distribution over the other, it was noted that the distribution of the input's energy/mass and UEV often had an impact on the PDF shape of the source's energy.

The sensitivity analysis section addressed two of the objectives of the study. The system sources that had a large impact on the variance of the yield UEV were determined and organized by distribution. The impact of each source's energy/mass and UEV components on the yield UEV was quantified in this section. The impact of the source's distribution on the yield UEV variance was also quantified in this section.

The objectives outlined previously have been met. In the systems descriptions section, the origination of uncertainty in energy analyses was shown tabularly and graphically by source and PDF. The normal distribution was used to partition the energy of the yield uncertainty by each source's energy/mass and UEV components. The sources that contributed the most uncertainty were then found for each PDF using the sensitivity analysis. The sensitivity analysis also showed the influence of the input PDF on the yield UEV variance. Limitations and future work for this study are discussed in the following chapter.

Chapter 6: Discussion

In addressing the objective questions, this study has begun to identify and isolate sources of uncertainty in energy analyses. Limitations to this study and ideas for future work are discussed below.

One of the main limitations of this study was human error. Many crop production energy analyses examined were poorly documented. In energy analyses, typos or miscalculations are worth orders of magnitude and can entirely change the data set procured. When later energy analyses reference this inaccurately represented data, the field is then further skewed. A standard format and model for presenting uncertainty may be a check for practitioners on their presented research that eliminates much of this human error (Ingwersen 2010). Current efforts of creating a hub of UEVs and methods to produce UEVs could also lower this human error and clarify the energy process (Tilley et al. 2012).

Model uncertainty was determined to be outside of the scope for this study as the same sources were selected from each system. It is understood that different models can be created to obtain the variance of a specific yield UEV. However, it should be noted that the confidence interval of a specific yield UEV using one model is not necessarily transferable to other models' yield UEV. The analyst should therefore be wary of the models used to create UEVs and their variances when including them in the analyst's own study.

In standardizing uncertainty calculations found by modeled energy analyses, it may be beneficial to have a proposed minimal number of runs. The Monte Carlo random number generator simulated uncertainty for modeled energy/mass, UEV,

yield energy, and yield UEV. Literature has a large range (30-10,000) for defining what is conventionally ‘enough’ iterations for a simulation. This term is based on what the researchers are statistically able to say with their results. The current study ran Monte Carlo models 100 times. It would be interesting to note how much uncertainty is taken out of the output UEV when there are different amounts of runs conducted.

To obtain the confidence intervals surrounding the yield UEV, only the normal PDF simulations were used in this study. The coefficient of variation method was not conducted on the other distributions due both to time constraints and the unknown dangers of using the COV on other distributions. There is a COV equation for the lognormal distribution. Future work can be done to modify this methodology to examine the Monte Carlo lognormal PDF output. Comparisons of the confidence intervals produced by normal and lognormal COV equations could influence the use of one distribution over the other.

There is much future work to be conducted in exploring input distributions and interactions in forming output UEV values. When assuming probability distributions for the energy and UEV of each source, this study utilized PDFs that previous studies had assumed. This study assumed 1) independence among sources and 2) that source’s energy/mass and UEVs and the energy/mass output had the same distribution type. Based on these assumptions, the PDFs of the inputs were found to have a significant impact on the yield UEV variance. The difference between the Monte Carlo simulations’ output and the original systems might be lowered if instead of assuming that all input parent populations can be represented by a single

distribution, different distributions are implemented for different inputs. Another area of lowering the difference between the simulations and the original systems could be having energy follow one distribution while the UEV follows a different distribution. The distributions chosen for each energy and UEV value could be experimented with based on sensitivity analyses. The distribution combinations that produce the output that is a best fit to the original data are the optimal combinations.

Distributions could also be chosen based on the advice of experts in the fields (Ayyub and Klir 2006). Ingwersen has suggested that the lognormal distribution is the most accurate when considering natural sources' energy (Ingwersen 2010a) and UEV (Ingwersen 2010b) values. A possible optimal distribution of the natural sources of the crop production system for a stochastic model is a skewed version of the lognormal distribution that has the definitive endpoints of the uniform distribution. Since the PDFs of the inputs significantly impact the yield UEV, it is encouraged that future researchers document why input distributions were chosen.

The sources whose energy/mass inputs impacted the variance of the output UEV were found in this study by eliminating the inputs that overlapped between the Model 1 and 2. To confirm which energy/mass parameters energy analysts should focus lowering the uncertainty of, a third model should be created that removes UEV parameter variance from the Monte Carlo simulation. This third model ('energy/mass only variance') will identify the sources that significantly lower the output UEV variance. Model 3 could serve as a check to the information obtained by subtracting Model 2 from Model 1.

Chapter 7: Summary

The summary and generalizations this study suggests below are based on the normal distribution. The normal distribution for inputs was used to partition the total system uncertainty by input (Figure 8), and was not reproduced for the other two distributions. This study found that the input PDFs impacted the yield UEV variance and therefore the total system uncertainty as well. Conducting the same analysis for the lognormal and uniform distributions may provide other generalizations. However, the sensitivity analysis hints that all three input distributions support a positive relationship between the percent a source contributes to total solar energy and the percent a source contributes to total system uncertainty. Both models for each distribution showed the nitrogen fertilizer source to have the largest significant impacts on the yield UEV variance of all the sources. Nitrogen fertilizer also contributed the most to total energy for each model and distribution. Only the normal distribution for inputs is shown below, but future work on input distributions may provide more general statements regardless of distribution.

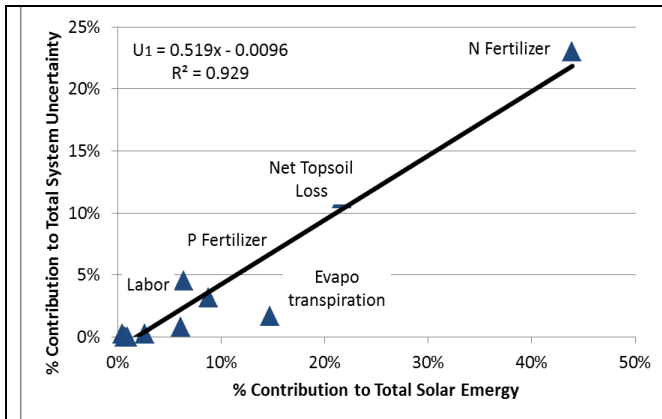


Figure 8a: Energy/mass and UEV variance

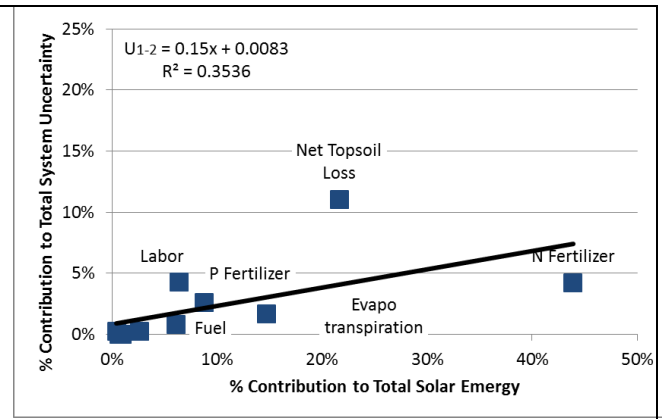


Figure 8b: Energy/mass only variance

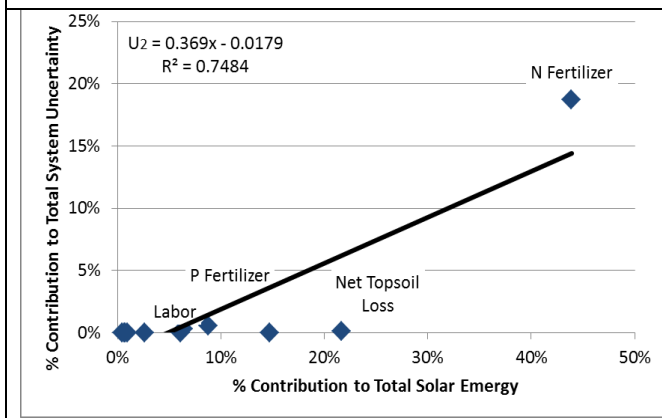


Figure 8c: UEV only variance

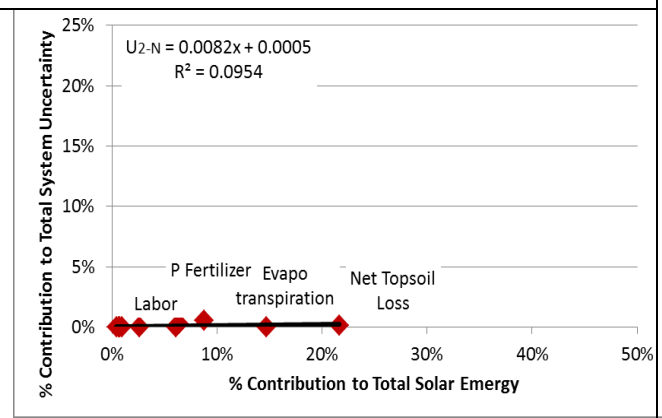


Figure 8d: UEV only variance minus nitrogen fertilizer

Figure 8: Relationship between uncertainty and energy input for each of the 11

sources for crop production. U_1 , U_2 , U_{1-2} , and U_{2-N} are respectively a source's contribution to uncertainty with total parameter variance, UEV only variance, energy/mass only variance, and UEV only variance with nitrogen removed, relative to each source's contribution to the yield energy.

The amount of uncertainty that a source contributes to the yield UEV is strongly related to the relative amount of energy it contributes to the yield energy (Figure 8a). That is, for crop systems, sources like nitrogen fertilizer that contributed the largest amount of energy to the yield also added the most variance to the yield UEV estimate (Figures 8a and 8c). Uncertainty came from both estimates of the rate of energy or material consumption and estimates of the UEV of the source. For UEV,

the largest contributor of uncertainty was nitrogen fertilizer (Figure 8c). While nitrogen fertilizer UEV contributed just under 20% to the total system uncertainty, no other source contributed more than 1% (Figure 8c and 8d). For energy/mass the largest source of uncertainty was the rate of net topsoil loss (more than 11%) (Figure 8b), but nitrogen fertilizer and labor also added nearly 5% to the total source uncertainty. Evaluation of crop uncertainty revealed that only 2 of 11 sources are responsible for the vast majority (more than 75%) of the total source uncertainty.

If the sources of uncertainty for crop systems are indicative of other energy systems, then the sources of uncertainty reside with only a few of the system sources, and tend to be the sources that contribute the largest amount of energy to the yield. Other energy transforming systems need to be evaluated in the manner described in this study to see where commonalities and differences in sources of uncertainty exist. From a practical perspective, the findings here indicate that uncertainty can be greatly reduced if analysts focus on reducing the uncertainty of the few system sources.

To compete with other environmental accounting and valuation techniques, the energy field must develop protocols for reliably characterizing, propagating, and analyzing uncertainty in models and output values. Since UEVs of outputs are cited by other energy analyses, there is an emphasis placed on documenting their uncertainty. By following the Monte Carlo method given in this study, future tabular energy analyses have a means for incorporating uncertainty into their output UEV calculation. Running a Monte Carlo simulation will provide the analyst with a ranking of each source that contributes to total uncertainty. Thus, the output from this form of sensitivity analyses can help the analyst reduce uncertainty. Steps in applying

these methods to more complex systems should be pursued, with the ultimate goal being to advance energy in the realm of policy decision making.

Appendices

Appendix i

Table 11: A key of systems studied. The numbers used in this table describing a system correspond to the numbers used in following tables.

System	Title of study	Specific system studied	Citation
1	Sustainability of bioethanol production from wheat with recycled residues as evaluated by Emergy assessment	Sandy Danish soil, conventional crop management	Coppola et al. 2009
2	Sustainability of bioethanol production from wheat with recycled residues as evaluated by Emergy assessment	Sandy loam Danish soil, conventional crop management	Coppola et al. 2009
3	Emergy evaluation of three cropping systems in southwestern Australia	Lupin-wheat rotation system	Lefroy and Rydberg 2003
4	Emergy evaluation of three cropping systems in southwestern Australia	Alley system	Lefroy and Rydberg 2003
5	Sustainable biomass production		Franzese et al. 2009
6	Sustainability assessment of slash-and-burn and fire-free agriculture in Northeastern Para, Brazil	Fire-free system	Rodrigues et al. 2003
7	Emergy of Florida Agriculture	Sweet corn	Brandt-Williams 2002
8	Emergy of Florida Agriculture	Grain corn	Brandt-Williams 2002

Appendix ii

Table 12a: Energy/mass data of original eight systems studied. This includes data minimums, maximums, means, and standard deviations. The yield is the amount of grain produced in Joules per hectare per year. The sources are split into those measured as energy (J/ha/yr) and those as a mass (converted to grams/ha/yr).					
Energy/Mass		System			
	Units	1	2	3	4
Sunlight	J/ha/yr	3.67E+13	3.73E+13	5.66E+13	4.81E+13
Evapotranspiration	J/ha/yr	2.80E+10	2.45E+10		
Net topsoil loss	J/ha/yr	7.46E+08		1.58E+10	5.20E+09
N Fertilizer	gN/ha/yr	1.22E+05	1.18E+05		
P Fertilizer	gP/ha/yr	1.23E+04	1.21E+04	1.29E+04	1.10E+04
Pesticides	g/ha/yr	1.38E+03	1.38E+03	2.00E+03	2.00E+03
Seed	g/ha/yr	1.70E+05	1.70E+05	3.25E+04	3.25E+04
Fuel	J/ha/yr	2.83E+09	3.16E+09	3.05E+08	2.59E+08
Steel machinery	g/ha/yr	1.98E+03	1.98E+03	1.17E+03	9.95E+02
Electricity	J/ha/yr	7.20E+08	1.20E+09	3.60E+06	3.06E+06
Labor	J/ha/yr	2.88E+06	2.88E+06	2.81E+06	2.81E+06
Yield	J/ha/yr	7.01E+10	1.17E+11	1.59E+10	1.36E+10
Energy/Mass		5	6	7	8
	Units				
Sunlight	J/ha/yr	5.53E+13	6.94E+13	6.35E+13	6.35E+13
Evapotranspiration	J/ha/yr		4.19E+10	6.05E+10	6.05E+10
Net topsoil loss	J/ha/yr	3.24E+09	4.70E+09	2.44E+10	4.25E+10
N Fertilizer	gN/ha/yr	1.69E+05		5.71E+04	5.71E+04
P Fertilizer	gP/ha/yr	8.20E+04	1.50E+04	3.95E+04	2.11E+04
Pesticides	g/ha/yr	5.38E+03		1.11E+04	1.69E+03
Seed	g/ha/yr	1.62E+04			
Fuel	J/ha/yr	6.97E+09	1.40E+08	1.25E+10	8.12E+09
Steel machinery	g/ha/yr	1.36E+04			
Electricity	J/ha/yr	2.00E+09			7.85E+08
Labor	J/ha/yr	1.08E+07	1.40E+07	2.54E+08	1.32E+07
Yield	J/ha/yr	1.12E+11	2.35E+10	1.04E+11	1.81E+10

Energy/Mass	Units	Min	Max	Mean	Std Dev
Sunlight	J/ha/yr	3.67E+13	6.94E+13	5.38E+13	1.22E+13
Evapotranspiration	J/ha/yr	2.45E+10	6.05E+10	4.31E+10	1.72E+10
Net topsoil loss	J/ha/yr	7.46E+08	4.25E+10	1.38E+10	1.52E+10
N Fertilizer	gN/ha/yr	5.71E+04	1.69E+05	1.05E+05	4.78E+04
P Fertilizer	gP/ha/yr	1.10E+04	8.20E+04	2.57E+04	2.46E+04
Pesticides	g/ha/yr	1.38E+03	1.11E+04	3.56E+03	3.61E+03
Seed	g/ha/yr	1.62E+04	1.70E+05	8.42E+04	7.86E+04
Fuel	J/ha/yr	1.40E+08	1.25E+10	4.29E+09	4.50E+09
Steel machinery	g/ha/yr	9.95E+02	1.36E+04	3.95E+03	5.42E+03
Electricity	J/ha/yr	3.06E+06	2.00E+09	7.85E+08	7.58E+08
Labor	J/ha/yr	2.81E+06	2.54E+08	3.79E+07	8.74E+07
Yield	J/ha/yr	1.36E+10	1.17E+11	5.92E+10	4.65E+10

Table 12b: UEV data of original eight systems studied. This includes data minimums, maximums, means, and standard deviations. The yield is the amount of grain produced in solar emjoules per Joules per hectare per year. The source UEVs are split into transformities (sej/J/ha/yr) and specific emergies (sej/g/ha/yr).

UEV	Units (ha/yr)	System			
		1	2	3	4
Sunlight	sej/J	1.00E+00	1.00E+00	1.00E+00	1.00E+00
Evapotranspiration	sej/J	2.59E+04	2.59E+04		
Net topsoil loss	sej/J	1.24E+05		1.05E+05	1.05E+05
N Fertilizer	sej/gN	2.41E+10	2.41E+10		
P Fertilizer	sej/gP	2.02E+10	2.02E+10	2.86E+10	2.86E+10
Pesticides	sej/g	1.85E+09	1.85E+09	4.77E+09	4.77E+09
Seed	sej/g	1.20E+09	1.20E+09	3.10E+07	3.10E+07
Fuel	sej/J	1.10E+05	1.10E+05	9.42E+04	9.42E+04
Steel machinery	sej/g	1.13E+10	1.13E+10	5.04E+09	5.04E+09
Electricity	sej/J	2.00E+05	2.00E+05	2.92E+05	2.92E+05
Labor	sej/J	1.24E+07	1.24E+07	1.93E+07	1.99E+07
Yield	sej/J	8.80E+04	5.10E+04	1.17E+05	9.27E+04
UEV	Units	System			
		5	6	7	8
Sunlight	sej/J	1.00E+00	1.00E+00	1.00E+00	1.00E+00
Evapotranspiration	sej/J		2.59E+04	2.59E+04	2.59E+04
Net topsoil loss	sej/J	1.24E+05	1.24E+05	1.24E+05	1.24E+05
N Fertilizer	sej/gN	6.37E+09		4.05E+10	4.05E+10
P Fertilizer	sej/gP	6.54E+09	2.99E+10	3.70E+10	3.70E+10
Pesticides	sej/g	2.48E+10		2.49E+10	2.49E+10
Seed	sej/g	8.68E+08			
Fuel	sej/J	1.11E+05	1.11E+05	1.11E+05	1.11E+05
Steel machinery	sej/g	1.12E+10			
Electricity	sej/J	2.51E+05			2.69E+05
Labor	sej/J	7.10E+06	1.50E+07	7.64E+06	7.64E+06
Yield	sej/J	7.34E+04	1.20E+05	2.12E+05	1.24E+06

UEV	Units	Min	Max	Mean	Std Dev
Sunlight	sej/J	1.00E+00	1.00E+00	1.00E+00	0.00E+00
Evapotranspiration	sej/J	2.59E+04	2.59E+04	2.59E+04	5.83E+00
Net topsoil loss	sej/J	1.05E+05	1.24E+05	1.19E+05	9.27E+03
N Fertilizer	sej/gN	6.37E+09	4.05E+10	2.71E+10	1.42E+10
P Fertilizer	sej/gP	6.54E+09	3.70E+10	2.60E+10	1.01E+10
Pesticides	sej/g	1.85E+09	2.49E+10	1.25E+10	1.16E+10
Seed	sej/g	3.10E+07	1.20E+09	6.66E+08	5.95E+08
Fuel	sej/J	9.42E+04	1.11E+05	1.07E+05	7.61E+03
Steel machinery	sej/g	5.04E+09	1.13E+10	8.78E+09	3.41E+09
Electricity	sej/J	2.00E+05	2.92E+05	2.51E+05	4.21E+04
Labor	sej/J	7.10E+06	1.99E+07	1.27E+07	5.12E+06
Yield	sej/J	5.10E+04	1.24E+06	2.49E+05	4.03E+05

Appendix iii

Table 13a: Sensitivity analysis for Model 1: Exact data and p values. Minimized the source energy/mass and UEV variance and then generated yield UEV. T tests' and f tests' p values were found by comparing the baseline to the minimized total variance of each source, and are recorded alongside the mean and standard deviation of the newly generated output. Significant p values ($\alpha < 0.05$) are bolded.

	Normal			
	Mean	p	Stddev	p
		value		value
Baseline	1.18E+05	1	5.30E+04	1
Sunlight	1.18E+05	0.25	5.30E+04	0.42
Evapotranspiration	1.35E+05	0.03	5.79E+04	0.38
Fuel	1.27E+05	0.37	4.89E+04	0.80
Net topsoil loss	1.25E+05	0.30	4.12E+04	0.01
Electricity	1.26E+05	0.28	4.76E+04	0.29
Labor	1.22E+05	0.57	4.62E+04	0.18
Seed	1.27E+05	0.24	4.79E+04	0.32
Steel machinery	1.37E+05	0.02	5.17E+04	0.97
Pesticides	1.32E+05	0.10	5.04E+04	0.83
P Fertilizer	1.35E+05	0.02	4.65E+04	0.20
N Fertilizer	1.25E+05	0.28	4.09E+04	0.01

	Lognormal			
	Mean	p	Stddev	p
		value		value
Baseline	1.59E+05	1	8.59E+04	1
Sunlight	1.27E+05	0.34	5.51E+04	0.00
Evapotranspiration	1.31E+05	0.01	6.44E+04	0.00
Fuel	1.47E+05	0.26	6.10E+04	0.00
Net topsoil loss	1.39E+05	0.06	6.38E+04	0.00
Electricity	1.64E+05	0.66	7.89E+04	0.40
Labor	1.48E+05	0.31	7.39E+04	0.13
Seed	1.59E+05	0.99	7.52E+04	0.19
Steel machinery	1.58E+05	0.89	6.38E+04	0.00
Pesticides	1.59E+05	1.00	6.31E+04	0.00
P Fertilizer	1.53E+05	0.58	7.40E+04	0.14
N Fertilizer	9.33E+04	0.00	3.73E+04	0.00
	Uniform			
	Mean	p	Stddev	p
		value		value
Baseline	1.70E+05	1	4.30E+04	1
Sunlight	1.74E+05	0.41	3.97E+04	0.42
Evapotranspiration	1.70E+05	0.94	4.29E+04	0.99
Fuel	1.54E+05	0.01	4.14E+04	0.70
Net topsoil loss	1.34E+05	0.00	3.34E+04	0.01
Electricity	1.70E+05	0.93	4.23E+04	0.87
Labor	1.46E+05	0.00	3.41E+04	0.02
Seed	1.66E+05	0.54	4.25E+04	0.90
Steel machinery	1.82E+05	0.05	4.33E+04	0.94
Pesticides	1.67E+05	0.66	3.43E+04	0.03
P Fertilizer	1.66E+05	0.53	4.01E+04	0.49
N Fertilizer	1.61E+05	0.10	3.23E+04	0.00

Table 13b: Sensitivity analysis for Model 2: Exact data and p values. Minimized the source UEV variance and then generated yield UEV. T tests' and f tests' p values were found by comparing the baseline to the minimized total variance of each source, and are recorded alongside the mean and standard deviation of the newly generated output. Significant p values ($\alpha < 0.05$) are bolded.				
	Normal			
	Mean	p	Stddev	p
		value		value
Baseline	1.24E+05	1	2.64E+04	1
Sunlight	1.28E+05	0.21	2.69E+04	0.84
Evapotranspiration	1.28E+05	0.25	2.71E+04	0.79
Fuel	1.37E+05	0.00	2.80E+04	0.57
Net topsoil loss	1.27E+05	0.41	2.47E+04	0.52
Electricity	1.27E+05	0.37	2.81E+04	0.54
Labor	1.32E+05	0.03	2.44E+04	0.44
Seed	1.25E+05	0.80	2.57E+04	0.78
Steel machinery	1.31E+05	0.04	2.14E+04	0.04
Pesticides	1.29E+05	0.16	2.58E+04	0.82
P Fertilizer	1.29E+05	0.13	2.50E+04	0.60
N Fertilizer	1.28E+05	0.07	6.31E+03	0.00
	Lognormal			
	Mean	p	Stddev	p
		value		value
Baseline	1.36E+05	1	3.38E+04	1
Sunlight	1.30E+05	0.34	2.76E+04	0.78
Evapotranspiration	1.32E+05	0.44	2.95E+04	0.18
Fuel	1.32E+05	0.46	3.85E+04	0.19
Net topsoil loss	1.28E+05	0.10	2.84E+04	0.09
Electricity	1.33E+05	0.54	3.80E+04	0.25
Labor	1.31E+05	0.31	3.15E+04	0.48
Seed	1.31E+05	0.37	3.56E+04	0.60
Steel machinery	1.30E+05	0.18	2.94E+04	0.16
Pesticides	1.32E+05	0.51	3.58E+04	0.56
P Fertilizer	1.32E+05	0.42	3.48E+04	0.78
N Fertilizer	1.21E+05	0.00	5.09E+03	0.00

	Uniform			
	Mean	p	Stddev	p
		value		value
Baseline	1.54E+05	1	2.03E+04	1
Sunlight	1.55E+05	0.72	1.94E+04	0.66
Evapotranspiration	1.57E+05	0.34	2.07E+04	0.83
Fuel	1.55E+05	0.59	1.97E+04	0.78
Net topsoil loss	1.59E+05	0.05	2.05E+04	0.92
Electricity	1.57E+05	0.21	2.01E+04	0.91
Labor	1.55E+05	0.66	1.69E+04	0.07
Seed	1.54E+05	0.86	2.07E+04	0.84
Steel machinery	1.56E+05	0.53	2.12E+04	0.66
Pesticides	1.58E+05	0.14	1.85E+04	0.36
P Fertilizer	1.51E+05	0.24	1.99E+04	0.83
N Fertilizer	1.55E+05	0.50	9.13E+03	0.00

Bibliography

- Amponsah, N.Y., O. Le Corre, 2010. Critical Review of the Usage of Unit Emergy Values in Recent Studies. In: Brown, M.T. (Ed.), Emergy Synthesis 6: Proceedings of the 6th Biennial Emergy Conference: Theory and Applications of the Emergy Methodology. Center for Environmental Policy, Gainesville, FL. 33-43.
- Ayyub, B., G. Klir, 2006. Uncertainty Modeling and Analysis in Engineering and the Sciences. Taylor & Francis Group, Boca Raton, FL. 378p.
- Blumenthal, J.M., D.D. Baltensperger, K.G. Cassman, S.C. Mason, A.D. Pavlista, 2008. Importance and effect of nitrogen on crop quality and health. In: Hatfield, J.L., and R.F. Follett (Eds.), Nitrogen in the Environment: Sources, Problems, and Management, second edition. Amsterdam. 51-70.
- Brandt-Williams, S., 2002. Handbook of Emergy Evaluation Folio 4: Emergy of Florida Agriculture. Center for Environmental Policy, University of Florida, Gainesville, FL. 44p.
- Brown, M.T., G. Protano, S. Ulgiati, 2011. Assessing geobiosphere work of generating global reserves of coal, crude oil, and natural gas. Ecological Modelling (Elsevier) 222: 879-887.
- Campbell, D.E., 2001. A note on uncertainty in estimates of transformities based on global water budgets. In: Brown, M.T. (Ed.), Emergy Synthesis 2: Proceedings of the 2nd Biennial Emergy Conference: Theory and Applications of the Emergy Methodology. Center for Environmental Policy, Gainesville, FL. 349-354.

- Cohen, M.J., 2001. Dynamic Energy Simulation of Soil Genesis and Techniques for Estimating Transformity Confidence Envelopes. In: Brown, M.T. (Ed.), Energy Synthesis 2: Proceedings of the 2nd Biennial Energy Conference: Theory and Applications of the Emergy Methodology. Center for Environmental Policy, Gainesville, FL. 355-370.
- Coppola, F., S. Bastianoni, H. Østergård, 2009. Sustainability of bioethanol production from wheat with recycled residues as evaluated by Emergy assessment. Biomass and Bioenergy 33: 1626-1642.
- Fluck, R.C., 1992. Energy for Florida Corn for Grain. Florida Cooperative Extension Service: Fact Sheet EES-92. Gainesville, FL. 1-2.
- Franzese, P. P., T. Rydberg, G.F. Russo, S. Ulgiati, 2009. Sustainable biomass production: A comparison between Gross Energy Requirement and Emergy Synthesis methods. Ecological Indicators (Elsevier) 9(5): 959-970.
- Hau, J.L., B.R. Bakshi, 2004. Promise and problems of emergy analysis. Ecological Modelling 178: 215-225.
- Ingwersen, W.W., 2010a. Uncertainty characterization for emergy values. Ecological Modelling 221(3): 445-452.
- Ingwersen, W.W., 2010b. An Uncertainty Model for Emergy. In: Brown, M.T. (Ed.), Energy Synthesis 6: Proceedings of the 6th Biennial Energy Conference: Theory and Applications of the Emergy Methodology. Center for Environmental Policy, Gainesville, FL. 555-559.
- Jaffe, J. and R.N. Stavins. On the value of formal assessment of uncertainty in regulatory analysis. Regulation & Governance: 1. 154-171.

- Lefroy, E., T. Rydberg, 2003. Emergy evaluation of three cropping systems in southwestern Australia. *Ecological Modelling* 161: 195-211.
- Lloyd, S., Ries, R., 2007. Characterizing, propagating, and analyzing uncertainty in life cycle assessment. *Industrial Ecology* 11: 161-179.
- Odum, H. T., 1996. *Environmental Accounting: Emergy and Environmental Decision Making*. John Wiley & Sons, New York. 370p.
- Rai, S.N., D. Krewski, 1998. Uncertainty and variability analysis in multiplicative risk models. *Risk Analysis* 18: 37-45.
- Rodrigues, G. S., P.C. Kitamura, T.D. Sa, K. Vielhauer, 2003. Sustainability assessment of slash-and-burn and fire-free agriculture in Northeastern Para, Brazil. In: Brown, M.T. (Ed.), *Emergy Synthesis 2: Proceedings of the 2nd Biennial Emergy Conference: Theory and Applications of the Emergy Methodology*. Center for Environmental Policy, Gainesville, FL. 95-108.
- Sonnemann, G.W., M. Schuhmacher, F. Castells, 2003. Uncertainty assessment by a Monte Carlo simulation in a life cycle inventory of electricity produced by a waste incinerator. *Journal of Cleaner Production* 11: 279-292.
- Tilley, D.R., Agostinho, F., Campbell, E., Ingwersen, W., Lomas, P., Winfrey, B., Zucaro, A., and Zhang. P., (2012). The ISAER transformity database. International Society for Advancement of Emergy Research. Available at www.emergydatabase.org.
- Tilley, D.R. and M.T. Brown. 2006. Dynamic emergy accounting for assessing the environmental benefits of subtropical wetland stormwater management systems. *Ecological Modelling* 192: 327–361.

Ulgiati, S., F. Agostinho, P.L. Lomas, E. Ortega, S. Viglia, P. Zhang, and A. Zucaro,
2010. Criteria for Quality Assessment of Unit Emergy Values. In: Brown,
M.T. (Ed.), Emergy Synthesis 6: Proceedings of the 6th Biennial Emergy
Conference: Theory and Applications of the Emergy Methodology. Center for
Environmental Policy, Gainesville, FL. 559-610.

Winston, W.L., 1991. Operations Research Applications and Algorithms (2nd ed.).
Boston: PWS-Kent. 1262p.